NATIONAL CENTER FOR EARTHQUAKE
ENGINEERING RESEARCH
State University of New York at Buffalo

EXPERIMENTAL AND ANALYTICAL STUDY OF A COMBINED SLIDING DISC BEARING AND HELICAL STEEL SPRING ISOLATION SYSTEM

by

M. C. Constantinou, A. S. Mokha and A. M. Reinhorn
Department of Civil Engineering
State University of New York at Buffalo
Buffalo, New York 14260

Technical Report NCEER-90-0019

October 4, 1990

This research was conducted at the State University of New York at Buffalo and was partially supported by the National Science Foundation under Grant No. ECE 86-07591.

NOTICE

This report was prepared by the State University of New York at Buffalo as a result of research sponsored by the National Center for Earthquake Engineering Research (NCEER). Neither NCEER, associates of NCEER, its sponsors, State University of New York at Buffalo, nor any person acting on their behalf:

a. makes any warranty, express or implied, with respect to the use of any information, apparatus, method, or process disclosed in this report or that such use may not infringe upon privately owned rights; or

b. assumes any liabilities of whatsoever kind with respect to the use of, or the damage resulting from the use of, any information, apparatus, method or process disclosed in this report.

EXPERIMENTAL AND ANALYTICAL STUDY OF A COMBINED SLIDING DISC BEARING AND HELICAL STEEL SPRING ISOLATION SYSTEM

by

M.C. Constantinou[1], A.S. Mokha[2] and A.M. Reinhorn[3]

October 4, 1990

Technical Report NCEER-90-0019

NCEER Project Number 88-2002A

NSF Master Contract Number ECE 86-07591

1 Associate Professor, Department of Civil Engineering, State University of New York at Buffalo

2 Structural Engineer, Skidmore, Owings and Merill, 333 Bush St., San Francisco, CA 94104. Formerly Graduate Student, Department of Civil Engineering, State University of New York at Buffalo

3 Professor, Department of Civil Engineering, State University of New York at Buffalo

NATIONAL CENTER FOR EARTHQUAKE ENGINEERING RESEARCH
State University of New York at Buffalo
Red Jacket Quadrangle, Buffalo, NY 14261

PREFACE

The National Center for Earthquake Engineering Research (NCEER) is devoted to the expansion and dissemination of knowledge about earthquakes, the improvement of earthquake-resistant design, and the implementation of seismic hazard mitigation procedures to minimize loss of lives and property. The emphasis is on structures and lifelines that are found in zones of moderate to high seismicity throughout the United States.

NCEER's research is being carried out in an integrated and coordinated manner following a structured program. The current research program comprises four main areas:

- Existing and New Structures
- Secondary and Protective Systems
- Lifeline Systems
- Disaster Research and Planning

This technical report pertains to Program 2, Secondary and Protective Systems, and more specifically, to protective systems. Protective Systems are devices or systems which, when incorporated into a structure, help to improve the structure's ability to withstand seismic or other environmental loads. These systems can be passive, such as base isolators or viscoelastic dampers; or active, such as active tendons or active mass dampers; or combined passive-active systems.

Passive protective systems constitute one of the important areas of research. Current research activities, as shown schematically in the figure below, include the following:

1. Compilation and evaluation of available data.
2. Development of comprehensive analytical models.
3. Development of performance criteria and standardized testing procedures.
4. Development of simplified, code-type methods for analysis and design.

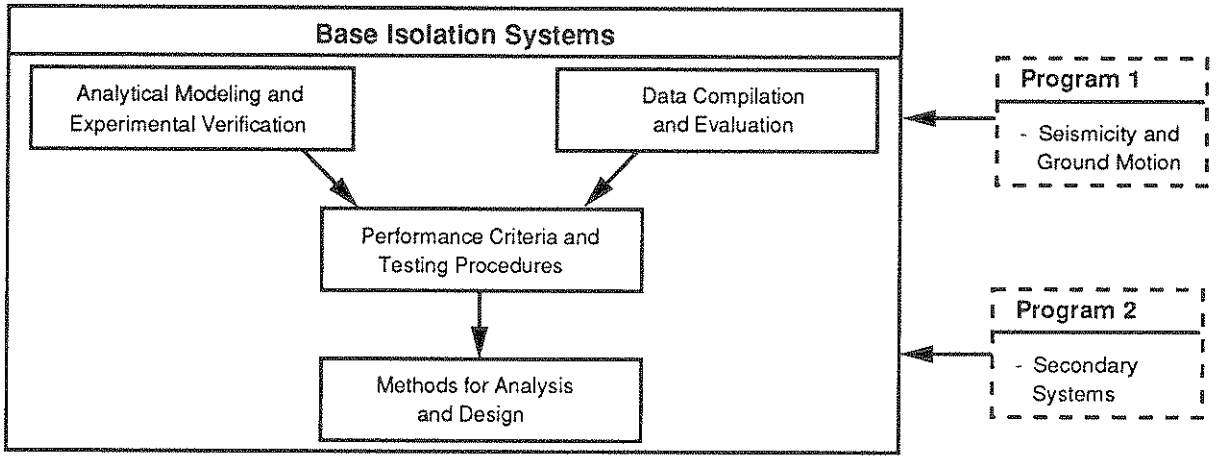

This report presents an evaluation of a sliding isolation system which consists of Teflon disc bearings and helical steel springs. The study is part of a series of experimental and analytical investigations being carried out at the University at Buffalo on a variety of base isolation systems. The isolation system was tested in a six-story quarter-scale model structure on the shake table at the University at Buffalo. Test results showed that the system has low sensitivity to the frequency content of input motion. Experimental results confirmed that system response could be predicted by analytical techniques.

ABSTRACT

A sliding isolation system consisting of Teflon disc bearings and helical steel springs is described. The system has been evaluated in shake table tests of a six-story, quarter scale, 52 Kip model structure and found to be capable of withstanding strong earthquake forces of significantly different frequency content. The isolation system has been designed to have strong frictional force and weak restoring force. Under these conditions, the isolated structure is insensitive to the frequency content of input and experimental results confirm this important property.

ACKNOWLEDGEMENTS

Financial support for this project has been provided by the National Center for Earthquake Engineering Research (Contract No. 88-2002A), by the National Science Foundation (Grant No. CES-8857080), by Watson Bowman Acme Corporation, Amherst, N.Y. and by GERB Vibration Control, Westmont, IL. The authors wish to express their sincere gratitude for the support received. Special thanks are due to Dr. Guenter Hueffmann, President and the technical staff of GERB Vibration Control for developing the helical spring units.

TABLE OF CONTENTS

SECTION	TITLE	PAGE
1	INTRODUCTION	1-1
2	TEST STRUCTURE AND INSTRUMENTATION	2-1
3	ISOLATION SYSTEM	3-1
4	TEST PROGRAM	4-1
5	TEST RESULTS	5-1
5.1	Effectiveness of System	5-1
5.2	Effect of Restoring Force	5-7
5.3	System Adequacy	5-13
5.4	Features of Response	5-15
6	ANALYTICAL PREDICTION OF RESPONSE	6-1
7	CONCLUSIONS	7-1
8	REFERENCES	8-1

LIST OF ILLUSTRATIONS

FIGURE	TITLE	PAGE
2-1	Six-Story Steel Test Structure (1ft = 304.8mm)	2-2
2-2	Instrumentation Diagram of Test Structure	2-5
3-1	Teflon Disc Bearing Design (1 inch = 25.4mm)	3-2
3-2	Teflon Disc Bearing	3-3
3-3	Helical Steel Spring Unit Under Deformation	3-5
3-4	Force-Displacement Loops of Isolation System (a) Frictional Force, (b) Frictional and Restoring Force From Four Spring Units Combined (1 inch = 25.4mm, 1 Kip = 4.46 kN)	3-7
4-1	Recorded Time Histories of Shake Table Acceleration; SB4HS Stands For Isolation System with Four Spring Units	4-3
5-1	Profiles of Floor Acceleration (Solid Line) and Displacement (Dashed Line) of Test Structure in Isolation System with Four Spring Units and Pacoima S16E Input (0.84g peak table acceleration)	5-6
5-2	Profiles of Floor Acceleration (Solid Line) and Displacement (Dashed Line) of Test Structure in Isolation System with Four Spring Units and El Centro S00E Input (0.31g peak table acceleration)	5-6
5-3	Profiles of Floor Acceleration (Solid Line) and Displacement (Dashed Line) of Test Structure in Isolation System with Four Spring Units and Hachinohe NS Input (0.22g peak table acceleration)	5-8

FIGURE	TITLE	PAGE
5-4	Profiles of Floor Acceleration (Solid Line) and Displacement (Dashed Line) of Test Structure in Isolation System with Four Spring Units and Mexico City N90W Input (0.18g peak table acceleration)	5-8
5-5	Profiles of Floor Acceleration (Solid Line) and Displacement (Dashed Line) of Test Structure in Isolation System with Two Spring Units and Hachinohe NS Input (0.22g peak table acceleration)	5-9
5-6	Profiles of Floor Acceleration (Solid Line) and Displacement (Dashed Line) of Test Structure in Isolation System with Two Spring Units and Miyagiken-Oki EW Input (0.42g peak table acceleration)	5-9
5-7	Profiles of Floor Acceleration (Solid Line) and Displacement (Dashed Line) of Test Structure in Isolation System without Spring Units and Hachinohe NS Input (0.21g peak table acceleration)	5-10
5-8	Profiles of Floor Acceleration (Solid Line) and Displacement (Dashed Line) of Test Structure in Isolation System without Spring Units and Miyagiken-Oki EW Input (0.43g peak table acceleration)	5-10
5-9	Peak Response of the Test Structure as Function of Isolation System Period (T_b) in Case of Hachinohe NS Input (0.22g peak table acceleration)	5-12
5-10	Peak Response of the Test Structure as Function of Isolation System Period (T_b) in Case of Miyagiken-Oki EW Input (0.42 peak table acceleration)	5-12

FIGURE	TITLE	PAGE
5-11	Fourier Amplitude Spectra of Sixth-Floor Acceleration of Structure for Fixed-Base Conditions and Isolation Conditions with Four (SB4HS), Two (SB2HS) and without (SB0HS) Spring Units. Observe that Frequency Content is not Affected by Stiffness of Spring Units	5-14
5-12	Bearing Displacement History and Base Shear-Displacement Loop of Isolation System with Four Spring Units for Harmonic Input of 2.4Hz Frequency. Forty Cycles Completed without Degradation (1in = 25.4mm)	5-16
5-13	Experimental Time Histories of Base (Bearing) Displacement, Structure Shear and Sixth Floor Displacement with Respect to Base and Base Shear-Bearing Displacement Loop in Case of Isolation System with Four Spring Units and for El Centro Input (0.31g peak table acceleration). Structure Shear is Shear at First Story. Base Shear is Shear at Bearing Level	5-19
5-14	Experimental Time Histories of Base (Bearing) Displacement, Structure Shear and Sixth-Floor Displacement with Respect to Base and Base Shear-Bearing Displacement Loop in Case of Isolation System with Four Spring Units and For Hachinohe NS Input (0.22g peak table acceleration)	5-20
5-15	Experimental Time Histories of Base (Bearing) Displacement, Structure Shear and Sixth-Floor Displacement with Respect to Base and Base Shear-Bearing Displacement Loop in Case of Isolation System with Four Spring Units and for Hachinohe NS Input (0.29g peak table acceleration)	5-21

FIGURE	TITLE	PAGE
5-16	Experimental Time Histories of Base (Bearing) Displacement, Structure Shear and Sixth-Floor Displacement with Respect to Base and Base Shear-Bearing Displacement Loop in Case of Isolation System with Four Spring Units and For Taft N21E Input (0.16g peak table acceleration)	5-22
5-17	Experimental Time Histories of Base (Bearing) Displacement, Structure Shear and Sixth-Floor Displacement with Respect to Base and Base Shear-Bearing Displacement Loop in Case of Isolation System with Four Spring Units and for Taft N21E Input (0.44g peak table acceleration)	5-23
5-18	Experimental Time Histories of Base (Bearing) Displacements, Structure Shear and Sixth-Floor Displacement with Respect to Base and Base Shear-Bearing Displacement Loop in Case of Isolation System with Four Spring Units and for Miyagiken-Oki EW Input (0.14g peak table acceleration)	5-24
5-19	Experimental Time Histories of Base (Bearing) Displacement, Structure Shear and Sixth-Floor Displacement with Respect to Base and Base Shear-Bearing Displacement Loop in Case of Isolation System with Four Spring Units and for Miyagiken-Oki EW Input (0.42g peak table acceleration)	5-25

FIGURE	TITLE	PAGE
5-20	Experimental Time Histories of Base (Bearing) Displacement, Structure Shear and Sixth-Floor Displacement with Respect to Base and Base Shear-Bearing Displacement Loop in Case of Isolation System with Four Spring Units and For Pacoima S74W Input (0.39 peak table acceleration)	5-26
5-21	Experimental Time Histories of Base (Bearing) Displacement, Structure Shear and Sixth-Floor Displacement with Respect to Base and Base Shear-Bearing Displacement Loop in Case of Isolation System with Four Spring Units and For Pacoima S74W Input (0.58g peak table acceleration)	5-27
5-22	Experimental Time Histories of Base (Bearing) Displacement, Structure Shear and Sixth-Floor Displacement with Respect to Base Shear-Bearing Displacement Loop in Case of Isolation System with Four Spring Units and For Pacoima S16E Input (0.48g peak table acceleration)	5-28
5-23	Experimental Time Histories of Base (Bearing) Displacement, Structure Shear and Sixth-Floor Displacement with Respect to Base and Base Shear-Bearing Displacement Loop in Case of Isolation System with Four Spring Units and for Pacoima S16E Input (0.73g peak table acceleration)	5-29
5-24	Experimental Time Histories of Base (Bearing) Displacement, Structure Shear and Sixth-Floor Displacement with Respect to Base and Base Shear-Bearing Displacement Loop in Case of Isolation System with Four Spring Units and for Pacoima S16E Input (0.84g peak table acceleration)	5-30

FIGURE	TITLE	PAGE
5-25	Experimental Time Histories of Base (Bearing) Displacement, Structure Shear and Sixth-Floor Displacement with Respect to Base and Base Shear-Bearing Displacement Loop in Case of Isolation System with Four Spring Units and for Mexico City N90W Input (0.13g peak table acceleration)	5-31
5-26	Experimental Time Histories of Base (Bearing) Displacement, Structure Shear and Sixth-Floor Displacement with Respect to Base and Base Shear-Bearing Displacement Loop in Case of Isolation System with Four Spring Units and for Mexico City N90W Input (0.15g peak table acceleration)	5-32
5-27	Experimental Time Histories of Base (Bearing) Displacement, Structure Shear and Sixth-Floor Displacement with Respect to Base and Base Shear-Bearing Displacement Loop in Case of Isolation System with Four Spring Units and for Mexico City N90W Input (0.18g peak table acceleration)	5-33
5-28	Experimental Time Histories of Base (Bearing) Displacement, Structure Shear and Sixth-Floor Displacement with Respect to Base and Base Shear-Bearing Displacement Loop in Case of Isolation System with Four Spring Units and for Mexico City N90W Input (0.21g peak table acceleration)	5-34

FIGURE	TITLE	PAGE
5-29	Experimental Time Histories of Base (Bearing) Displacement, Structure Shear and Sixth-Floor Displacement with Respect to Base and Base Shear-Bearing Displacement Loop in Case of Isolation System with Two Spring Units and for Mexico City N90W Input (0.21g peak table acceleration)	5-35
5-30	Experimental Time Histories of Base (Bearing) Displacement, Structure Shear and Sixth-Floor Displacement with Respect to Base and Base Shear-Bearing Displacement Loop in Case of Isolation System with Two Spring Units and for El Centro S00E Input (0.28g peak table acceleration)	5-36
5-31	Experimental Time Histories of Base (Bearing) Displacement, Structure Shear and Sixth-Floor Displacement with Respect to Base and Base Shear-Bearing Displacement Loop in Case of Isolation System with Two Spring Units and for Miyagiken-Oki EW Input (0.13g peak table acceleration)	5-37
5-32	Experimental Time Histories of Base (Bearing) Displacement, Structure Shear and Sixth-Floor Displacement with Respect to Base and Base Shear-Bearing Displacement Loop in Case of Isolation System with Two Spring Units and for Miyagiken-Oki EW Input (0.42g peak table acceleration)	5-38

FIGURE	TITLE	PAGE
5-33	Experimental Time Histories of Base (Bearing) Displacement, Structure Shear and Sixth-Floor Displacement with Respect to Base and Base Shear-Bearing Displacement Loop in Case of Isolation System with Two Spring Units and for Pacoima S16E Input (0.46g peak table acceleration)	5-39
5-34	Experimental Time Histories of Base (Bearing) Displacement, Structure Shear and Sixth-Floor Displacement with Respect to Base and Base Shear-Bearing Displacement Loop in Case of Isolation System with Two Spring Units and for Pacoima S74W Input (0.38g peak table acceleration)	5-40
5-35	Experimental Time Histories of Base (Bearing) Displacement, Structure Shear and Sixth-Floor Displacement with Respect to Base and Shear-Bearing Displacement Loop in Case of Isolation System with Two Spring Units and for Hachinohe NS Input (0.22g peak table acceleration)	5-41
5-36	Experimental Time Histories of Base (Bearing) Displacement, Structure Shear and Sixth-Floor Displacement with Respect to Base and Shear-Bearing Displacement Loop in Case of Isolation System without Spring Units and for Miyagiken-Oki EW Input (0.14g peak table acceleration)	5-42
5-37	Experimental Time Histories of Base (Bearing) Displacement, Structure Shear and Sixth-Floor Displacement with Respect to Base and Shear-Bearing Displacement Loop in Case of Isolation System without Spring Units and for Miyagiken-Oki EW Input (0.28g peak table acceleration)	5-43

FIGURE	TITLE	PAGE
5-38	Experimental Time Histories of Base (Bearing) Displacement, Structure Shear and Sixth-Floor Displacement with Respect to Base and Shear-Bearing Displacement Loop in Case of Isolation System without Spring Units and for Miyagiken-Oki EW Input (0.43g peak table acceleration)	5-44
5-39	Experimental Time Histories of Base (Bearing) Displacement, Structure Shear and Sixth-Floor Displacement with Respect to Base and Shear-Bearing Displacement Loop in Case of Isolation System without Spring Units and for Hachinohe NS Input (0.21g peak table acceleration)	5-45
6-1	Analytical Time Histories of Base (Bearing) Displacement, Structure Shear and Sixth-Floor Displacement with Respect to Base and Base Shear-Bearing Displacement Loop in Case of Isolation System with Four Spring Units and for Hachinohe NS Input (0.22g peak table acceleration). Compare with Figure 5-14	6-7
6-2	Analytical Time Histories of Base (Bearing) Displacement, Structure Shear and Sixth-Floor Displacement with Respect to Base and Base Shear-Bearing Displacement Loop in Case of Isolation System with Four Spring Units and for Pacoima S16E Input (0.84g peak table acceleration). Compare with Figure 5-24	6-8

FIGURE	TITLE	PAGE
6-3	Analytical Time Histories of Base (Bearing) Displacement, Structure Shear and Sixth-Floor Displacement with Respect to Base and Base Shear-Bearing Displacement Loop in Case of Isolation System with Four Spring Units and for Mexico City N90W Input (0.21 peak table acceleration). Compare with Figure 5-28.	6-9
6-4	Analytical Time Histories of Base (Bearing) Displacement, Structure Shear and Sixth-Floor Displacement with Respect to Base and Base Shear-Bearing Displacement Loop in Case of Isolation System with Two Spring Units and for Mexico City N90W Input (0.21g peak table acceleration). Compare with Figure 5-29	6-10
6-5	Analytical Time Histories of Base (Bearing) Displacement, Structure Shear and Sixth-Floor Displacement with Respect to Base and Base Shear-Bearing Displacement Loop in Case of Isolation System with Two Spring Units for El Centro S00E Input (0.28g peak table acceleration). Compare with Figure 5-30	6-11
6-6	Analytical Time Histories of Base (Bearing) Displacement, Structure Shear and Sixth-Floor Displacement with Respect to Base and Base Shear-Bearing Displacement Loop in Case of Isolation System with Two Spring Units for Miyagiken-Oki Input (0.42g peak table acceleration). Compare with Figure 5-32	6-12

FIGURE	TITLE	PAGE
6-7	Analytical Time Histories of Base (Bearing) Displacement, Structure Shear and Sixth-Floor Displacement with Respect to Base and Base Shear-Bearing Displacement Loop in Case of Isolation System with Two Spring Units and for Hachinohe NS Input (0.22g peak table acceleration). Compare with Figure 5-35	6-13
6-8	Analytical Time Histories of Base (Bearing) Displacement, Structure Shear and Sixth-Floor Displacement with Respect to Base and Base Shear-Bearing Displacement Loop in Case of Isolation System without Spring Units for Miyagiken-Oki EW Input (0.43g peak ground acceleration). Compare with Figure 5-38	6-14
6-9	Analytical Time Histories of Base (Bearing) Displacement, Structure Shear and Sixth-Floor Displacement with Respect to Base and Base Shear-Bearing Displacement Loop in Case of Isolation System without Spring Units and for Hachinohe NS Input (0.21g peak table acceleration). Compare with Figure 5-39	6-15
6-10	Analytical Time Histories of Structure Shear and Sixth-Floor Displacement in Case of Isolation System with Four Spring Units and Pacoima S16E Input (0.84g peak table acceleration). The Rocking Motion of Table Has Been Accounted for. Compare with Figure 5-24	6-16

FIGURE	TITLE	PAGE
6-11	Comparison of Analytical and Experimental Base (Bearing) Displacement Histories in Case of System without Spring Units and Hachinohe NS Input (0.21g peak table acceleration). Observe Difference in Bearing Permanent Displacement When Accidential Bearing Inclination is not Accounted	6-17

LIST OF TABLES

TABLE	TITLE	PAGE
2-I	Characteristics of Structure Under Fixed Base Conditions (Value in Parenthesis is Analytical)	2-3
5-I	Summary of Experimental Results	5-2

SECTION 1
INTRODUCTION

Elastomeric isolation systems are becoming widely accepted and found application in several building and bridge structures in the United States, Japan, New Zealand and elsewhere (Buckle 1986, Kelly 1988). Elastomeric isolation systems are spring-like systems. They shift the fundamental frequency of the structure to values lower than the predominant earthquake frequencies. This effect, coupled with increased energy absorption capability, results in significant reductions of the earthquake forces imparted to the structural system above the isolation interface. This reduction of forces is associated with large displacements at the isolation system which must be accommodated by the elastomeric supports. Elastomeric isolation systems are sensitive to the frequency content of the earthquake excitation. In particular, these systems are not very effective in protecting structures against long period motions like the 1985 Mexico City earthquake. Isolation against this motion, which has a predominant frequency of less than 0.5 Hz, would require a much lower than 0.5 Hz isolation system frequency, which is impractical.

An alternative method of isolation is by sliding systems. A structure supported entirely by sliding bearings would be experiencing forces at the isolation interface that are always bounded by the mobilized frictional force, regardless of the level of ground acceleration or its frequency content. However, a freely sliding structure would also have large permanent displacements, particu-

larly when the sliding interface is not perfectly leveled. Control of these permanent displacements within acceptable limits is accomplished by the use of recentering devices.

Several sliding isolation systems with recentering devices have been proposed. The most notable of these systems are the Friction Pendulum System (Zayas et al, 1987, Mokha et al 1990a), the TASS system (Kawamura et al, 1988) and the R-FBI system (Mostaghel and Khodaverdian, 1987). These systems have been studied both analytically and experimentally. They all utilize sliding interfaces consisting of Teflon or Teflon based materials in contact with polished metals. Recentering capability is provided in the three systems by different means. In the Friction Pendulum System (FPS), the sliding interface takes a spherical shape so that restoring force is provided by the weight of the structure during rising along the spherical surface. In the TASS system, rubber springs are used in parallel with elastomeric-TFE sliding bearings. In the R-FBI system, bearings consisting of several Teflon-steel interfaces are fitted in the center with a rubber core which provides restoring force when deformed in shear. A 50,000 gallon water tank in California is isolated by FPS bearings and three structures in Japan are isolated by the TASS system. Furthermore, FPS bearings have been very recently used in the seismic retrofit a three-story apartment building in the San Francisco marina area.

Testing of sliding isolation systems has been limited to shake table tests of single-story models (Zayas et al, 1987, Kawamura et al, 1988). Shake table tests with multistory models have been

recently conducted by Chalhoub and Kelly, 1989 on a combined sliding-elastomeric bearing system and by Mokha et al, 1990a on the Friction Pendulum System. Both series of tests demonstrated the effectiveness of the tested systems in protecting the structure above. Bearing displacements in these systems were better controlled than the ones in purely elastomeric systems, however accelerations were higher. In both tested systems, the mobilized frictional forces were of the same order or less than the developed restoring forces in strong earthquake excitations. They could be classified as sliding isolation systems with strong restoring force and both showed a sensitivity to long period motions like the 1985 Mexico City earthquake. In the tests of the FPS system with the Mexico City motion, resonance effects were clearly evident, whereas in the tests of the combined sliding-elastomeric bearing system with the same motion, a displacement control device in the elastomeric bearings was activated and prevented the bearings from moving too far.

The tests reported in this report have been carried out with a novel sliding isolation system. The model structure, a quarter scale six-story steel frame, was entirely supported by sliding Teflon disc bearings (Mokha et al, 1988). Recentering capability was provided by helical steel springs which carried no vertical load and deformed in shear. Three groups of tests were conducted, one without the steel springs, and two with springs of different total stiffness. In all cases, the mobilized peak frictional forces

were larger, by at least a factor of two, than the developed peak restoring forces in the springs, resulting in systems with weak or no restoring force. The tests demonstrated the following:

1. The system was effective in protecting the structural system above against motions of significantly different frequency content.
2. In the three groups of tests, with and without restoring force devices, the peak model acceleration, peak interstory drift and peak base shear were practically the same for the same table input. The restoring force devices (helical springs) served only as displacement control devices.
3. The frequency content of the response of the model structure in the three groups of tests was practically unaffected by the stiffness of helical springs. This phenomenon further indicates that the springs were effective in only controlling the bearing displacement and that they did not contribute to the effectiveness of the isolation system by lengthening the period of the structural system.

SECTION 2
TEST STRUCTURE AND INSTRUMENTATION

Figure 2-1 shows the test structure. It represents a section in the weak direction of a typical steel moment-resisting frame at approximately quarter scale. Concrete blocks were used to add mass as necessary for similitude requirements, bringing the weight to 51.4 Kips (229.2 kN). The base of the model consisted of two heavy W14x90 sections. The isolation system, consisting of four sliding Teflon disc bearings and helical steel spring units, was placed between the base and the shake table. The distribution of weight with height was: 7.65 Kips (34.1 kN) at sixth floor, 7.84 Kips (34.9 kN) at floors fifth to first and 4.56 Kips (20.3 kN) at the base.

The natural frequencies, mode shapes and modal damping factors of the test structure in its fixed-base condition were determined in shake table tests using a banded 0-50 Hz white noise input and employing modal identification techniques. The first three natural frequencies were found to be 2.34 Hz, 7.76 Hz and 13.28 Hz. A detailed description of the properties of the test structure together with analytically determined modal properties has been presented by Mokha et al, 1990a. Table 2-I lists the experimentally determined frequencies, mode shapes and modal damping ratios of the test structure. Analytically determined quantities are listed in the same table in parenthesis. These quantities compare well with the experimental ones. It should be noted that the analytically

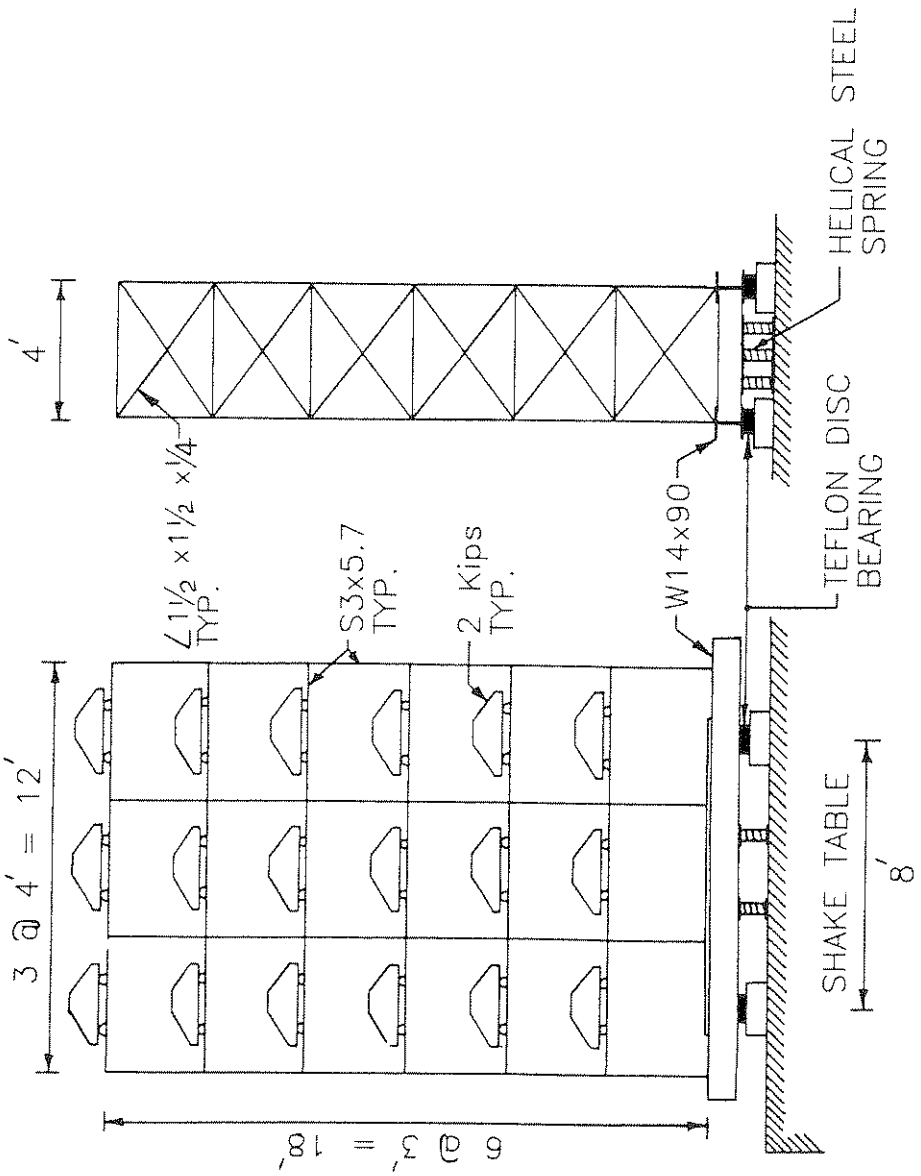

Fig. 2-1 - Six-Story Steel Test Structure (1ft = 304.8mm).

Table 2-I - Characteristics of Structure Under Fixed Base Conditions
(Value in Parenthesis is Analytical)

Mode (1)	Frequency Hz (2)	Damping Ratio (3)	Mode Shape (4)					
			Floor 1	Floor 2	Floor 3	Floor 4	Floor 5	Floor 6 (top)
1	2.34 (2.14)	0.0142	0.214 (0.164)	0.437 (0.395)	0.632 (0.611)	0.797 (0.791)	0.921 (0.923)	1 (1)
2	7.76 (7.72)	0.0204	0.563 (0.520)	1 (1)	0.900 (0.956)	0.326 (0.386)	-0.423 (-0.401)	-0.997 (-0.996)
3	13.28 (12.04)	0.0235	0.822 (0.804)	0.750 (0.863)	-0.248 (-0.230)	-1 (-1)	-0.435 (-0.383)	0.850 (0.817)
4	19.04 (17.98)	0.0155	1 (1)	-0.010 (0.104)	-0.827 (-0.996)	0.283 (0.240)	0.639 (0.908)	-0.461 (-0.619)
5	24.80 (24.02)	0.0059	0.739 (1)	-0.851 (-0.769)	0.229 (-0.027)	0.708 (0.805)	-1 (-0.946)	0.425 (0.397)
6	28.92 (28.82)	0.0086	0.515 (0.679)	-0.850 (-0.919)	1 (1)	-0.902 (-0.879)	0.605 (0.580)	-0.209 (-0.196)

determined frequencies are lower than the experimental ones, indicating that the model structure is actually stiffer than the theory predicted.

The instrumentation consisted of accelerometers and sonic displacement transducers which were placed at each floor to measure the horizontal acceleration of each floor and base in the longitudinal (testing direction) and transverse directions. Displacement transducers were placed only in the longitudinal direction and at both sides of the model in order to measure displacements of each floor and base with respect to a stationary frame as well as any torsional motion of the model. Furthermore, transducers were used to directly measure the displacement of the base with respect to the shake table. Accelerometers were also placed above each sliding bearing, to measure vertical acceleration and help determined whether the model uplifted from its supports. A total of 39 channels of data were recorded.

The instrumentation diagram of the test structure is shown in Figure 2-2. Only 30 channels are shown in Figure 2-2, the rest were used to monitor the motion of the shake table.

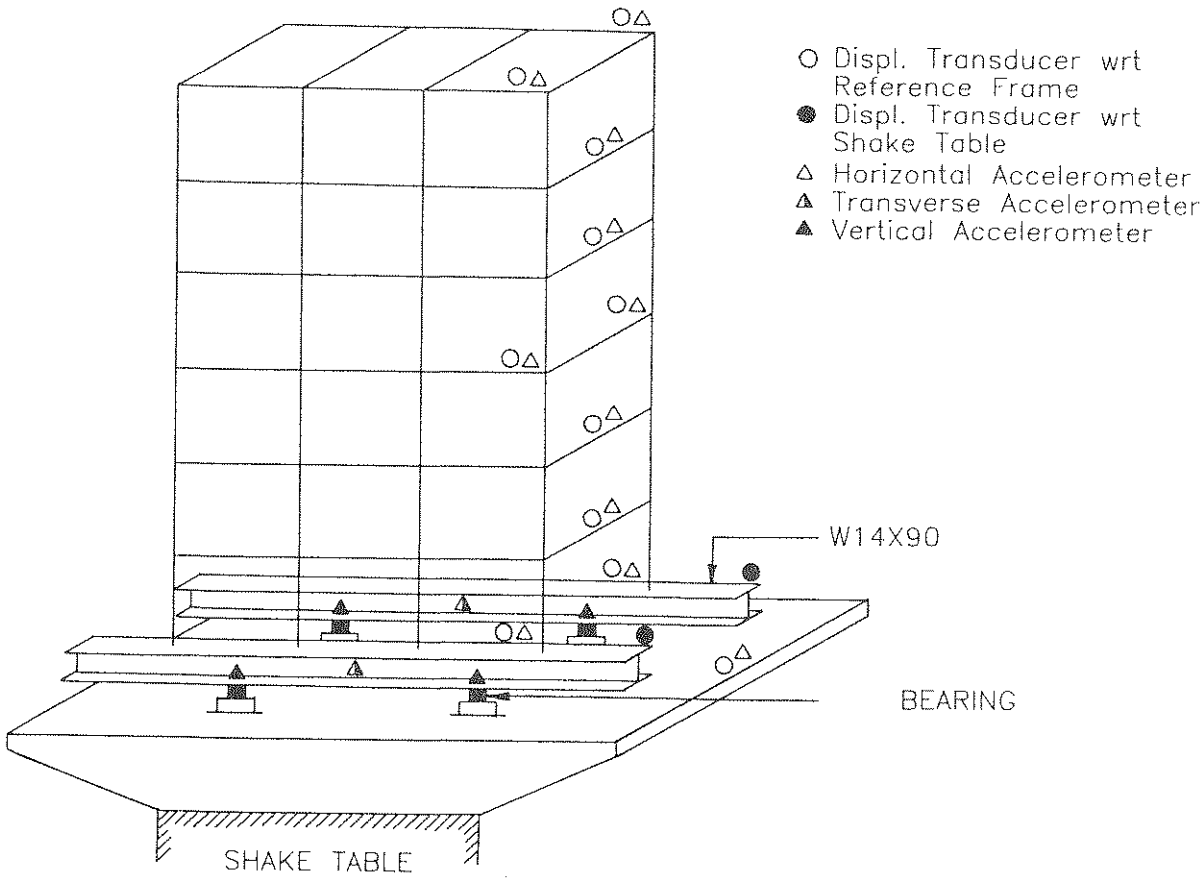

Fig. 2-2 - Instrumentation Diagram of Test Structure.

SECTION 3
ISOLATION SYSTEM

The isolation system consisted of four sliding Teflon disc bearings which were placed under the base at 8 feet (2.44m) distance as shown in Figure 2-1. The entire weight of the model was carried by these bearings. The ratio of height of model to distance between bearings was 2.25, indicating a slender configuration.

The Teflon disc bearing design is shown in Figure 3-1. The upper plate of the bearing is faced with a polished stainless steel plate which was commercially polished to degree No. 8. Measurements of the surface roughness in the testing direction gave a value of 1.6 μin (0.04 μm) in the arithmetic average scale (R_a). The bottom part of the bearing consists of a plate with a 3.7 in (94 mm) diameter unfilled Teflon sheet recessed on its top. The steel plate is supported by a high hardness Adiprene (Urethane rubber) disc. The disc is held by a shear restriction mechanism. The Adiprene disc allows some limited rotation of the plate above so that Teflon and stainless steel are in full contact. As designed the bearing could accommodate 4.4 in (111.8 mm) movement in all directions. However, in these tests, the bolts shown in Figure 3-1 were used as displacement limits so that the maximum displacement the bearing could accommodate was 2.8 in (71.1 mm).

Figure 3-2 shows a photograph of the Teflon disc bearing. The circular Teflon sheet, recessed in its backing plate and supported

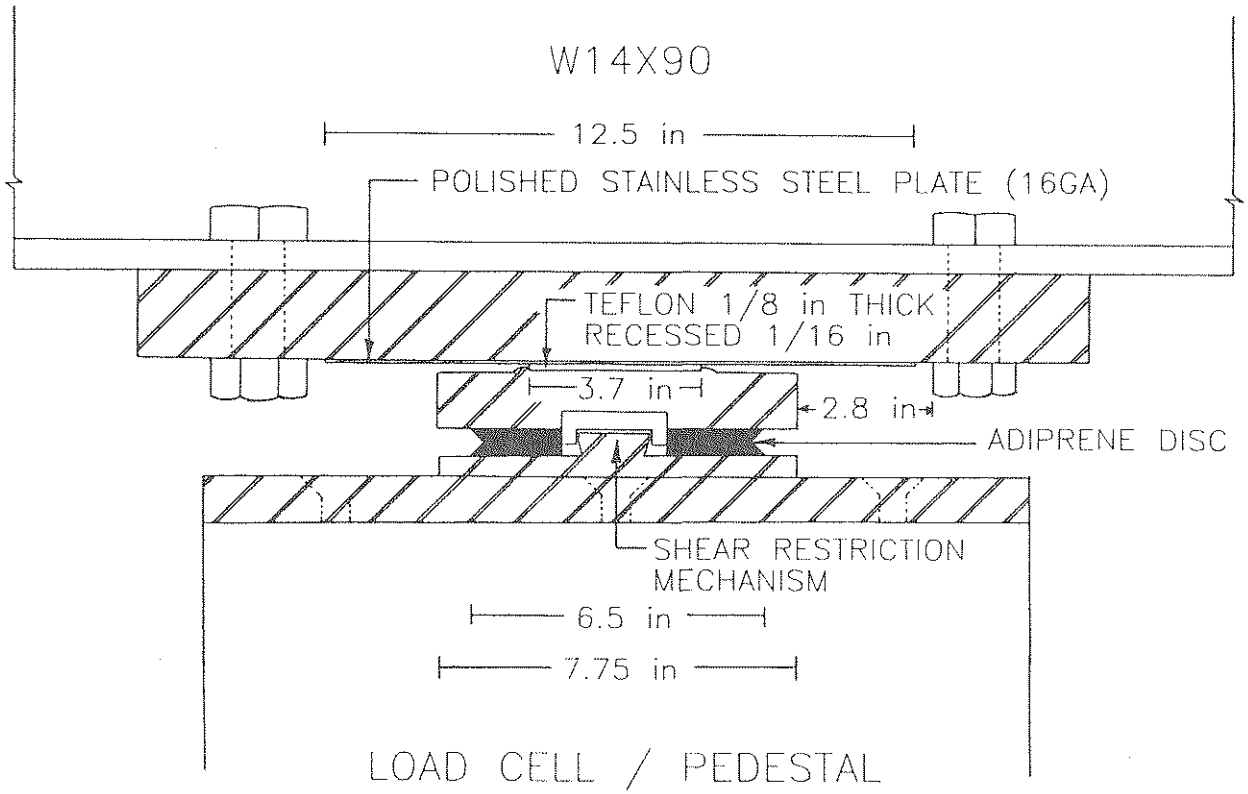

Fig. 3-1 - Teflon Disc Bearing Design (1 inch = 25.4mm).

Fig. 3-2 - Teflon Disc Bearing.

by the Adiprene disc and shear restriction mechanism, is reflected in the highly polished stainless steel plate of the top part of the bearing.

The bearings were placed on top of axial load cells which were raised with a system of leveling plates and bolts until all four bearings were subjected to the same load. In this position the load cells were bolted to the shake table, grouted and steel plates were welded all around, reducing them to simple pedestals as shown in Figures 2-1 and 3-1.

The top sliding plate of each bearing was leveled by the following procedure. A washer was placed between this plate and the W14x90 section above and the four connecting bolts were used to level the bearing within carpenter's accuracy. In this position, the plate was grouted. Measurements of the inclination of the plates revealed that on the average, the four sliding plates were inclined by 0.4 degrees in a single direction.

Restoring force capability was provided by helical steel spring units, each one of which consisted of three helical steel springs of 7.5 in (190.5 mm) free length, external diameter of 3.1 in (78.7 mm) and 0.512 in (13 mm) of wire diameter. The springs did not carry any axial load and they provided restoring force by deforming in shear. Figure 3-3 shows one spring unit under shear deformation of 1.8 in (45.7 mm).

The properties of the isolation system were determined by the following test. The base of the model was connected to a reaction frame by two stiff rods which were instrumented with load cells.

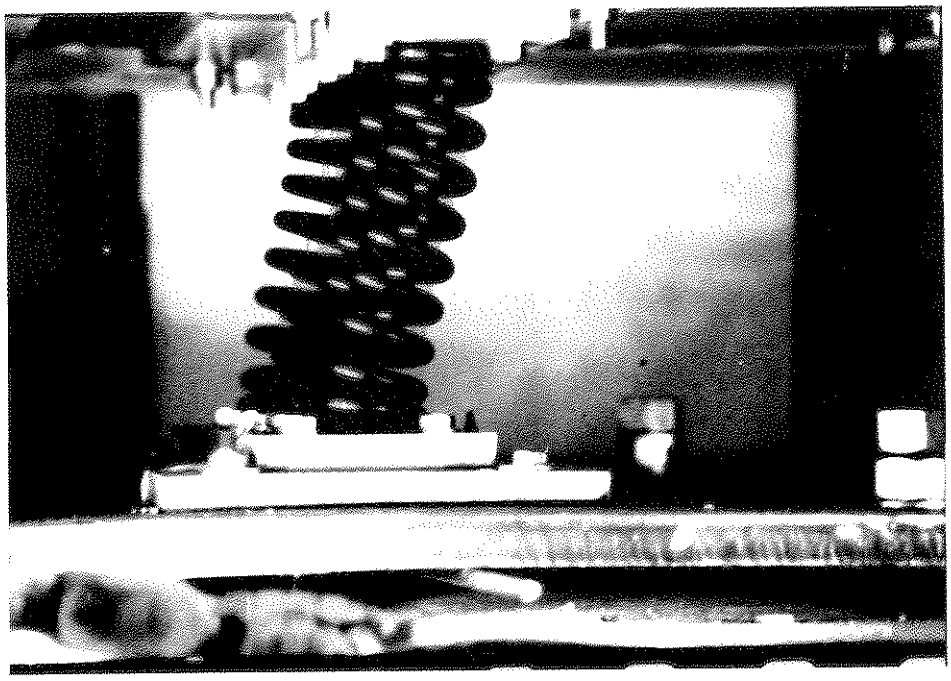

Fig. 3-3 - Helical Steel Spring Unit Under Deformation.

The shake table was driven in sinusoidal motion of specified frequency and displacement amplitude and measurements of the force transmitted through the isolation system to the motionless base were made. Figure 3-4a shows recorded force-displacement loops in two such tests in which the model was supported only by the sliding bearings and the table was driven at an amplitude of 1.75 in. The test at a frequency of 0.016 Hz was the first to be conducted and the effects of breakaway (or static) friction are evident. The value of sliding coefficient of friction was measured and found to vary between a value of 0.032 at very slow velocity of sliding and about 0.12 at high velocity of sliding. These values were consistent with previous tests by the authors under similar conditions (Mokha et al, 1988 and 1990b).

When all four spring units were added to the isolation system, the recorded loops exhibited the stiffness of the springs as shown in Figure 3-4b. Again in these tests the table was driven at an amplitude of 1.75 in. For a displacement of up to about 0.5 in (12.7 mm), the springs had a lower stiffness (a common characteristic of helical steel springs). For the four units the total initial stiffness was 1.54 Kip/in (0.27 kN/mm). Beyond this limit on displacement, the stiffness had a value of 2.68 Kip/in (0.47 kN/mm). The following quantity having dimensions of time is defined:

$$T_b = 2\pi\left(\frac{W}{gK_2}\right)^{1/2} \qquad (3.1)$$

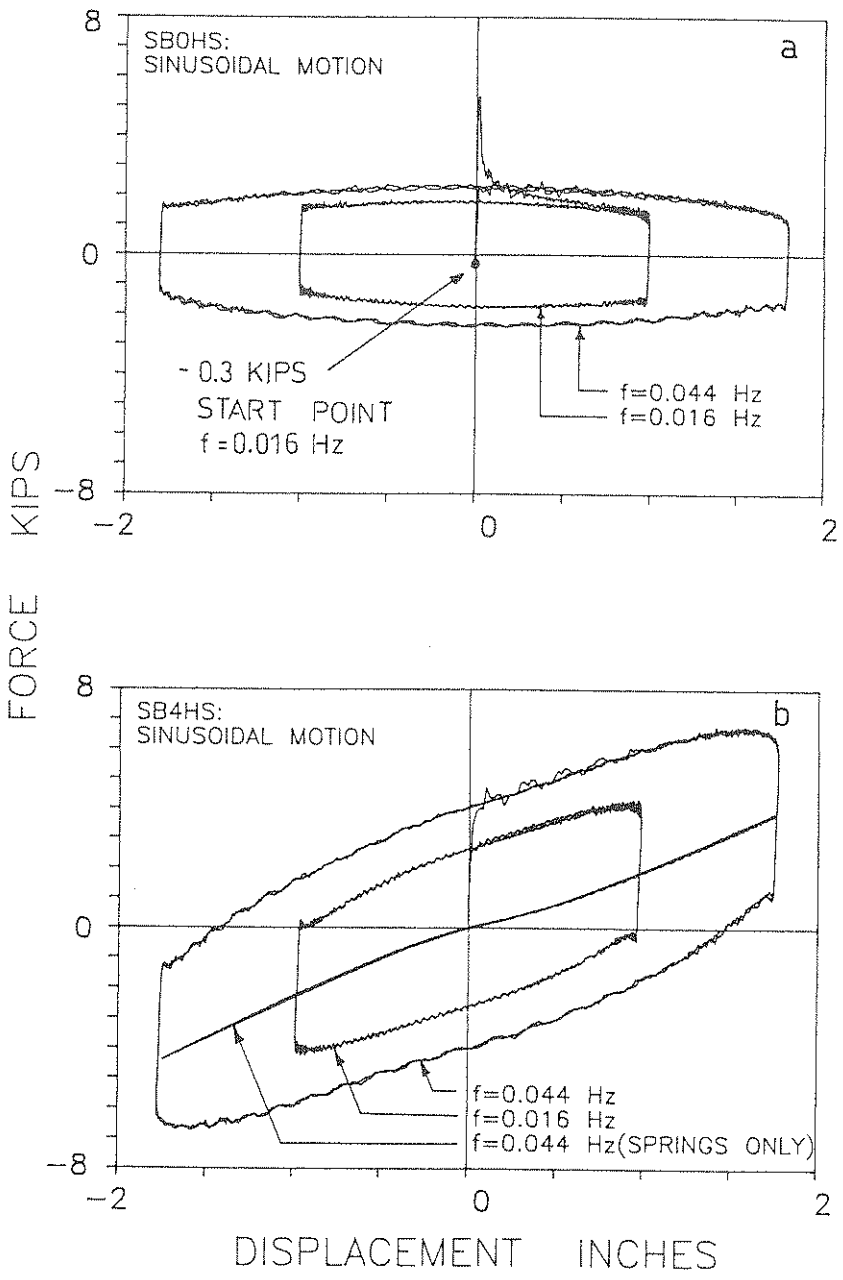

Fig. 3-4 - Force-Displacement Loops of Isolation System (a) Frictional Force, (b) Frictional and Restoring Force From Four Spring Units Combined (1 inch = 25.4mm, 1 Kip = 4.46kN).

where W is the weight of the structure and K_2 is the stiffness of the spring units beyond the limit of about 0.5 in (12.7 mm) on displacement. T_b represents the period of free vibration of the isolated structure when the superstructure is considered a rigid body and friction is disregarded. In the tested system, T_b takes the value of 1.4 sec. when all four spring units are used and the value of 1.98 sec. when two units are used. When the springs are removed, T_b becomes infinite.

An important observations to be made in the results of Figure 3-4 is that the coefficient of friction in Figure 3-4b is considerably larger than that in Figure 3-4a. The tests results shown in Figure 3-4b were conducted after completing several high velocity tests. This phenomenon prompted the authors to conduct a set of tests on Teflon-steel interfaces and study the effect of loading history on the frictional properties (Mokha et al, 1990c). It was found that friction of these interfaces increases when the interface is previously worn by a large number of high velocity cycles of motion. In the earthquake motion tests that followed, friction continued to rise so that its maximum value increased from about 0.12 in the first tests to about 0.19, where it became stable.

In general, it was found that the coefficient of sliding friction followed with good accuracy the following relationship which was proposed by Constantinou et al, 1990:

$$\mu(\dot{U}_b) = f_{max} - Df\exp(-\alpha|\dot{U}_b|) \qquad (3.2)$$

where $\dot{U}_b$ is the velocity at the sliding interface and f_{max} and (f_{max} - Df) are the maximum and minimum mobilized coefficients of friction, respectively. During the earthquake motion tests, the values of f_{max} and (f_{max} - Df) varied from 0.15 to 0.19 and from 0.06 to 0.10, respectively. Parameter a was approximately constant at a value of 0.55 sec/inch (21.6 sec/m).

Based on the above quoted values of the friction coefficient, the mobilized peak frictional force was 9.8 kips whereas the peak restoring force was 4.8 kips (configuration with four spring units at displacement of 2 in.). Accordingly, the ratio of peak frictional force to peak restoring force in the tested system was larger then two.

SECTION 4
TEST PROGRAM

The model structure was subjected to seven different earthquake signals on the shake table. The characteristics of these earthquake signals ranged from high frequency (Miyagiken - Oki) to predominantly low frequency motions (Hachinohe and Mexico City). The signals used are listed below:

1. Imperial Valley Earthquake (El Centro S00E) of May 18, 1940. Component S00E, peak ground acceleration (PGA) = 0.34g, predominant frequency range (PFR) = 1 - 4 Hz.
2. Kern County Earthquake (Taft N21E) of July 21, 1952. Component N21E, PGA = 0.16 g, PFR = 0.5 - 5 Hz.
3. San Fernando Earthquake (Pacoima S74W) of February 9, 1971. Component S74W. PGA = 1.08g, PFR = 0.25 - 2 Hz.
4. San Fernando Earthquake (Pacoima S16E) of February 9, 1971. Component S16E, PGA = 1.17 g, PFR = 0.25 - 6 Hz.
5. Miyagiken-Oki Earthquake (Miyagiken-Oki) of June 12, 1978 (Tohoku Univ., Sendai, Japan). Component EW, PGA = 0.16g, PFR = 0.5 - 5 Hz.
6. Tokachi-Oki Earthquake, Japan (Hachinohe) of May 16, 1968. Component NS, PGA = 0.23g, PFR = 0.25 - 1.5 Hz.
7. Mexico City Earthquake (Mexico City) of September 19, 1985 (SCT Building Station). Component N90W, PGA = 0.17g, PFR = 0.35 - 0.55 Hz.

Of these records, the last two are long period motions with Mexico City being almost a sinusoidal wave at frequency of 0.5 Hz. The records were time-compressed by a factor of two for similitude. Each earthquake signal was run at increasing levels of peak table acceleration until the peak interstory drift reached approximately the elastic limit of the test structure, which was determined to be about 0.2 inches (5.1 mm) or 0.0055 times the story height.

Furthermore, one test was conducted with sinusoidal table motion of 2.4 Hz frequency and large number of cycles. This test was conducted so that any deteriorating behavior of the isolation system is observed.

Figure 4-1 shows plots of time histories of some of the motions used in the testing program as recorded in tests of the isolation system with four spring units. These motions are shown in scaled time. The percentage figure shown in the caption of each plot applies to the acceleration of the actual record. For example, the figure 85% implies that the acceleration of the actual record has been multiplied by the factor 0.85, time-scaled and fitted through the shake table. Of interest to note is the high frequency tail of some of these records (El Centro, Taft and Miyagiken-Oki). This is evidence of table-structure interaction.

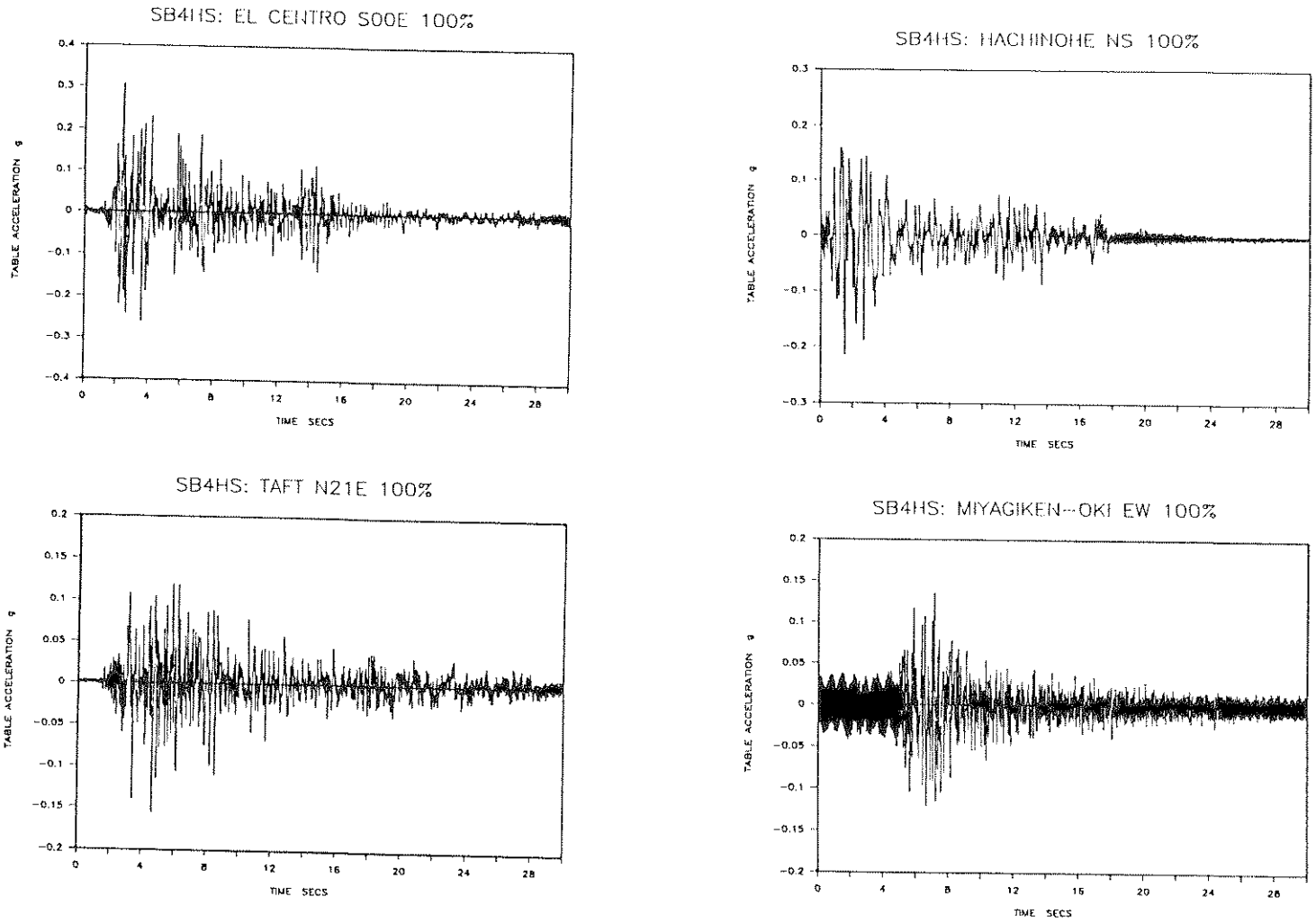

Fig.4-1 - Recorded Time Histories of Shake Table Acceleration. SB4HS Stands For Isolation System with Four Spring Units.

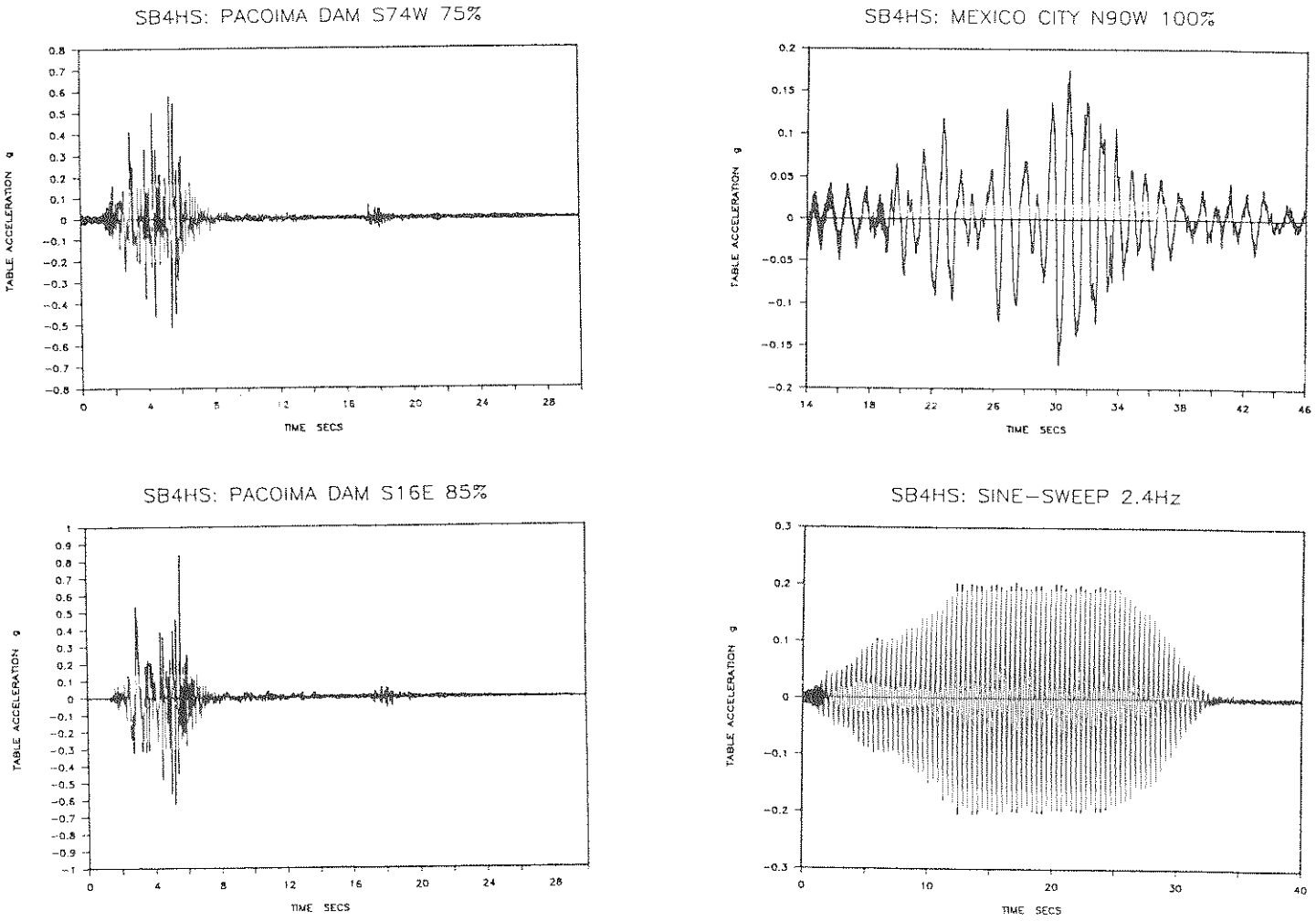

Fig. 4-1 - Continued.

SECTION 5
TEST RESULTS

Table 5-I lists the input signals in the test program, the isolation system condition, the peak table acceleration and the maximum response of the model in terms of base shear over weight (51.4 Kips) ratio, bearing displacement, peak model acceleration, peak interstory drift and permanent bearing displacement at the end of free vibration response. The base shear was computed from the floor and base acceleration records assuming that the mass of the model is concentrated at the level of the floor and base. Four isolation conditions are identified in Table 5-I. Fixed for fixed-base conditions and SB4HS, SB2HS and SBOHS for the sliding system with four, two and no helical spring units, respectively. The earthquake excitation in Table 5-I is presented with a percentage figure which applies to the peak ground acceleration of the actual record. For example, the case Taft N21E 300% corresponds to the actual Taft record with the peak acceleration increased approximately by a factor of three.

5.1 Effectiveness of System

The effectiveness of the isolation system in protecting the structure above is evident in a comparison of the test results with El Centro motion. Under fixed base conditions, the peak interstory drift reached a value close to the elastic limit at a peak table acceleration of 0.1g. In the isolated condition with four spring units (condition with T_b, Eq. (3.1), equal

Table 5-I - Summary of Experimental Results

Excitation (1)	Isolation Condition (2)	Pk. Table Accel. (g) (3)	Bearing Displ. (in) (4)	Base Shear*/ Weight (5)	Pk. Model Base Accel. (g) (6)	Pk. Model Floor Accel** (g) (7)	Pk. Model Inter-story Drift** (inch) (8)	Permanent Displ. (inch) (9)
El Centro S00E 30%	Fixed	0.10	--	0.255	--	0.47 (6)	0.171 (2)	--
El Centro S00E 100%	SB4HS	0.31	0.411	0.180	0.49	0.92 (6)	0.165 (3)	0.074
Hachinohe NS 100%	SB4HS	0.22	0.660	0.179	0.51	0.65 (6)	0.130 (3)	0.092
Hachinohe NS 150%	SB4HS	0.29	0.884	0.189	0.54	0.72 (6)	0.138 (3)	0
Taft N21E 100%	SB4HS	0.16	0.160	0.148	0.23	0.59 (6)	0.116 (3)	0.086
Taft N21E 300%	SB4HS	0.44	0.560	0.177	0.56	0.83 (6)	0.146 (3)	0
Miyagiken-Oki EW 100%	SB4HS	0.14	0.043	0.131	0.15	0.41 (6)	0.095 (2)	0.002
Miyagiken-OKI EW 300%	SB4HS	0.42	0.430	0.186	0.6	0.82 (3)	0.143 (3)	0.018
Pacoima S74W 50%	SB4HS	0.39	0.330	0.170	0.44	0.77 (6)	0.145 (3)	0.054
Pacoima S74W 75%	SB4HS	0.58	0.650	0.188	0.61	0.97 (6)	0.174 (3)	0.049
Pacoima S16E 50%	SB4HS	0.48	0.760	0.187	0.54	0.88 (6)	0.154 (2,3)	0.160
Pacoima S16E 75%	SB4HS	0.73	1.300	0.196	0.67	1.00 (6)	0.191 (3)	0.024
Pacoima S16E 85%	SB4HS	0.84	1.570	0.208	0.69	1.08 (1)	0.206 (3)	0
Mexico N90W 70%	SB4HS	0.13	0.220	0.146	0.19	0.26 (6)	0.105 (3)	0.120
Mexico N90W 85%	SB4HS	0.15	0.570	0.157	0.28	0.32 (6)	0.108 (3)	0.030
Mexico N90W 100%	SB4HS	0.18	0.910	0.178	0.35	0.38 (6)	0.124 (2)	0.050

Table 5-I (Continued) - Summary of Experimental Results

Excitation (1)	Isolation Condition (2)	Pk. Table Accel. (g) (3)	Bearing Displ. (in) (4)	Base Shear*/ Weight (5)	Pk. Model Base Accel. (g) (6)	Pk. Model Floor Accel** (g) (7)	Pk. Model Inter-story Drift** (inch) (8)	Permanent Displ. (inch) (9)
Mexico N90W 120%	SB4HS	0.21	2.120	0.223	0.42	0.51 (6)	0.149 (2)	0.010
Sinusoidal 2.4Hz	SB4HS	0.20	0.290	0.156	0.34	0.68 (6)	0.120 (3)	0
Mexico N90W 120%	SB2HS	0.21	2.050	0.186	0.43	0.43 (6)	0.141 (3)	0.770
El Centro S00E 100%	SB2HS	0.28	0.900	0.178	0.54	0.90 (6)	0.164 (4)	0.620
Miyagiken-Oki EW 100%	SB2HS	0.13	0.080	0.134	0.14	0.39 (6)	0.097 (3)	0.070
Miyagiken-Oki EW 300%	SB2HS	0.42	0.900	0.176	0.59	0.88 (3)	0.149 (3)	0.690
Pacoima S16E 50%	SB2HS	0.46	0.930	0.189	0.57	0.89 (6)	0.159 (3)	0.660
Pacoima S74W 50%	SB2HS	0.38	0.520	0.174	0.45	0.83 (6)	0.159 (3)	0.320
Hachinohe NS 100%	SB2HS	0.22	1.280	0.183	0.57	0.67 (6)	0.138 (3)	0.670
Miyagiken-Oki EW 100%	SB0HS	0.14	0.063	0.135	0.13	0.38 (6)	0.096 (3)	0.040
Miyagiken-Oki EW 200%	SB0HS	0.28	0.700	0.163	0.39	0.63 (6)	0.131 (3)	0.700
Miyagiken-Oki EW 300%	SB0HS	0.43	1.350	0.176	0.61	0.86 (3)	0.149 (2)	1.350
Hachinohe NS 100%	SB0HS	0.21	2.080	0.188	0.46	0.63 (6)	0.141 (3)	2.080

*Shear at bearing level, 1 inch = 25.4 mm
**Quantity in parenthesis is story or floor at which maximum was recorded.

to 1.4 secs), a lower value on the peak drift was obtained at a peak table acceleration of 0.31g. Accordingly, the capacity of the frame to withstand this motion while remaining undamaged has been increased in the isolated condition by a factor of at least three in comparison to the fixed-base condition.

Bearing displacements in the case of the system with four spring units are small and in general about half of those measured in tests with elastomeric isolation systems and similar size and scale models (Griffith et al, 1988). However, recorded peak model accelerations are considerably larger than in the previously mentioned tests of elastomeric isolation systems, and in general are larger than the peak table acceleration.

It has been common to determine the effectiveness of elastomeric isolation systems by the degree to which the table acceleration has been reduced in the structure above (e.g. Griffith et al, 1988). This measure of effectiveness is, of course, valid only in systems in which all stories move in phase. In such cases, accelerations and inertia forces point to the same direction and, unless they are low, they may lead to large story shear, overturning moment and drift. However, when out of phase response prevails, the inertia forces may be large but they point in opposing directions, leading to reduce story shear, overturning moment and drift. This kind of behavior dominates the response of sliding systems. It has been previously observed by the authors in tests of the Friction Pendulum System (Mokha et al, 1990a) and in the tests described in this report.

Evidence for this behavior is provided in Figure 5-1 which shows profiles of acceleration (solid line) and displacement (dashed line) of the tested frame at times at which the indicated peak responses were recorded. Excitation is the Pacoima record, component S16E scaled to peak acceleration of 0.84g. The isolation system was with four spring units. The peak bearing displacement, peak interstory drift, peak overturning moment and base shear occur when model accelerations are less than 0.6g, thus less than the peak table acceleration. The peak model acceleration of 1.08g occurs at a much later time, at the first floor and while all other floor accelerations are less than 0.6g and in opposing directions. Clearly, the response is out of phase with dominant higher mode participation.

Figure 5-2 shows profiles of acceleration and displacement of the same system, but for the El Centro input, scaled to peak acceleration of 0.31g. Again the acceleration response is out of phase. The peak model acceleration occurs at the sixth floor and is equal to 0.92g, almost three times the table acceleration. However, the peak interstory drift occurs at a different time, when the peak model acceleration is 0.47g (1.5 times the table acceleration) and when the response is dominated by higher mode participation. Interstory drift and not the peak model acceleration represents in this case a useful measure of stress and deformation levels in the structures.

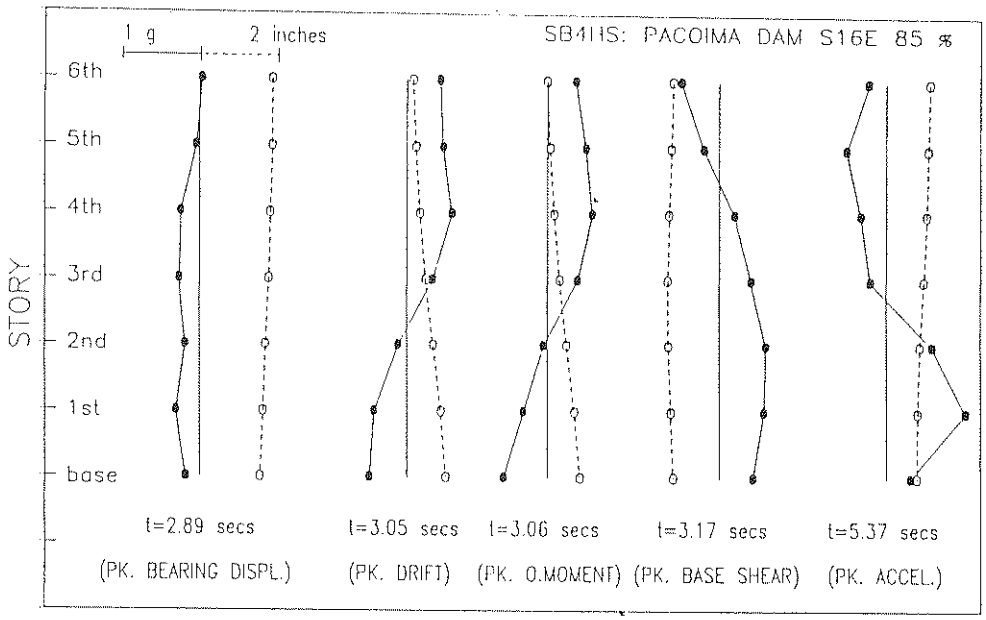

Fig. 5-1 - Profiles of Floor Acceleration (Solid Line) and Displacement (Dashed Line) of Test Structure in Isolation System with Four Spring Units and Pacoima S16E Input (0.84g peak table acceleration).

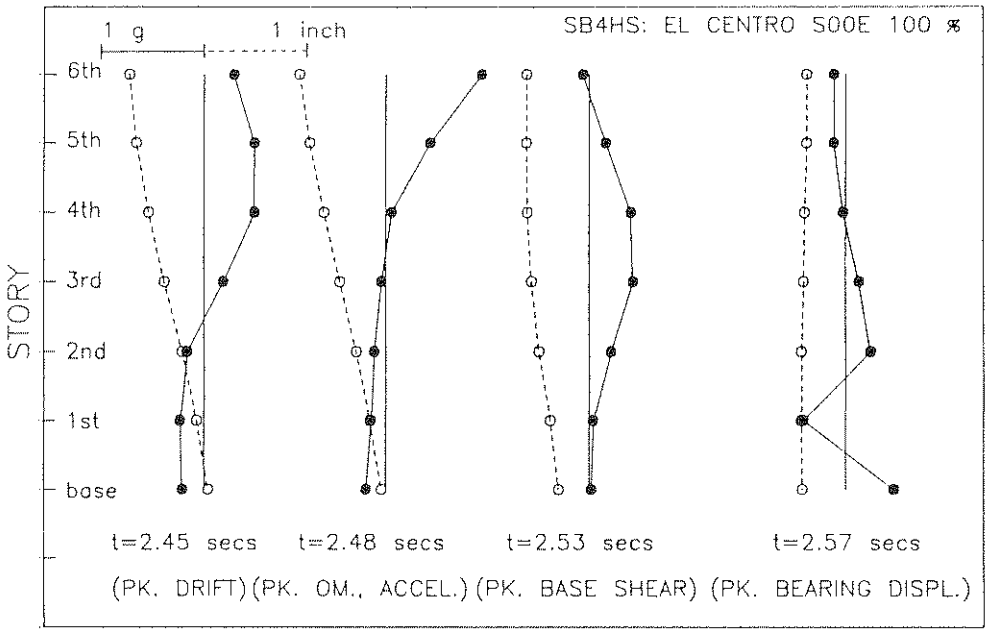

Fig. 5-2 - Profiles of Floor Acceleration (Solid Line) and Displacement (Dashed Line) of Test Structure in Isolation System with Four Spring Units and El Centro S00E Input (0.31g peak table acceleration).

A somewhat different picture develops in the long period motions. Figures 5-3 and 5-4 show profiles of acceleration and displacement of the same system when excited by the Hachinohe NS (0.22g) and Mexico City (0.18g peak table acceleration) motions. The higher mode participation in the response is not as dominant as in the other motions. However, at the time at which the peak interstory drift occurs the model accelerations are lower than the peak value shown in Table 5-I.

Similar behavior is observed in the tests with two and no spring units as shown in Figures 5-5 through 5-8, respectively.

Concluding, we note that the accelerations in the model structure are large and in general larger than the peak table acceleration. However, the response is out of phase with dominant higher mode participation. The floor inertia forces, while large, point to opposing directions leading to reduced interstory drift, overturning moment and shear.

5.2 Effect of Restoring Force

The helical spring units were designed to provide weak restoring force with the specific purpose of controlling the bearing displacement and not for shifting the fundamental frequency of the system to low values.

Tests with four spring units (T_b = 1.4 secs), two spring units (T_b = 1.98 secs) and no spring units ($T \sim \infty$) were conducted with the Japanese Miyagiken-Oki (two tests) and Hachinohe (one

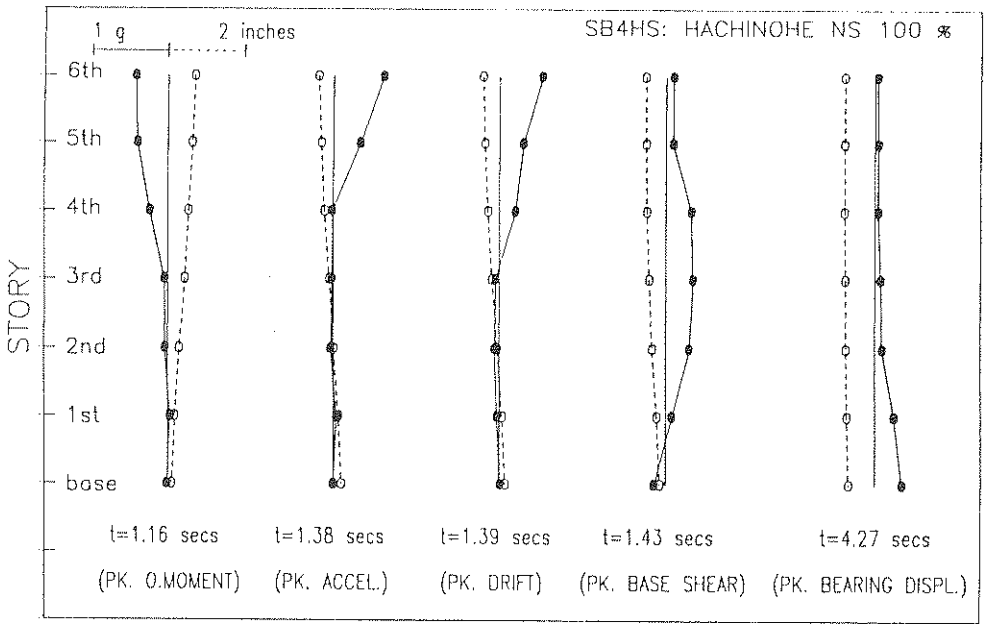

Fig. 5-3 - Profiles of Floor Acceleration (Solid Line) and Displacement (Dashed Line) of Test Structure in Isolation System with Four Spring Units and Hachinohe NS Input (0.22g peak table acceleration).

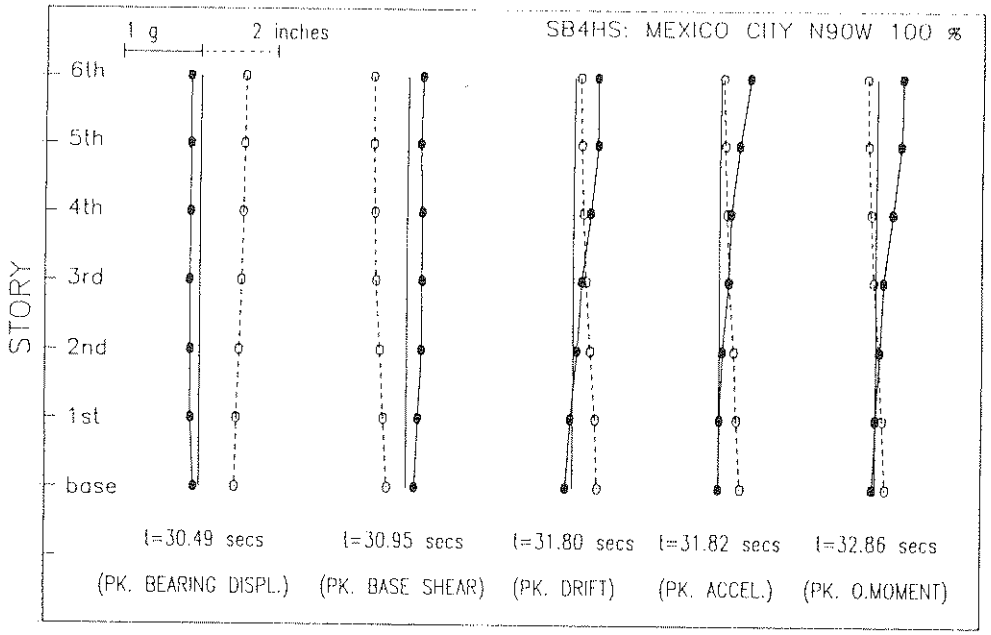

Fig. 5-4 - Profiles of Floor Acceleration (Solid Line) and Displacement (Dashed Line) of Test Structure in Isolation System with Four Spring Units and Mexico City N90W Input (0.18g peak table acceleration).

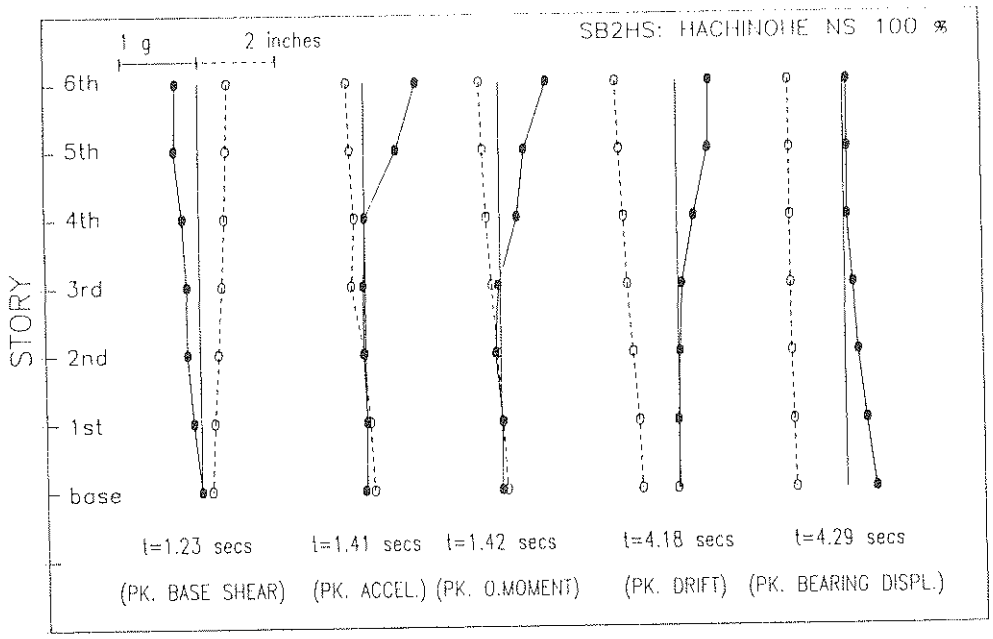

Fig. 5-5 - Profiles of Floor Acceleration (Solid Line) and Displacement (Dashed Line) of Test Structure in Isolation System with Two Spring Units and Hachinohe NS Input (0.22g peak table acceleration).

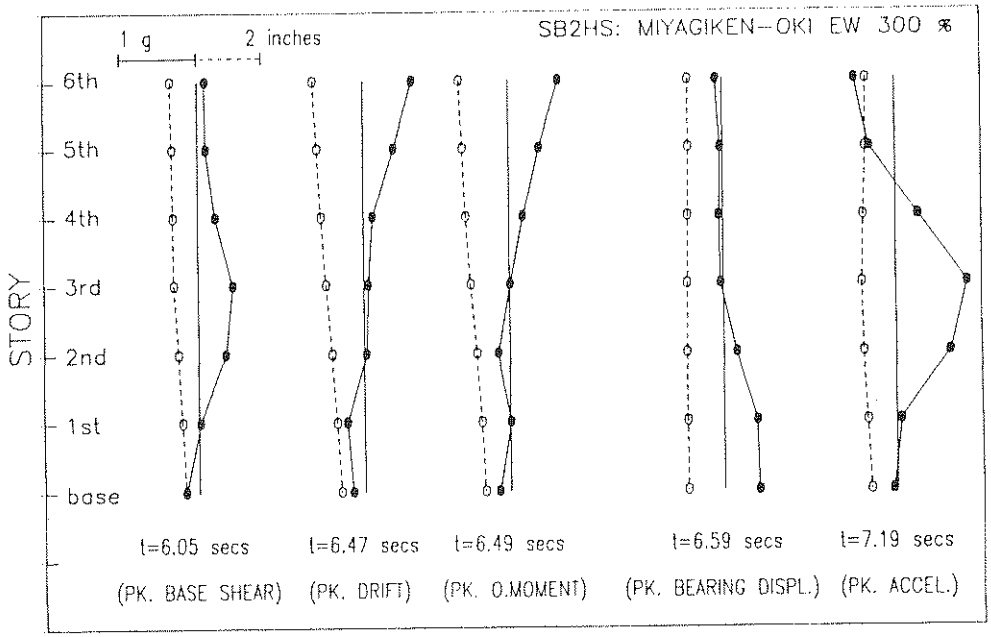

Fig. 5-6 - Profiles of Floor Acceleration (Solid Line) and Displacement (Dashed Line) of Test Structure in Isolation System with Two Spring Units and Miyagiken-Oki EW Input (0.42g peak table acceleration).

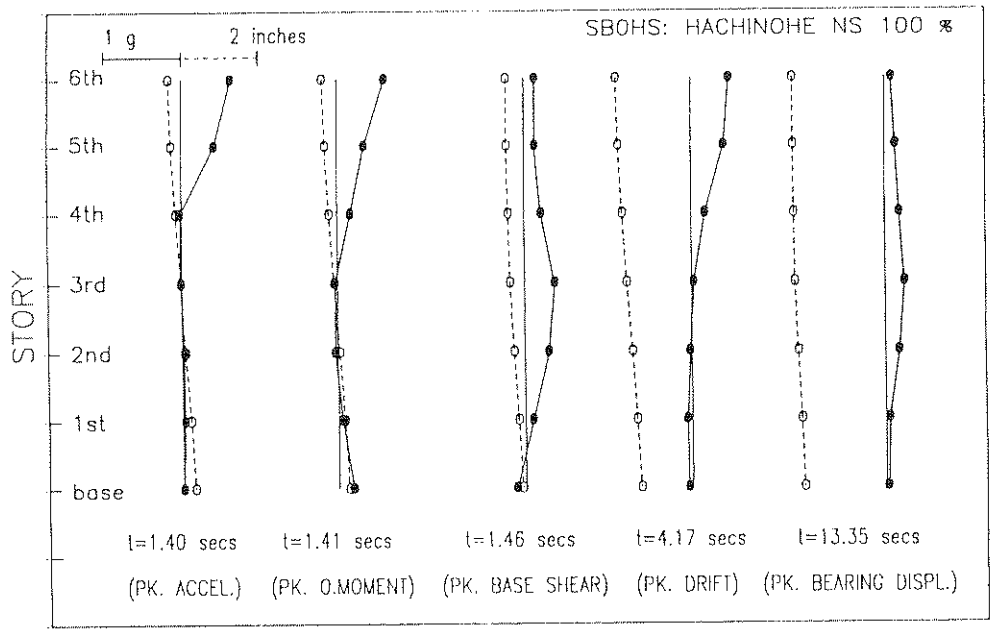

Fig. 5-7 - Profiles of Floor Acceleration (Solid Line) and Displacement (Dashed Line) of Test Structure in Isolation System Without Spring Units and Hachinohe NS Input (0.21g peak table acceleration).

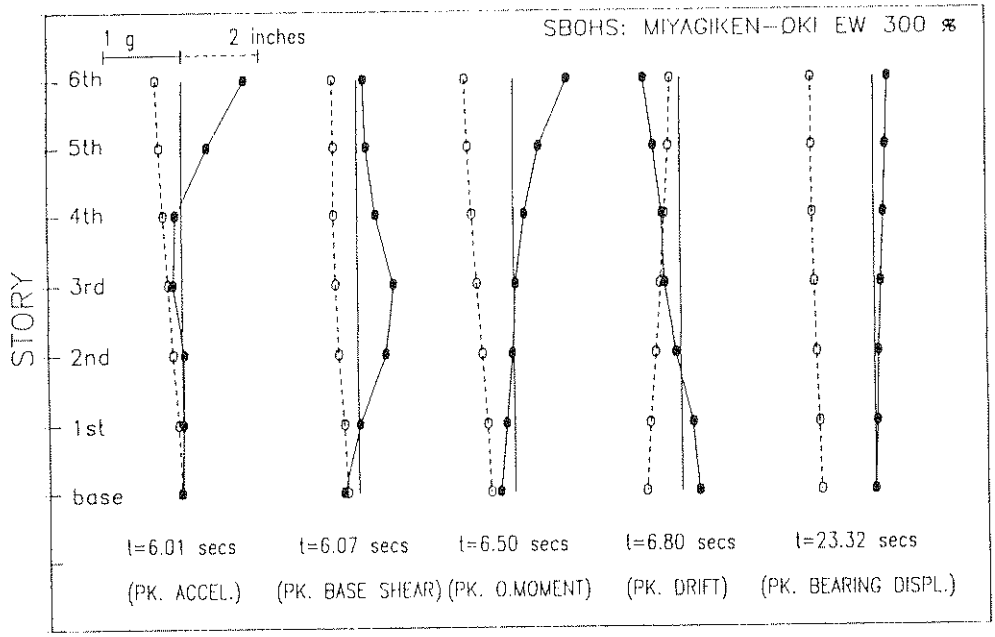

Fig. 5-8 - Profiles of Floor Acceleration (Solid Line) and Displacement (Dashed Line) of Test Structure in Isolation System Without Spring Units and Miyagiken-Oki EW Input (0.43g peak table acceleration).

test) records. The first is a high frequency motion, whereas the second is a low frequency motion. The results of Table 5-I clearly indicate that the response of the test structure in terms of peak base shear, peak model acceleration and peak interstory drift was practically unaffected by the stiffness of the spring units. The results show that the springs were effective only in limiting the bearing displacement. In particular, the configuration with four spring units resulted in very low permanent displacements which, in general, were less than six percent of the bearing design displacement (2.8 in or 71.1 mm). On the other hand, the configurations with two and no spring units resulted in excessive permanent displacements.

This interesting behavior is vividly illustrated in Figures 5-9 and 5-10 which show recorded peak responses as function of parameter T_b (Eq. (3-1)) for the Hachinohe input (peak table acceleration of 0.22g) and the Miyagiken-Oki input (peak table acceleration of 0.42g).

It should be noted that the large permanent bearing displacements in the system without spring units have been primarily a result of the accidental inclination of the sliding interface in a single direction, which was determined to be about 0.4 degrees. This in effect increases the coefficient of friction in one direction and decreases it in the opposite direction. This difference may appear to be small but is very important and analytical evidence for this will be provided later in this report.

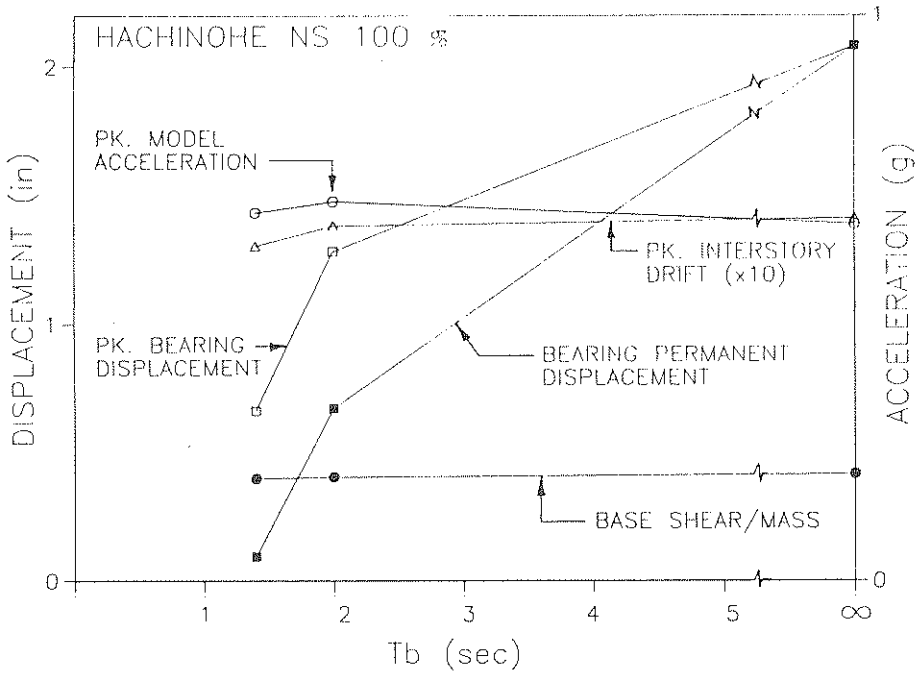

Fig. 5-9 - Peak Response of the Test Structure as Function of Isolation System Period (T_b) in Case of Hachinohe NS Input (0.22g Peak Table Acceleration).

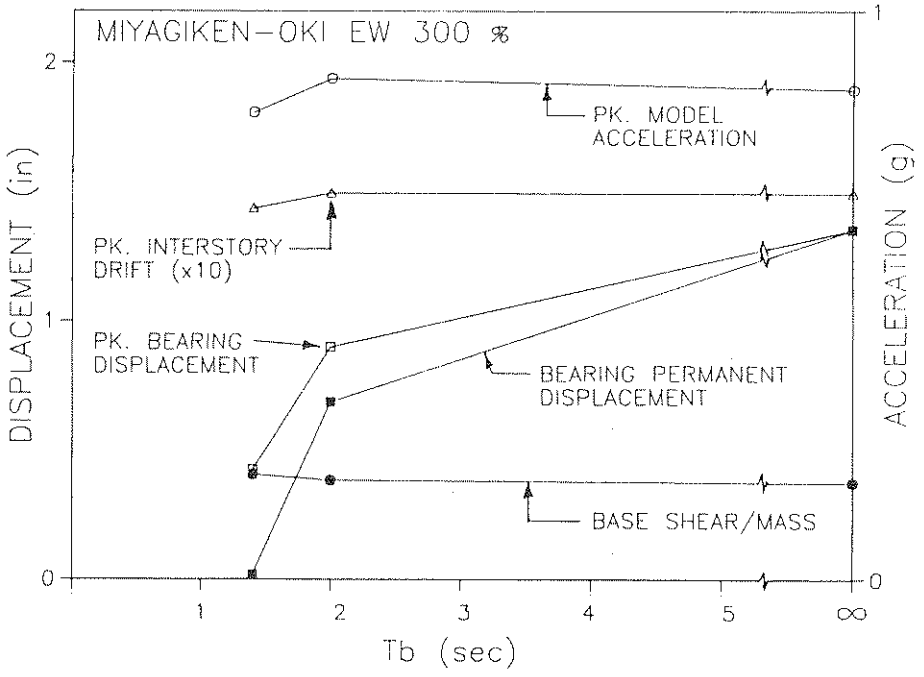

Fig. 5-10 - Peak Response of the Test Structure as Function of Isolation System Period (T_b) in Case of Miyagiken-Oki EW Input (0.42g peak table acceleration).

The stiffness of the restoring force devices had also an insignificant effect on the frequency content of the response of the tested structure. Evidence for this is provided in Figure 5-11 which shows Fourier amplitude spectra of the recorded sixth floor acceleration of the test structure. The dashed line corresponds to the Fourier spectra of the fixed base structure when excited by the scaled-down El Centro 1940 motion. The distinct peaks at 2.34 and 7.76 Hz correspond to the first two frequencies of the superstructure. The solid line corresponds to Fourier spectra of the isolated model with four, two and no spring units and for the Hachinohe input. The three spectra are almost identical and exhibit distinct peaks at the fundamental frequencies of the superstructure. As intended in the design, the spring units did not shift the frequencies of the test structure to lower values.

The results indicate that restoring force devices in sliding isolation systems are important in controlling bearing displacements within acceptable limits. The stiffness of these devices should be selected so that permanent displacements are small. Designing for lower than necessary stiffness does not increase the degree of isolation.

5.3 System Adequacy

An adequate isolation system should not deteriorate when subjected to a large number of cycles of loading. In one test in the configuration with four spring units, the shake table was

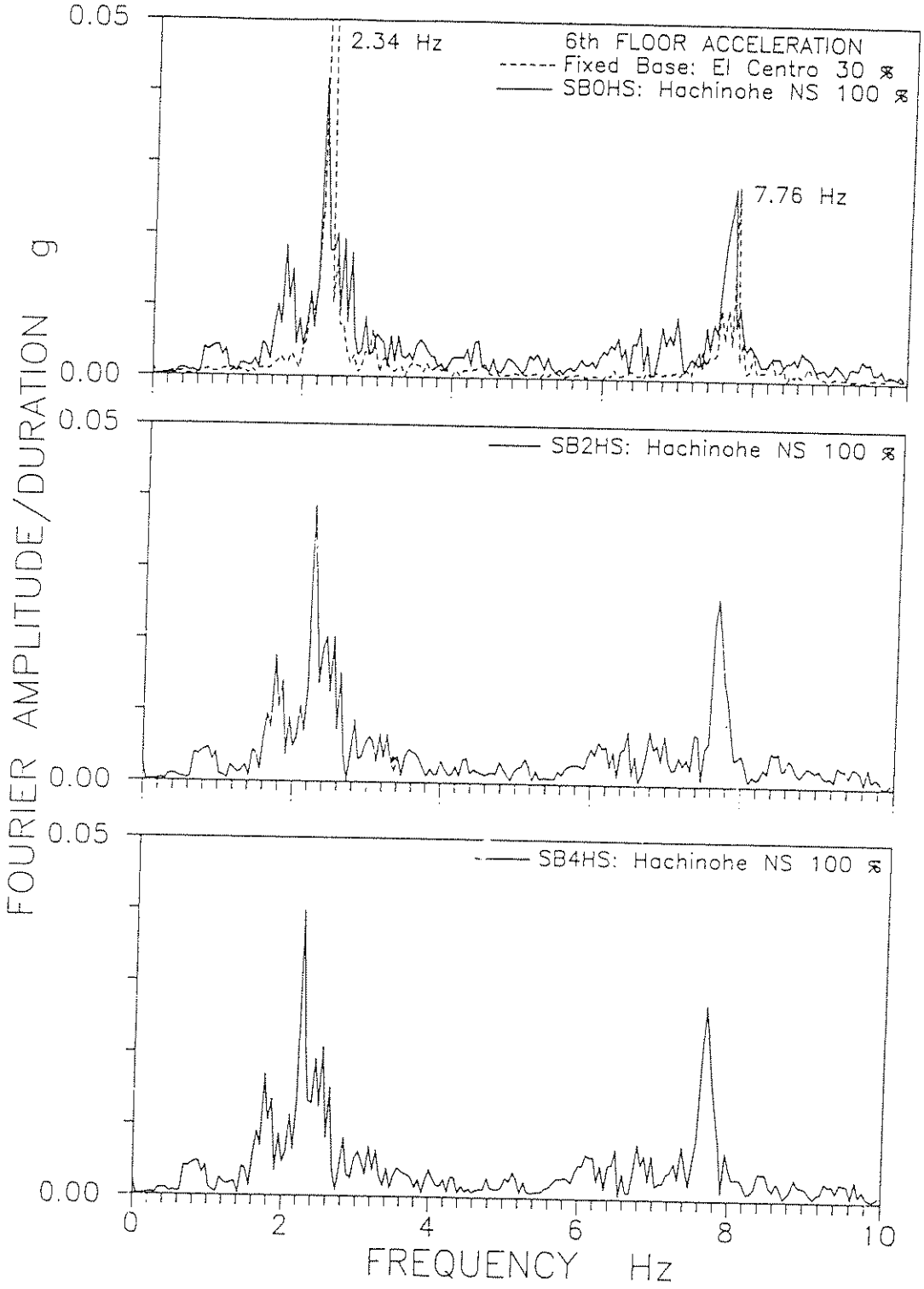

Fig. 5-11 - Fourier Amplitude Spectra of Sixth-Floor Acceleration of Structure for Fixed-Based Conditions and Isolation Conditions with Four (SB4HS), Two (SB2HS) and Without (SB0HS) Spring Units. Observe that Frequency Content is not Affected by Stiffness of Spring Units.

driven at a frequency of 2.4 Hz and amplitude was varied until the table acceleration reached a value of 0.2g. At least forty cycles of motion were completed with bearing displacement exceeding 0.2 in (5 mm) and peak sliding velocity between 3 and 4 in/sec (75 to 100 mm/sec). The recorded base (bearing) displacement history and the base shear - displacement loops with displacement larger than 0.2 in are shown in Figure 5-12. The isolation system showed very stable characteristics without any degradation under repeated cyclic loading.

5.4 Features of Response

The recorded response of the isolated model structure is presented in Figures 5-13 through 5-39 in terms of time histories of base (bearing) displacement, structural shear over weight (51.4 Kips) ratio (structural shear is shear at first story) and sixth floor displacement with respect to base and base shear (at bearing level) over weight ratio versus bearing displacement loops. Figures 5-13 through 5-28 present results for the system with four spring units (SB4HS), Figures 5-29 through 5-35 present results for the system with two spring units (SB2HS) and Figures 5-36 through 5-39 present results for the system without spring (SBOHS).

Note the following in these figures:

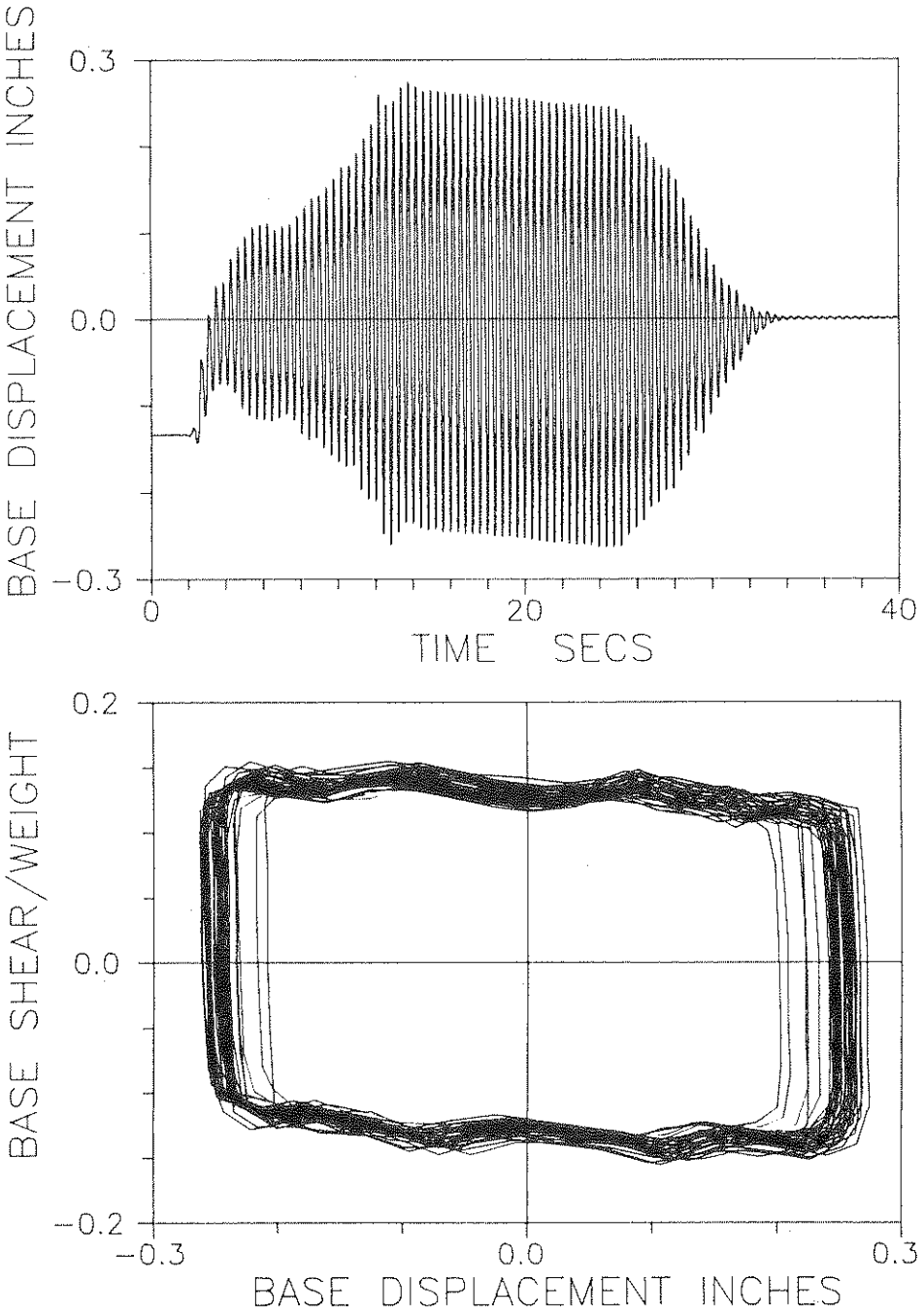

Fig. 5-12 - Bearing Displacement History and Base Shear-Displacement Loop of Isolation System with Four Spring Units for Harmonic Input of 2.4 Hz Frequency. Forty Cycles Completed Without Degradation (1 in = 25.4mm).

1. The time histories of structural shear and sixth floor displacement are almost identical in the three groups of tests with and without spring units. Of course, this should be expected as the springs were weak and did not alter the frequency characteristics of the system.
2. The bearing displacement histories in the three groups of tests exhibit very similar characteristics except for the drift in a preferred direction in the systems with two and no spring units. This is a result of the accidental average inclination of the bearings in that direction.
3. The tail of the time histories of structural shear and sixth floor displacement shows a peculiar behavior (large values, and is some cases, beat phenomena) which appears to be inconsistent with the corresponding table translational input (see Figure 4-1) and bearing displacement history. This behavior could be explained when one considers rocking motion of the table. Unfortunately, the rocking motion of table was not monitored in the tests. Rather, the vertical acceleration just above each sliding bearing was measured (see Figure 2-2 for instrumentation diagram). These records were used to obtain approximations to the rocking motion of the table. Indeed, this motion was sizable and responsible for the observed behavior. More details will be provided later in this report when the analytical prediction of the response is discussed.

Finally, we note that during the entire testing program no uplift occurred at the bearings and no torsional motion was detected.

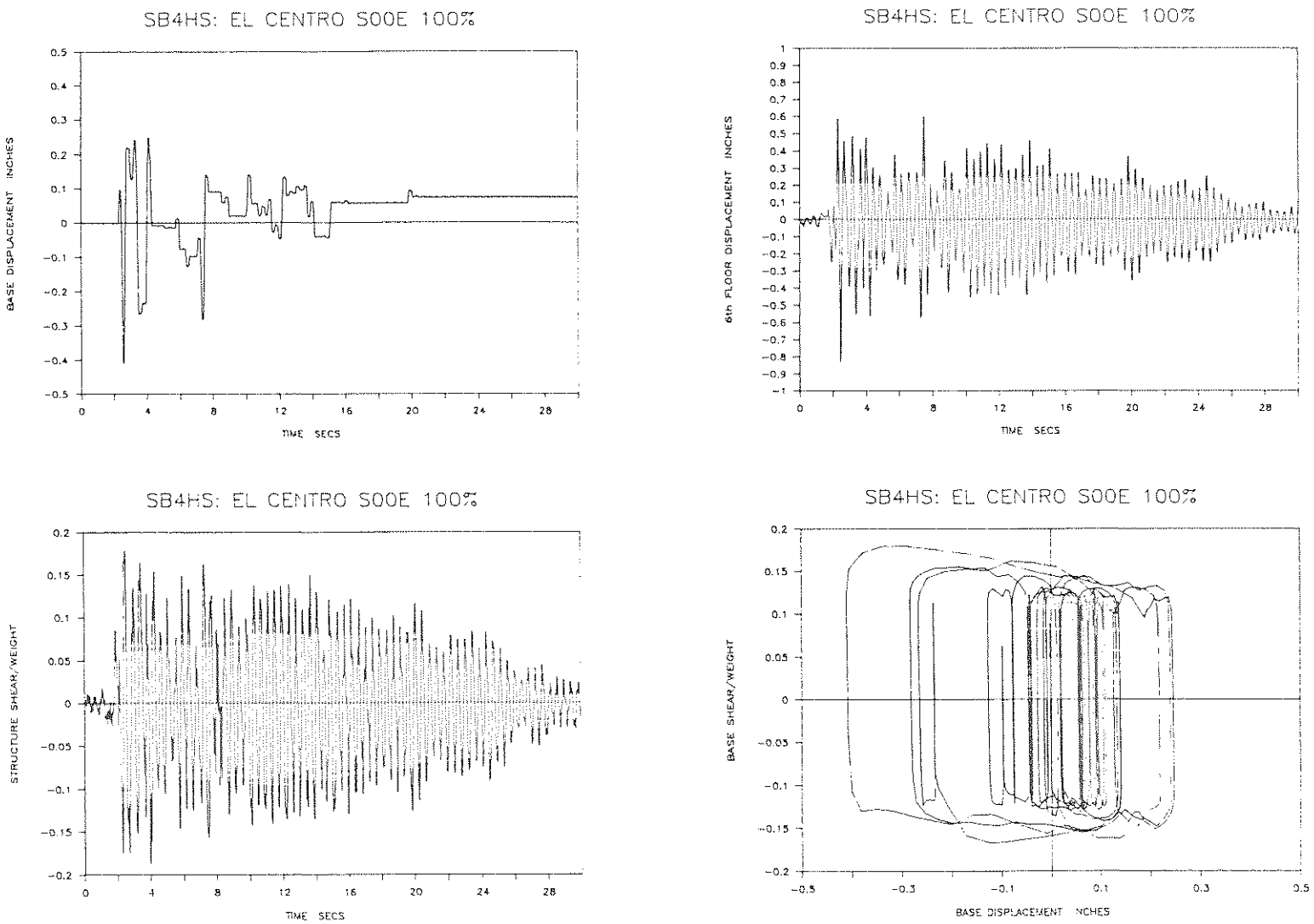

Fig. 5-13 - Experimental Time Histories of Base (Bearing) Displacement, Structure Shear and Sixth Floor Displacement with Respect to Base and Base Shear-Bearing Displacement Loop in Case of Isolation System with Four Spring Units and for El Centro Input (0.31g peak table acceleration). Structure Shear is Shear at First Story. Base Shear is Shear at Bearing Level.

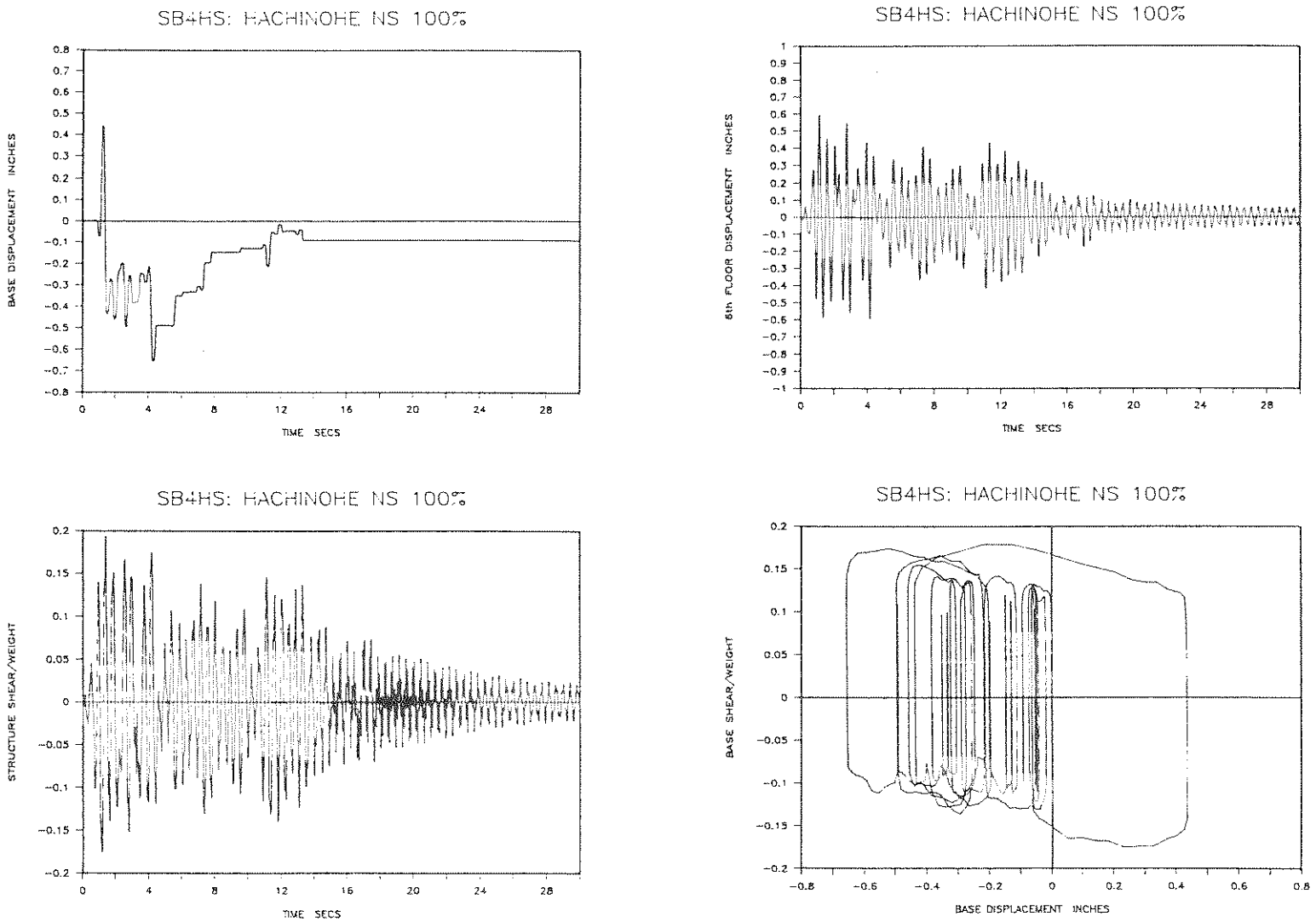

Fig. 5-14 - Experimental Time Histories of Base (Bearing) Displacement, Structure Shear and Sixth-Floor Displacement with Respect to Base and Base Shear-Bearing Displacement Loop in Case of Isolation System with Four Spring Units and for Hachinohe NS Input (0.22g peak table acceleration).

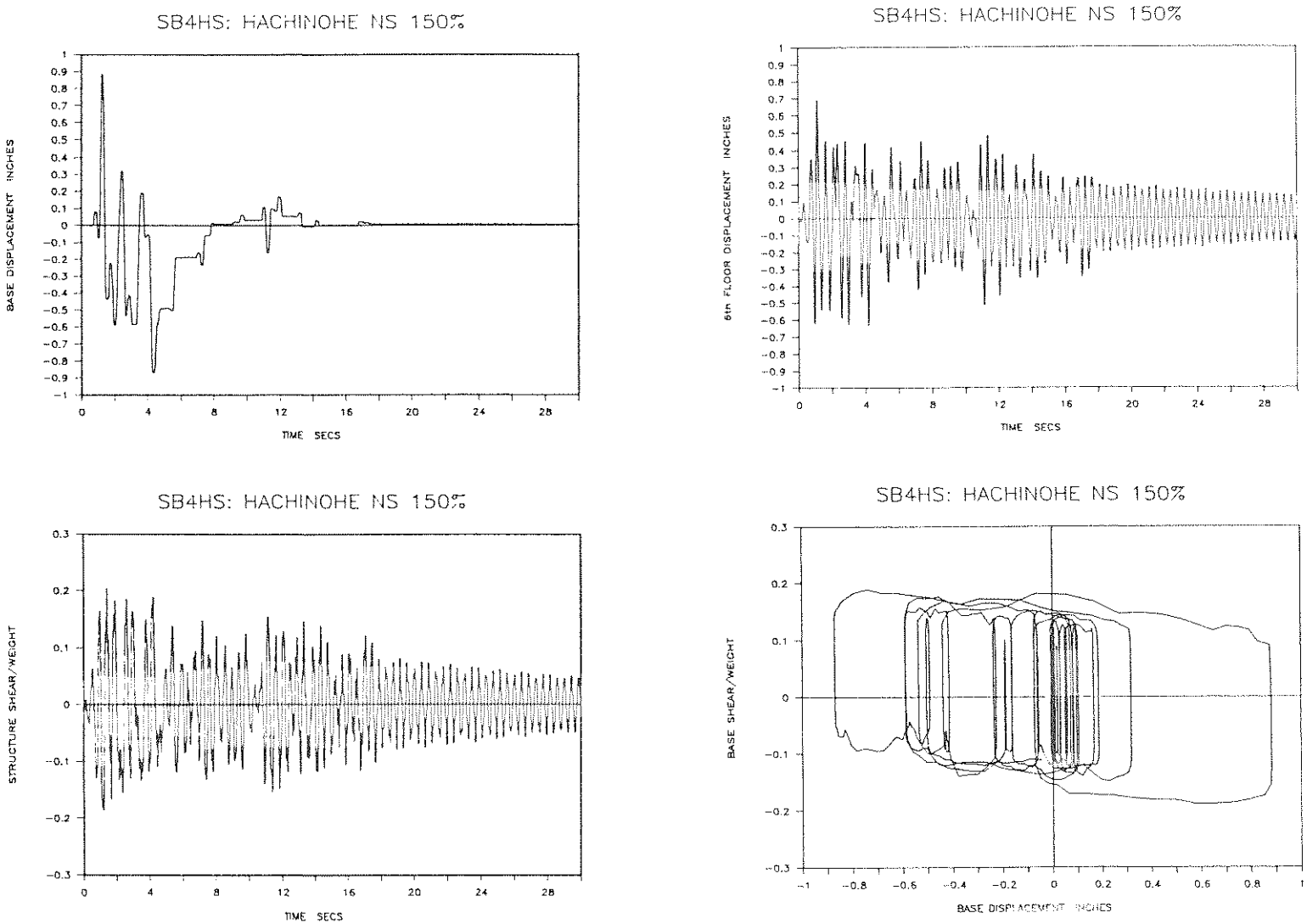

Fig. 5-15 - Experimental Time Histories of Base (Bearing) Displacement, Structure Shear and Sixth-Floor Displacement with Respect to Base and Base Shear-Bearing Displacement Loop in Case of Isolation System with Four Spring Units and for Hachinohe NS Input (0.29g peak table acceleration).

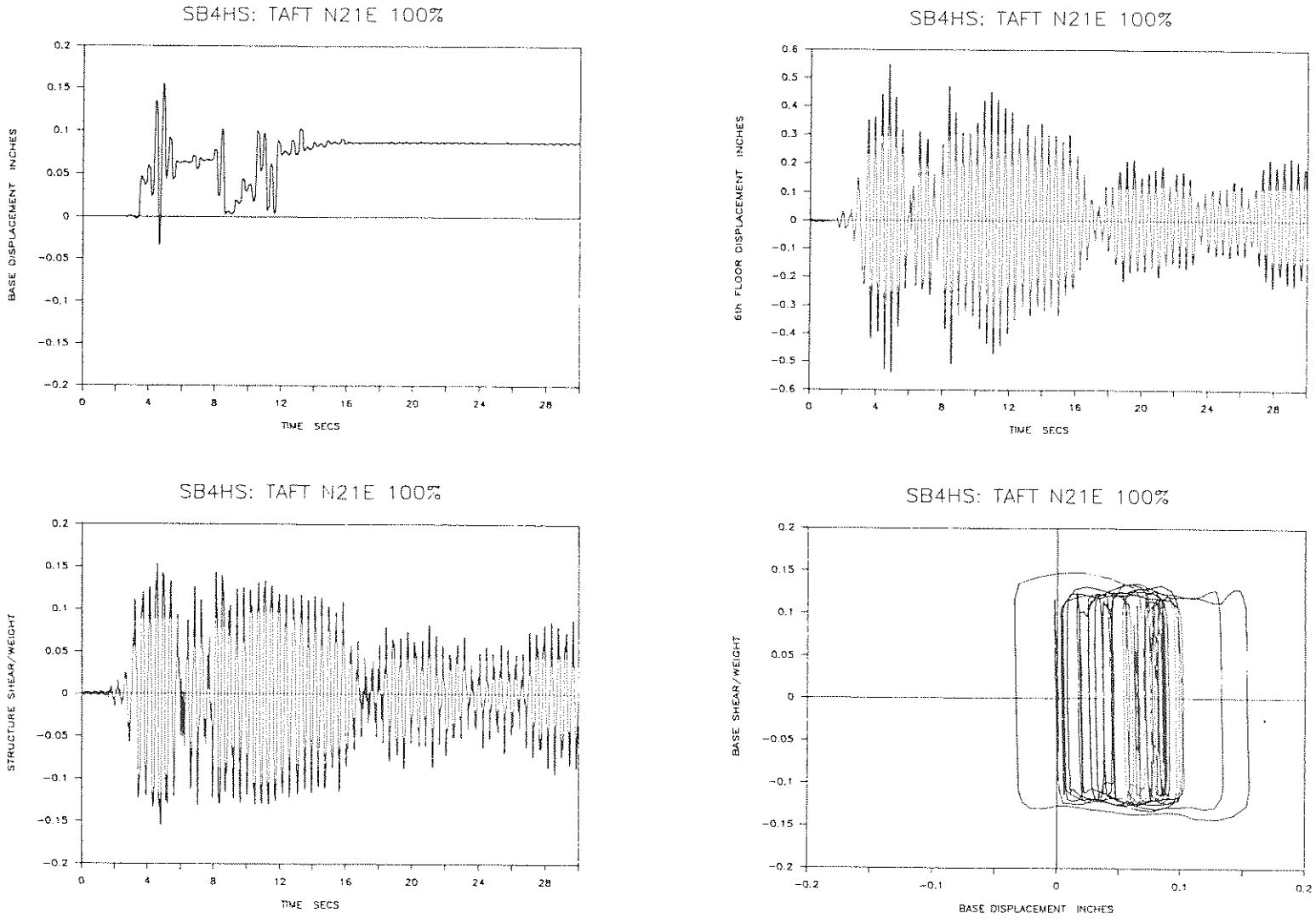

Fig. 5-16 - Experimental Time Histories of Base (Bearing) Displacement, Structure Shear and Sixth-Floor Displacement with Respect to Base and Base Shear-Bearing Displacement Loop in Case of Isolation System with Four Spring Units and for Taft N21E Input (0.16g peak table acceleration).

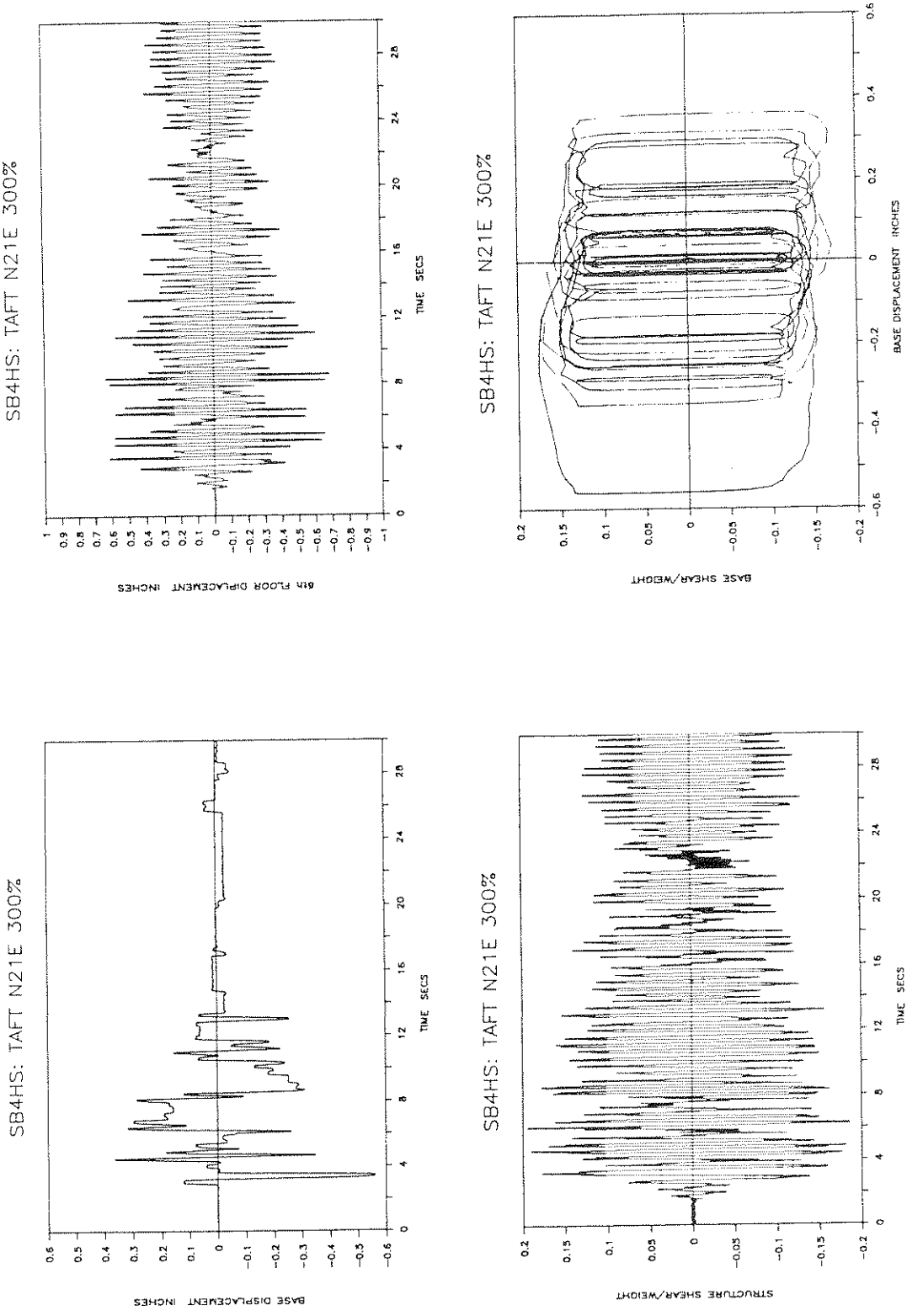

Fig. 5-17 - Experimental Time Histories of Base (Bearing) Displacement, Structure Shear and Sixth-Floor Displacement with Respect to Base and Base Shear-Bearing Displacement Loop in Case of Isolation System with Four Spring Units and for Taft N21E Input (0.44g peak table acceleration).

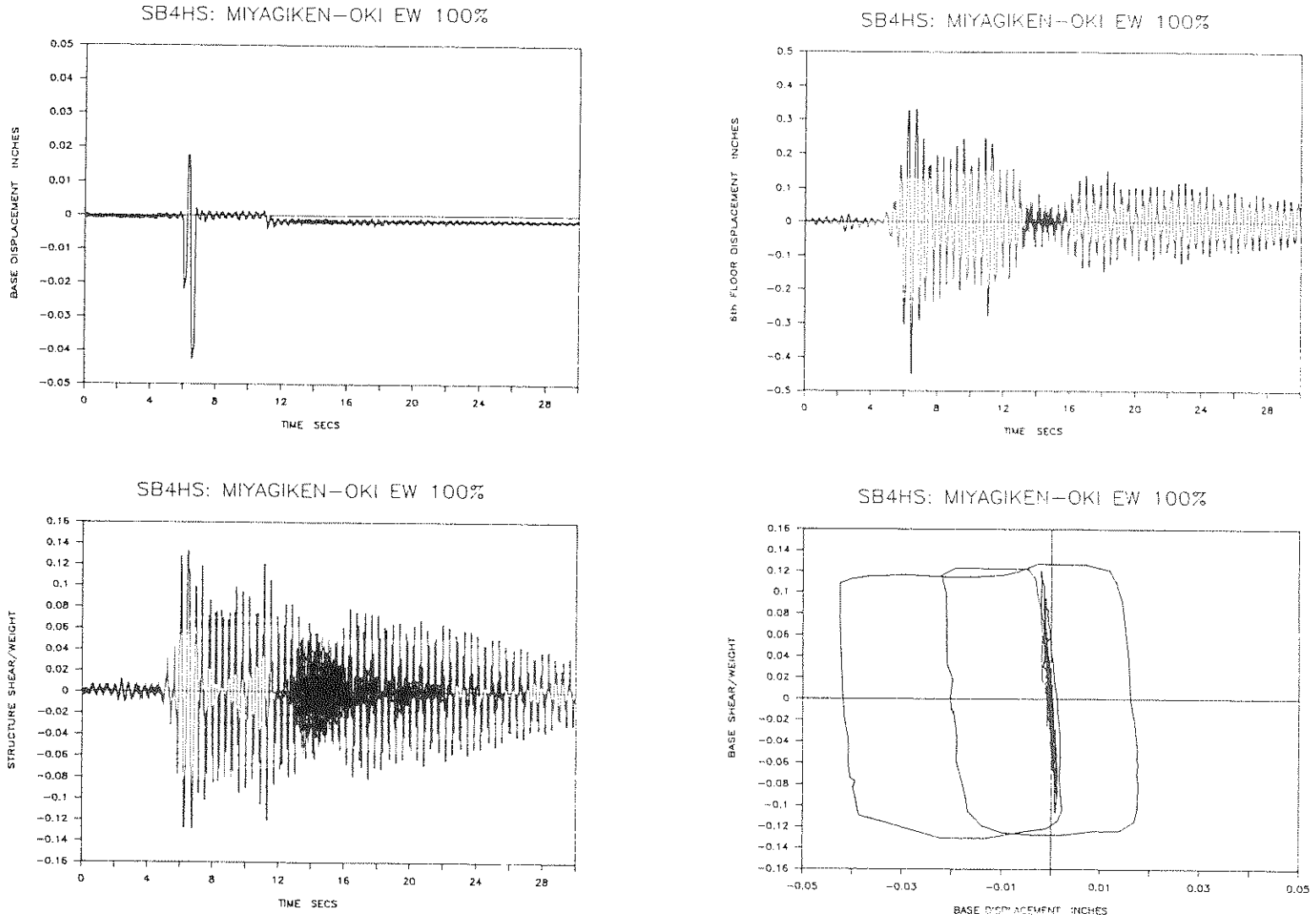

Fig. 5-18 - Experimental Time Histories of Base (Bearing) Displacement, Structure Shear and Sixth-Floor Displacement with Respect to Base and Base Shear-Bearing Displacement Loop in Case of Isolation System with Four Spring Units and for Miyagiken-Oki EW Input (0.14g peak table acceleration).

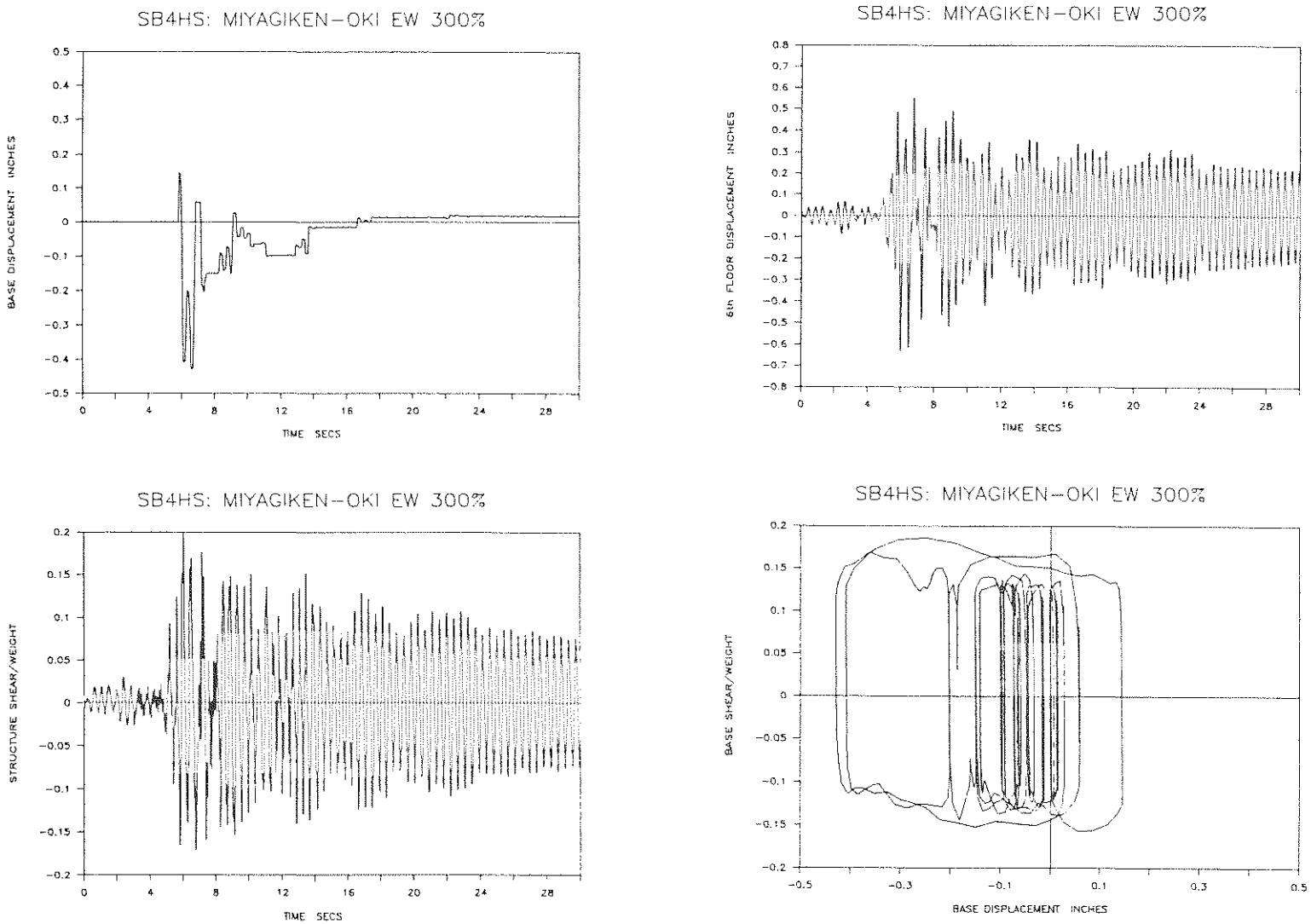

Fig. 5-19 - Experimental Time Histories of Base (Bearing) Displacement, Structure Shear and Sixth-Floor Displacement with Respect to Base and Base Shear-Bearing Displacement Loop in Case of Isolation System with Four Spring Units and for Miyagiken-Oki EW Input (0.42g peak table acceleration).

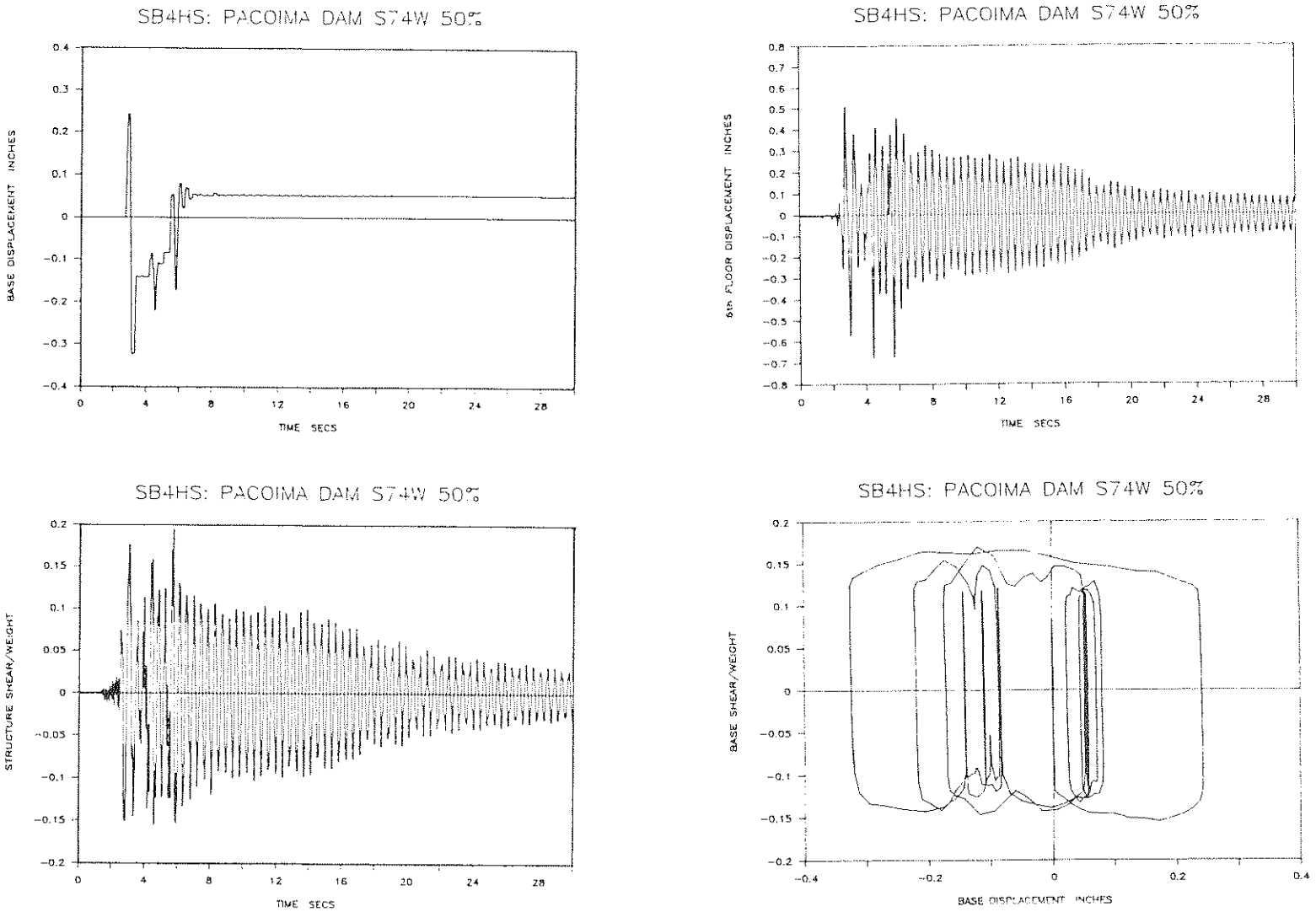

Fig. 5-20 - Experimental Time Histories of Base (Bearing) Displacement, Structure Shear and Sixth-Floor Displacement with Respect to Base and Base Shear-Bearing Displacement Loop in Case of Isolation Systemwith Four Spring Units and for Pacoima S74W Input (0.39g peak table acceleration).

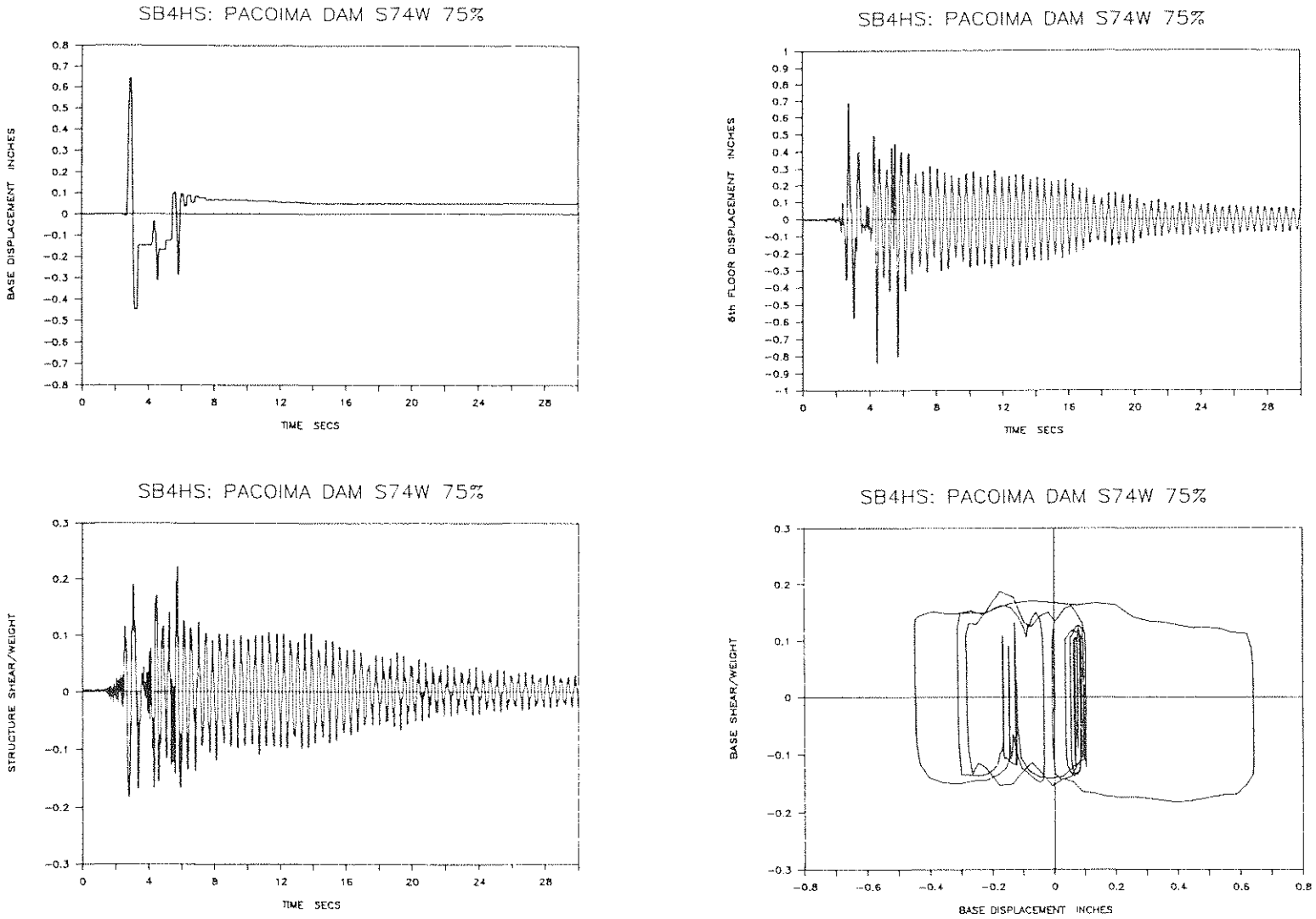

Fig. 5-21 - Experimental Time Histories of Base (Bearing) Displacement, Structure Shear and Sixth-Floor Displacement with Respect to Base and Base Shear-Bearing Displacement Loop in Case of Isolation System with Four Spring Units and for Pacoima S74W Input (0.58g peak table acceleration).

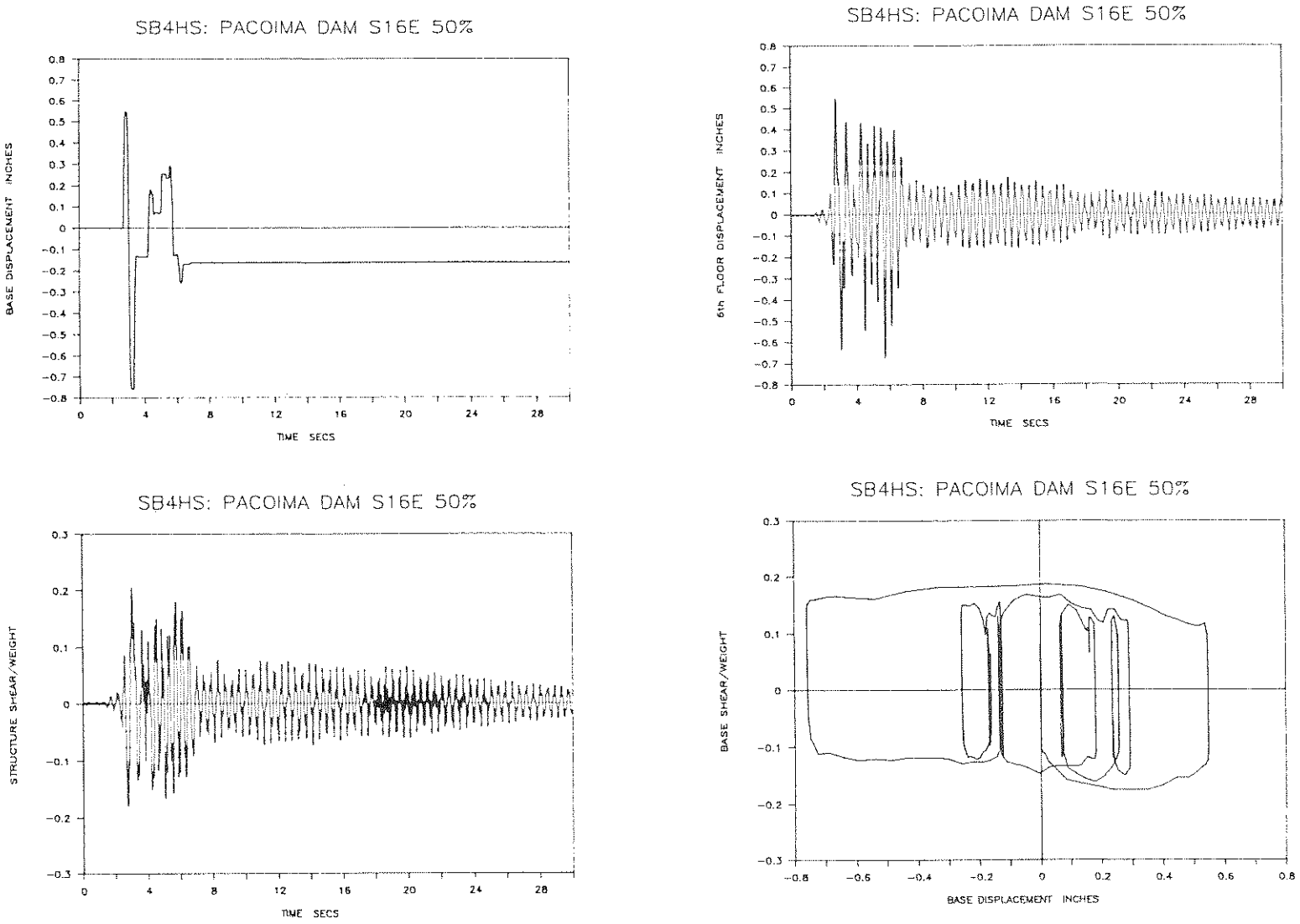

Fig. 5-22 - Experimental Time Histories of Base (Bearing) Displacement, Structure Shear and Sixth-Floor Displacement with Respect to Base and Base Shear-Bearing Displacement Loop in Case of Isolation System with Four Spring Units and for Pacoima S16E Input (0.48g peak table acceleration).

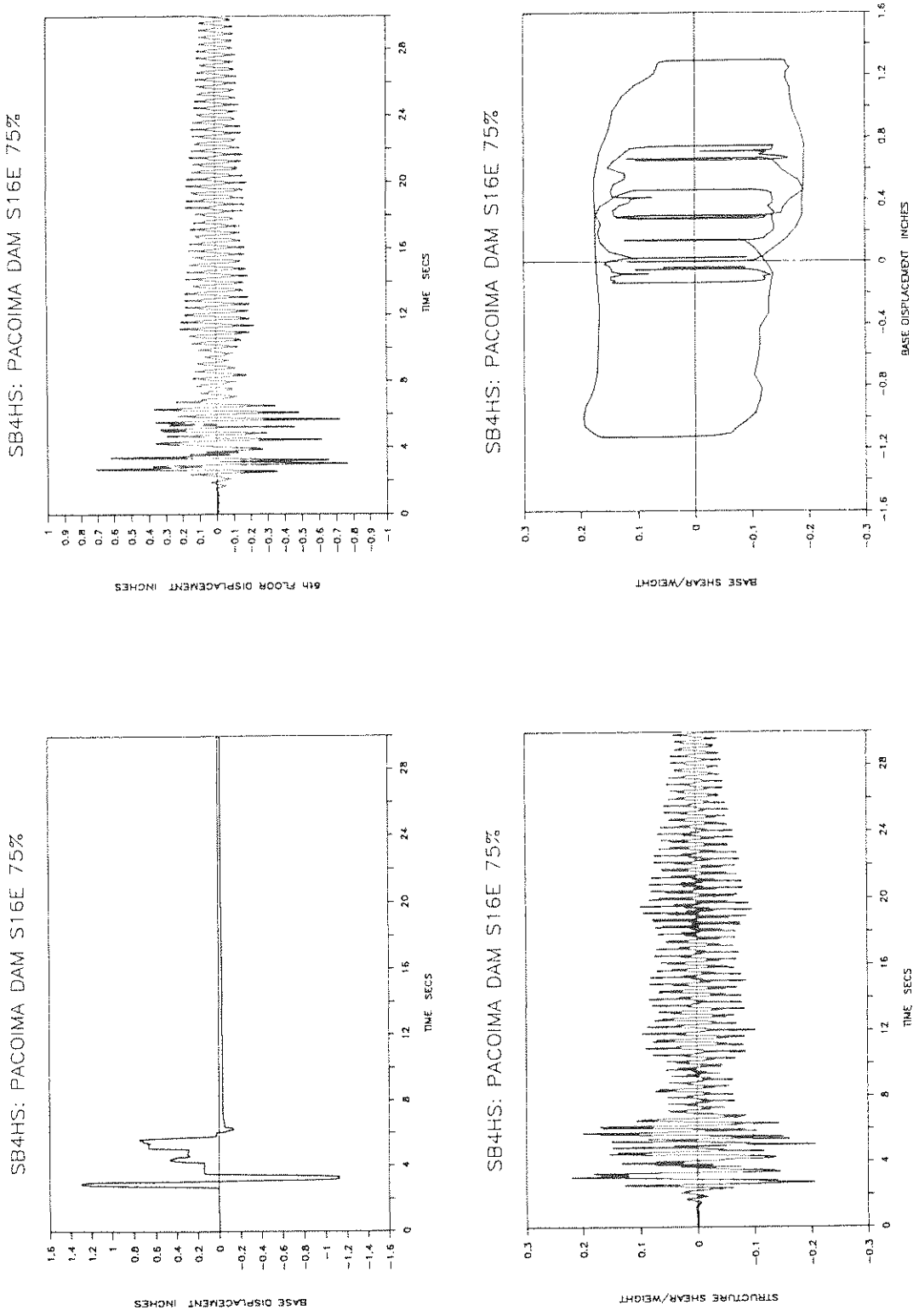

Fig. 5-23 - Experimental Time Histories of Base (Bearing) Displacement, Structure Shear and Sixth-Floor Displacement with Respect to Base and Base Shear-Bearing Displacement Loop in Case of Isolation System with Four Spring Units and for Pacoima S16E Input (0.73g peak table acceleration).

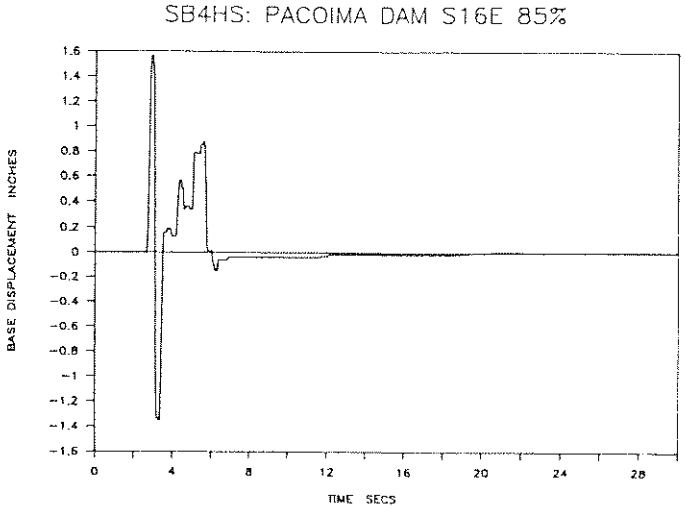

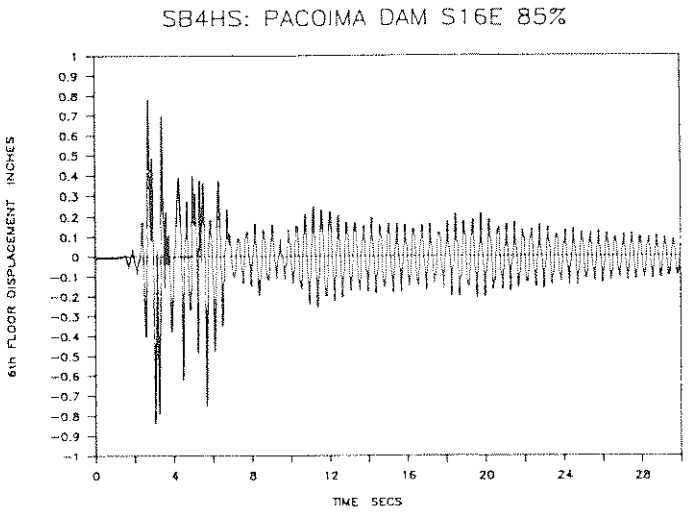

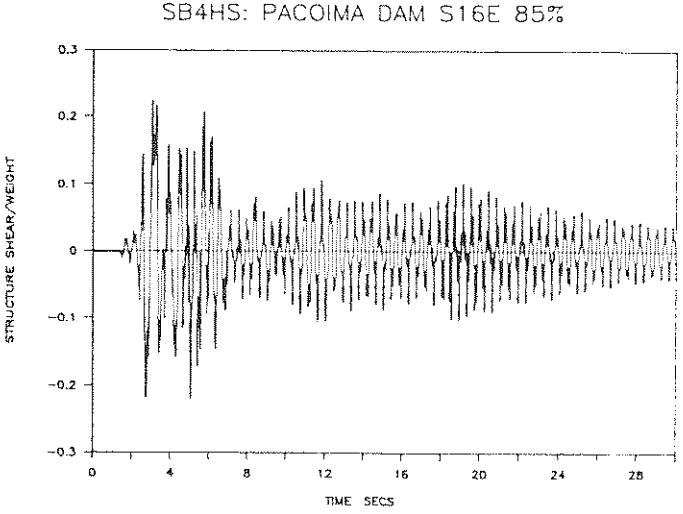

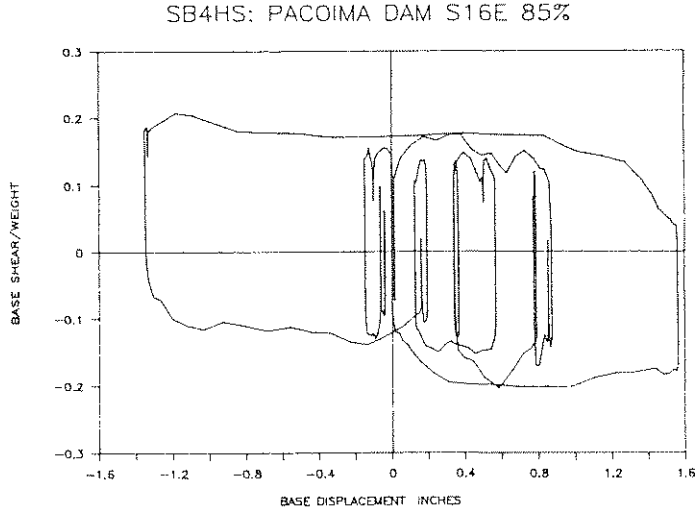

Fig. 5-24 - Experimental Time Histories of Base (Bearing) Displacement, Structure Shear and Sixth-Floor Displacement with Respect to Base and Base Shear-Bearing Displacement Loop in Case of Isolation System with Four Spring Units and for Pacoima S16E Input (0.84g peak table acceleration).

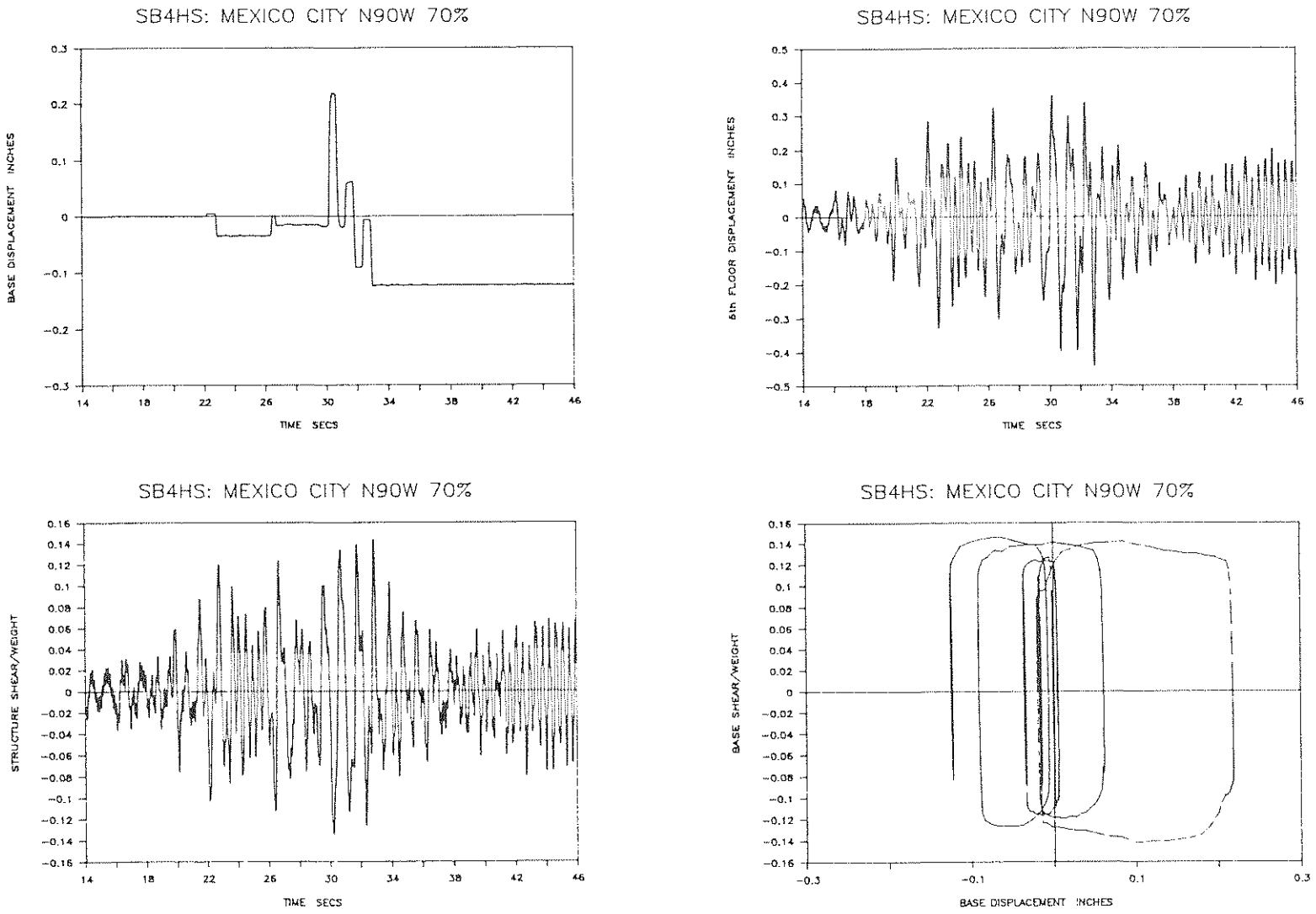

Fig. 5-25 - Experimental Time Histories of Base (Bearing) Displacement, Structure Shear and Sixth-Floor Displacement with Respect to Base and Base Shear-Bearing Displacement Loop in Case of Isolation System with Four Spring Units and for Mexico City N90W Input (0.13g peak table acceleration).

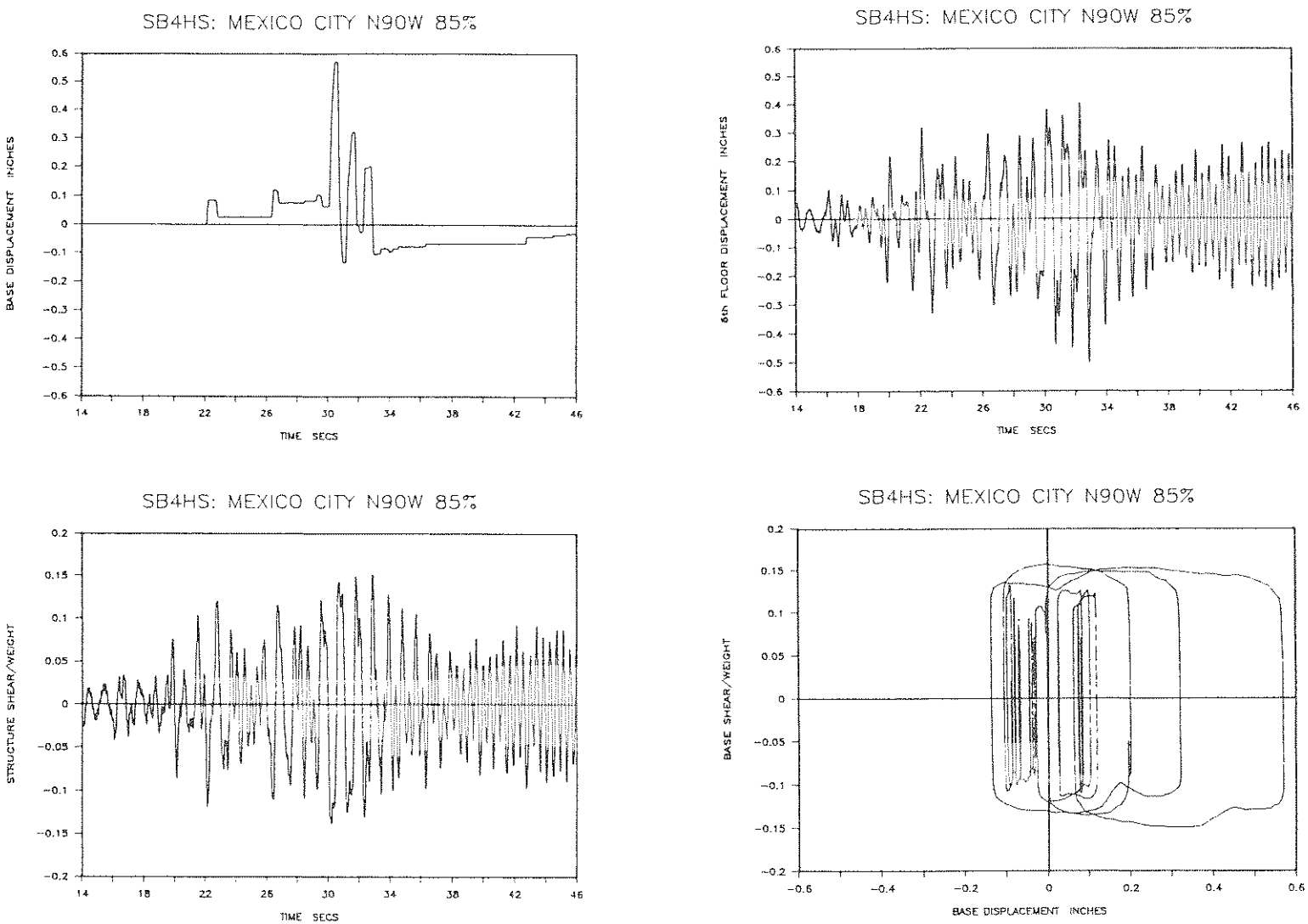

Fig. 5-26 - Experimental Time Histories of Base (Bearing) Displacement, Structure Shear and Sixth-Floor Displacement with Respect to Base and Base Shear-Bearing Displacement Loop in Case of Isolation System with Four Spring Units and for Mexico City N90W Input (0.15g peak table acceleration).

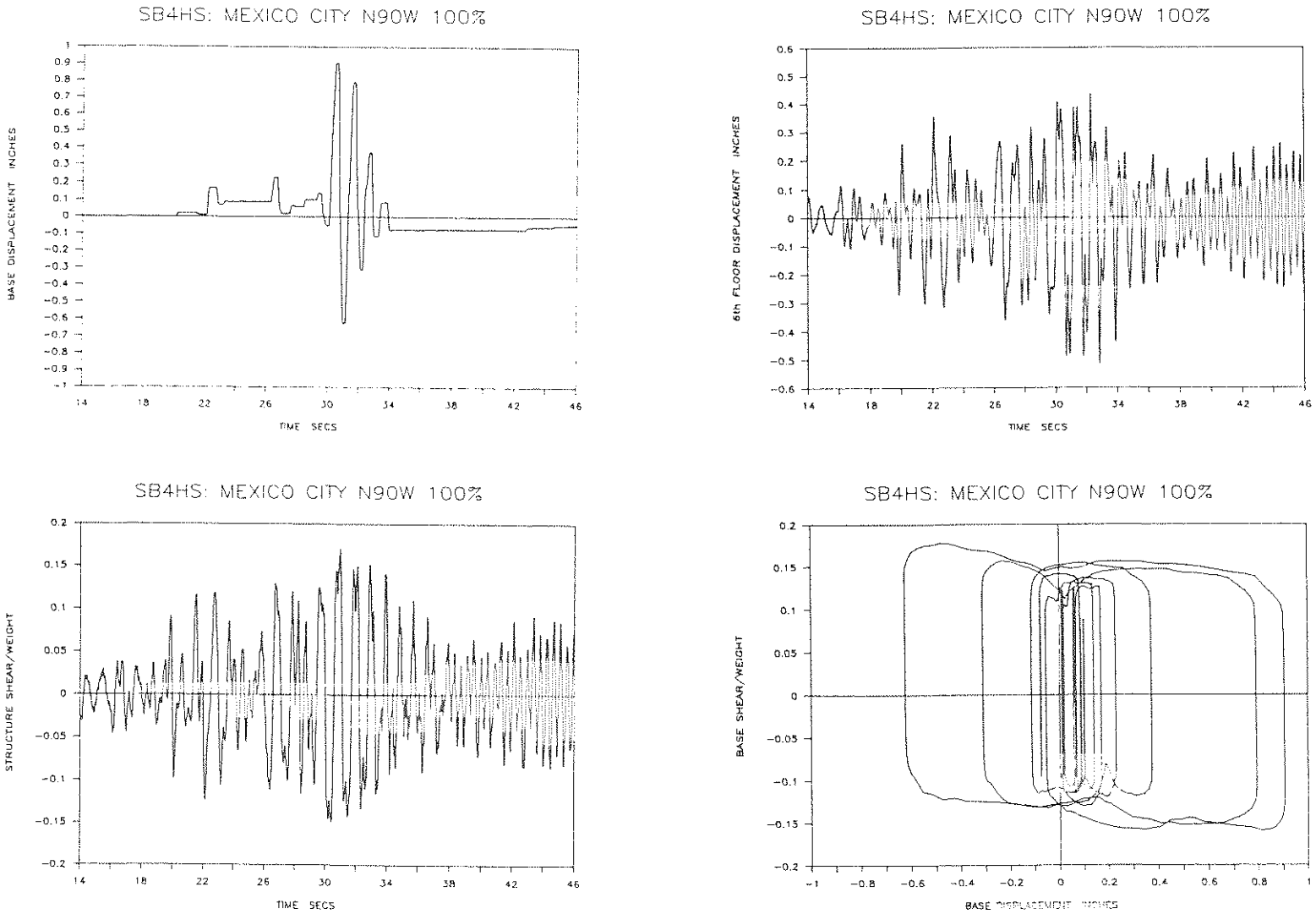

Fig. 5-27 - Experimental Time Histories of Base (Bearing) Displacement, Structure Shear and Sixth-Floor Displacement with Respect to Base and Base Shear-Bearing Displacement Loop in Case of Isolation System with Four Spring Units and for Mexico City N90W Input (0.18g peak table acceleration).

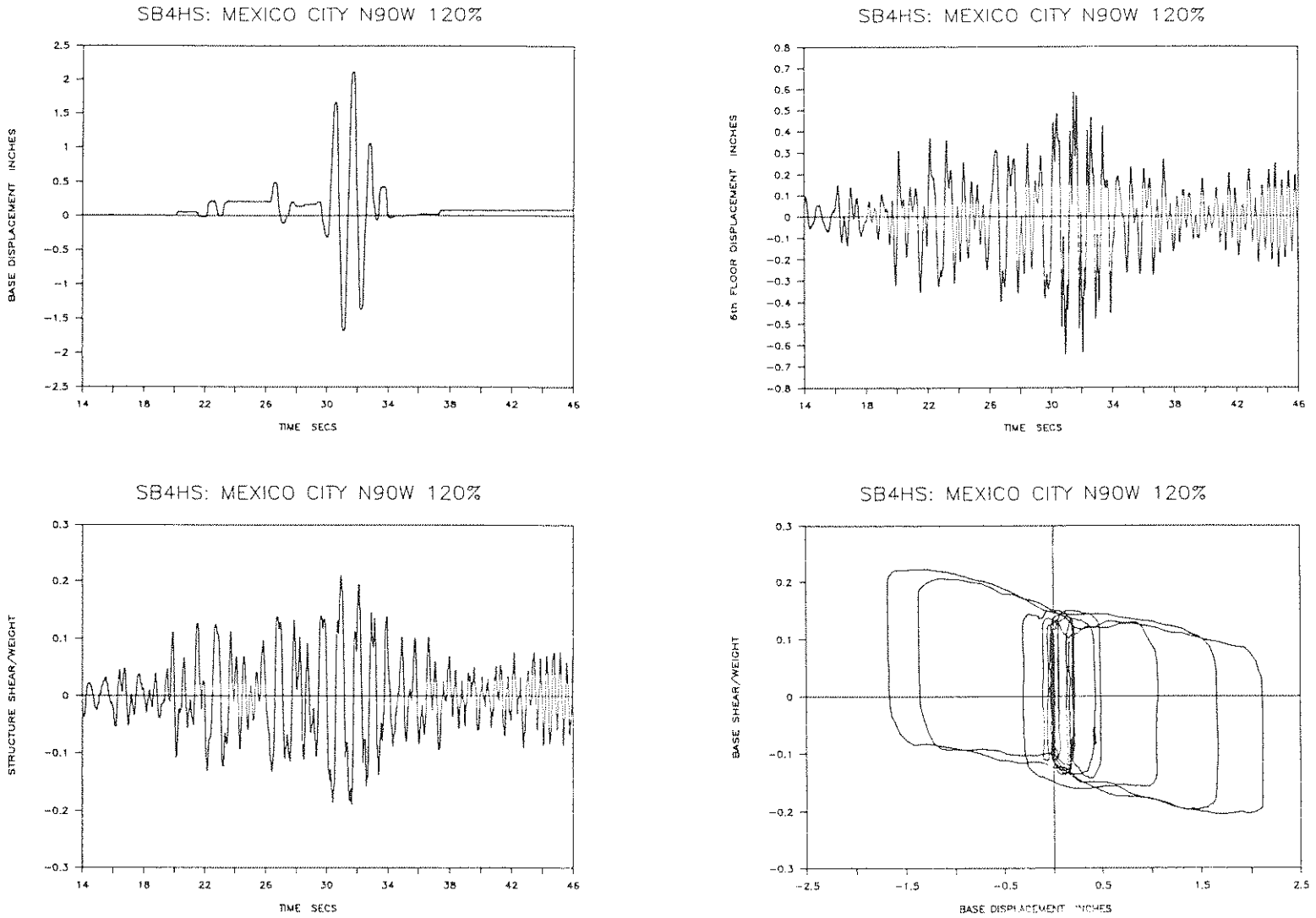

Fig. 5-28 - Experimental Time Histories of Base (Bearing) Displacement, Structure Shear and Sixth-Floor Displacement with Respect to Base and Base Shear-Bearing Displacement Loop in Case of Isolation System with Four Spring Units and for Mexico City N90W Input (0.21g peak table acceleration).

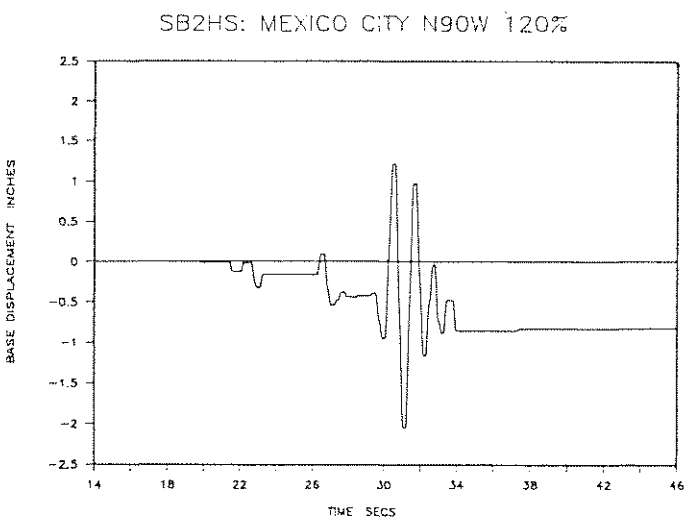

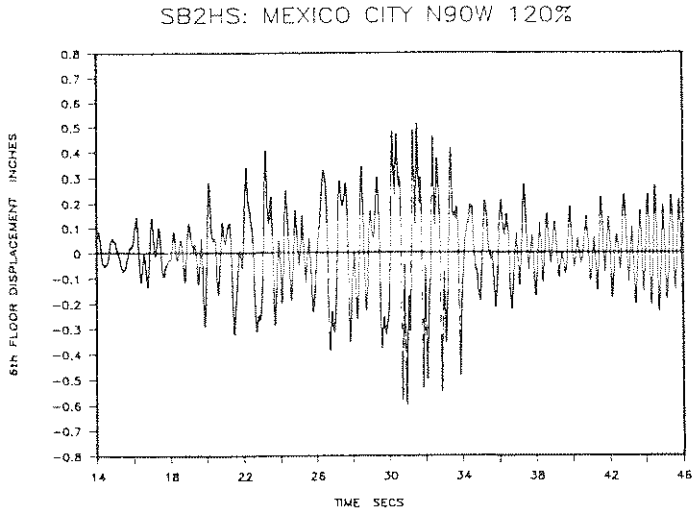

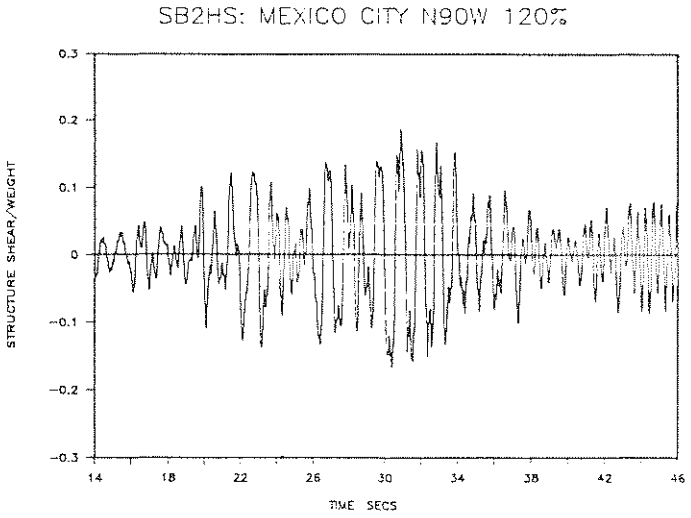

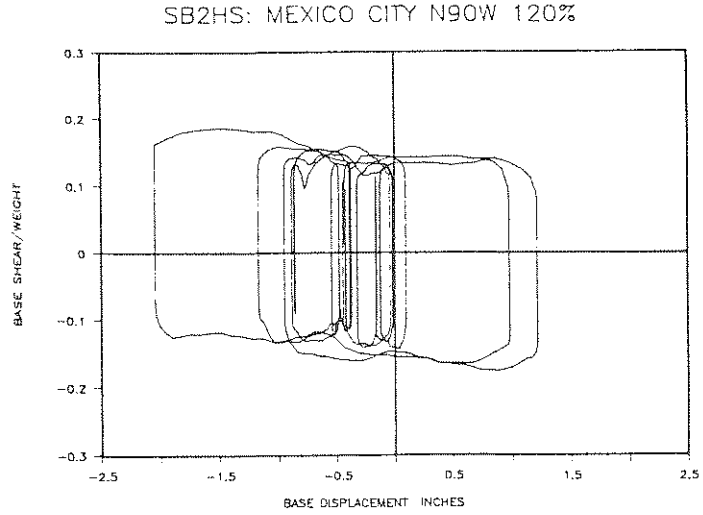

Fig. 5-29 - Experimental Time Histories of Base (Bearing) Displacement, Structure Shear and Sixth-Floor Displacement with Respect to Base and Base Shear-Bearing Displacement Loop in Case of Isolation System with Two Spring Units and for Mexico City N90W Input (0.21g peak table acceleration).

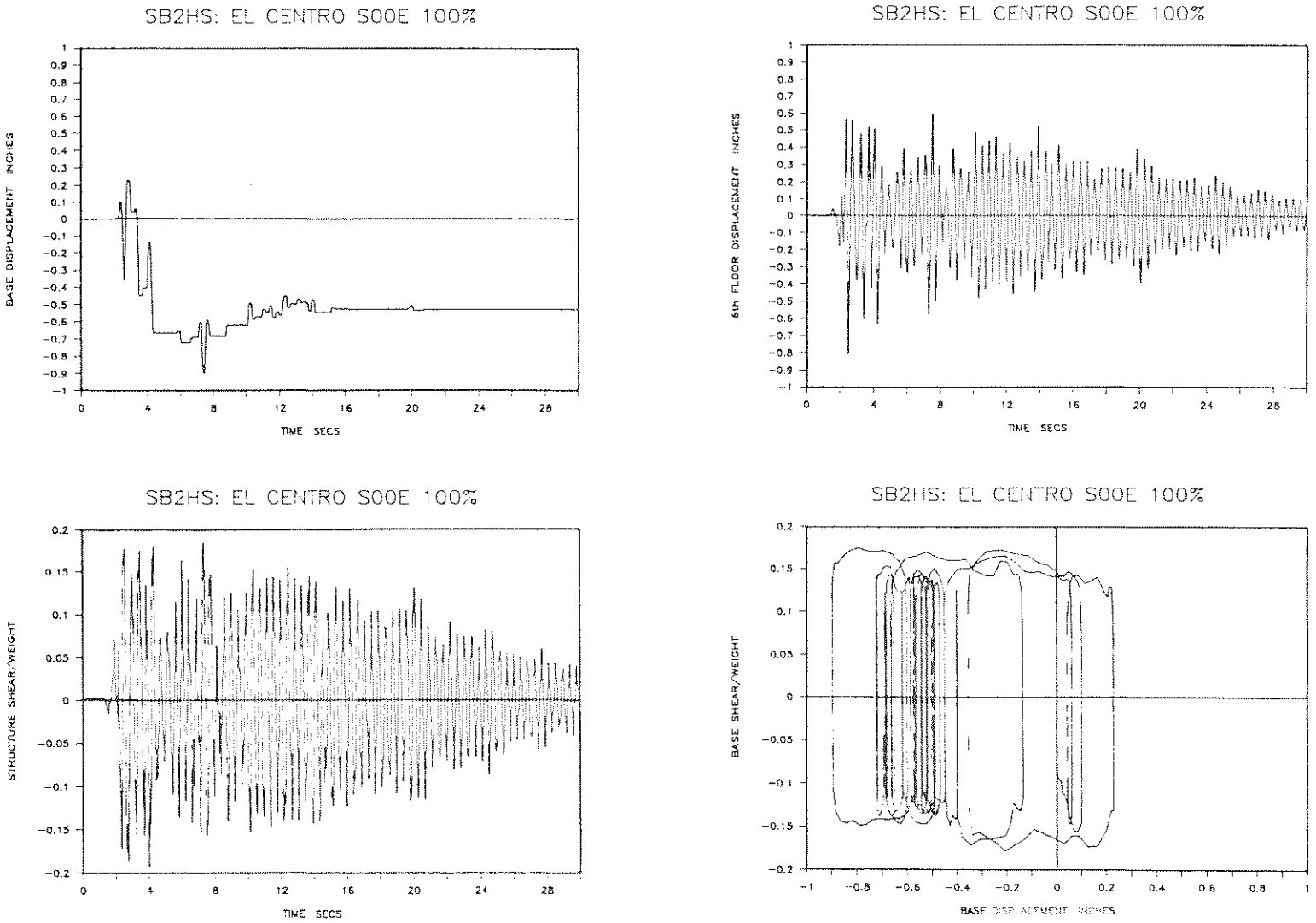

Fig. 5-30 - Experimental Time Histories of Base (Bearing) Displacement, Structure Shear and Sixth-Floor Displacement with Respect to Base and Base Shear-Bearing Displacement Loop in Case of Isolation System with Two Spring Units and for El Centro S00E Input (0.28g peak table acceleration).

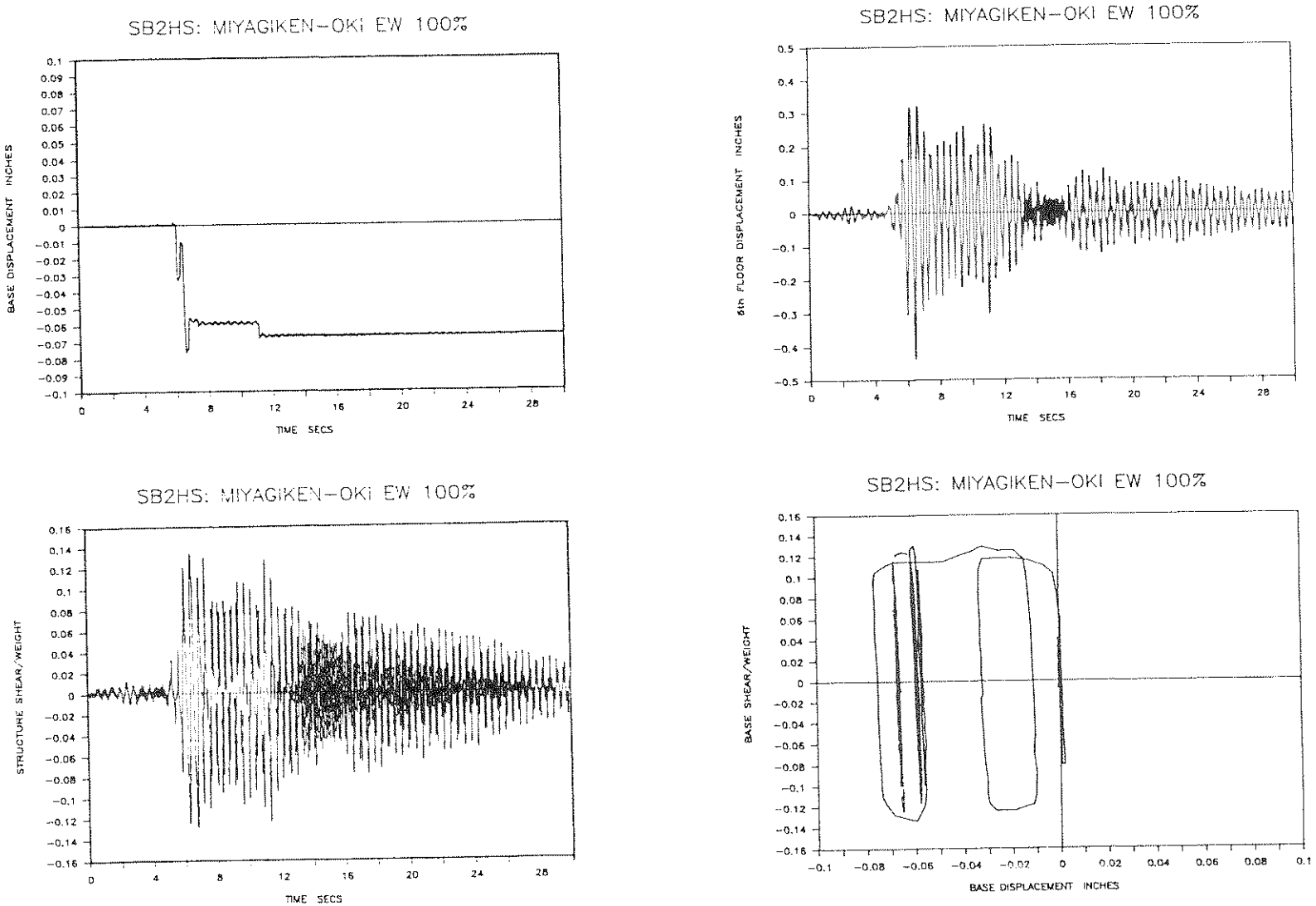

Fig. 5-31 - Experimental Time Histories of Base (Bearing) Displacement, Structure Shear and Sixth-Floor Displacement with Respect to Base and Base Shear-Bearing Displacement Loop in Case of Isolation System with Two Spring Units and for Miyagiken-Oki EW Input (0.13g peak table acceleration).

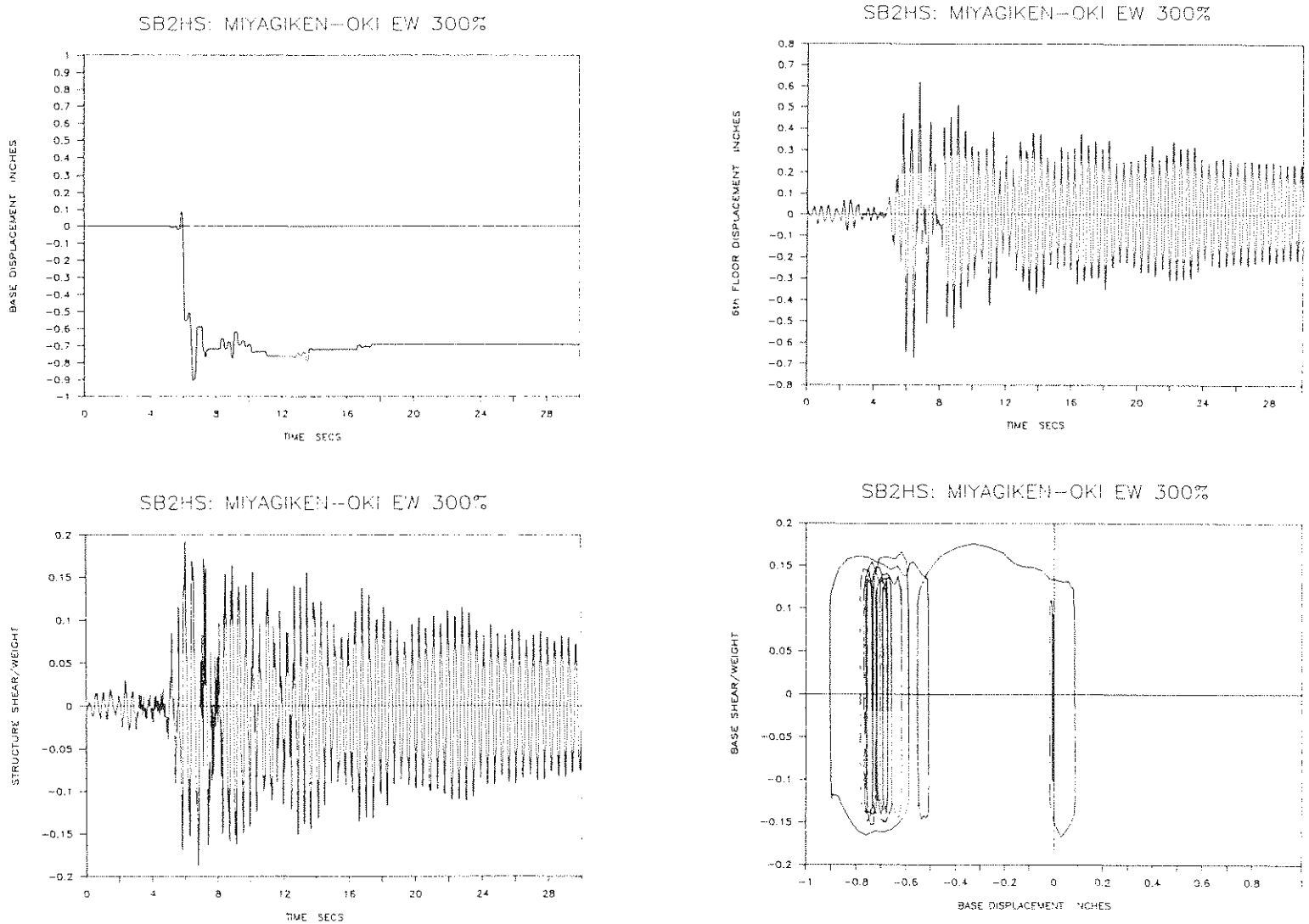

Fig. 5-32 - Experimental Time Histories of Base (Bearing) Displacement, Structure Shear and Sixth-Floor Displacement with Respect to Base and Base Shear-Bearing Displacement Loop in Case of Isolation System with Two Spring Units and for Miyagiken-Oki EW Input (0.42g peak table acceleration).

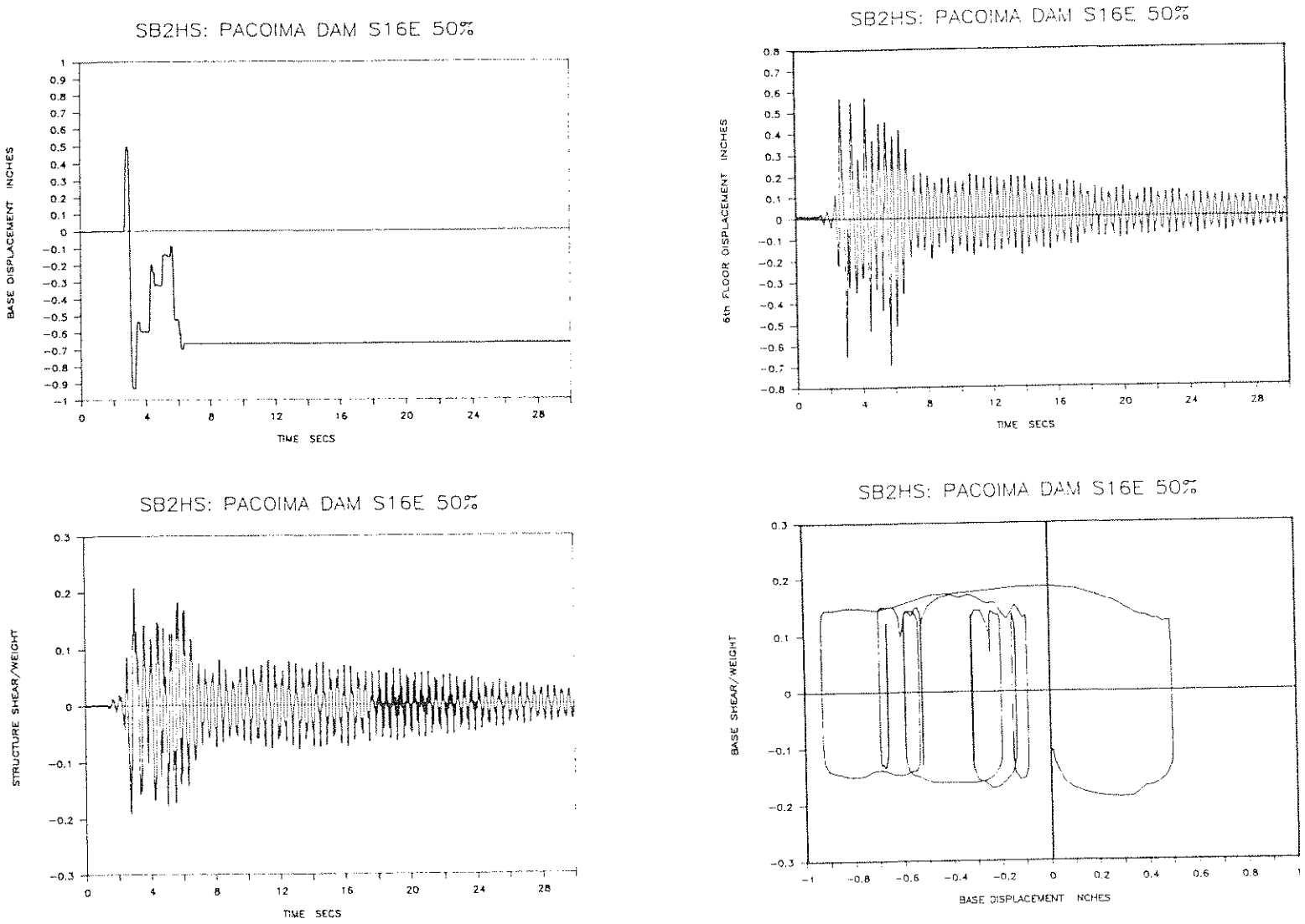

Fig. 5-33 - Experimental Time Histories of Base (Bearing) Displacement, Structure Shear and Sixth-Floor Displacement with Respect to Base and Base Shear-Bearing Displacement Loop in Case of Isolation System with Two Spring Units and for Pacoima S16E Input (0.46g peak table acceleration).

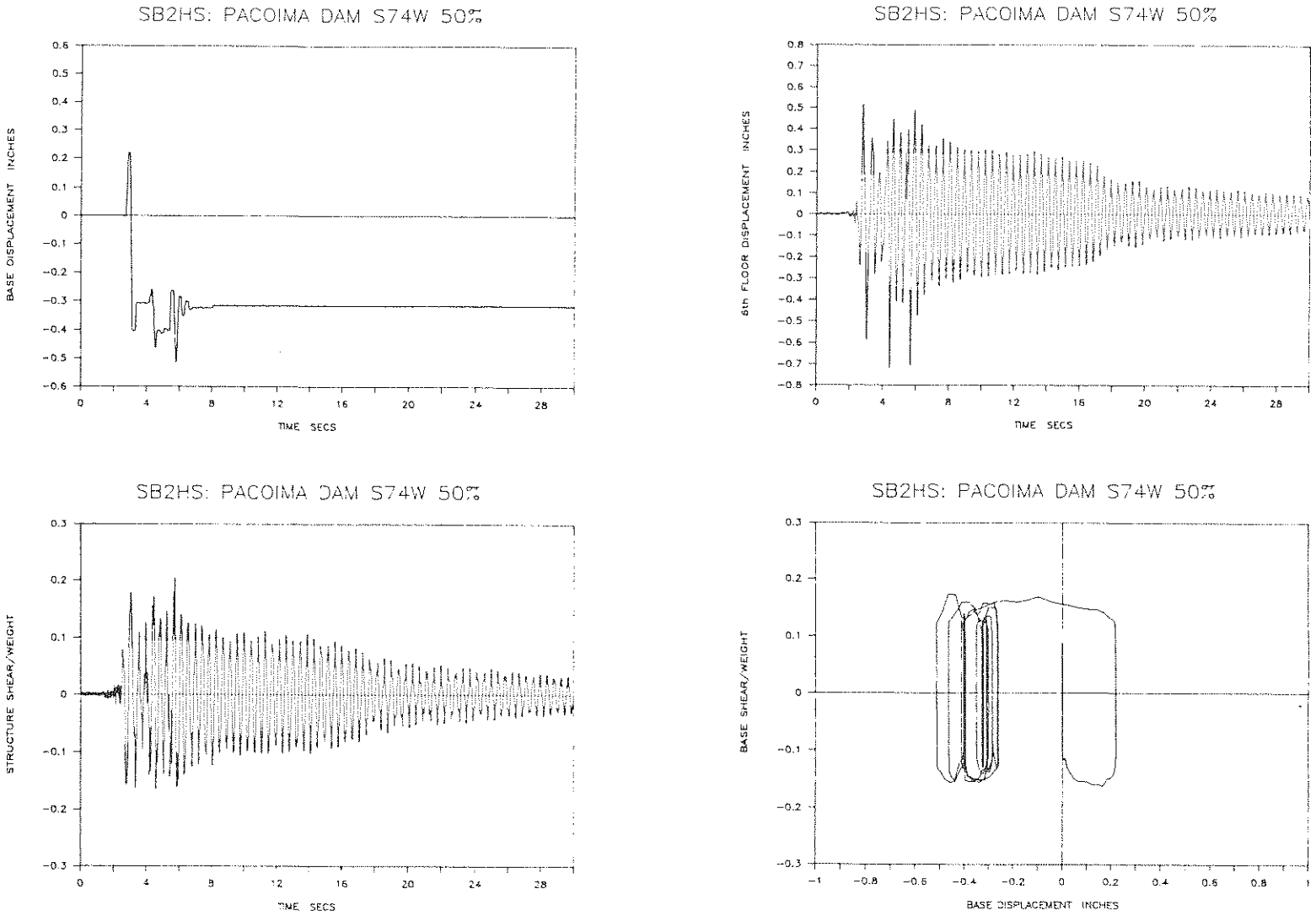

Fig. 5-34 - Experimental Time Histories of Base (Bearing) Displacement, Structure Shear and Sixth-Floor Displacement with Respect to Base and Base Shear-Bearing Displacement Loop in Case of Isolation System with Two Spring Units and for Pacoima S74W Input (0.38g peak table acceleration).

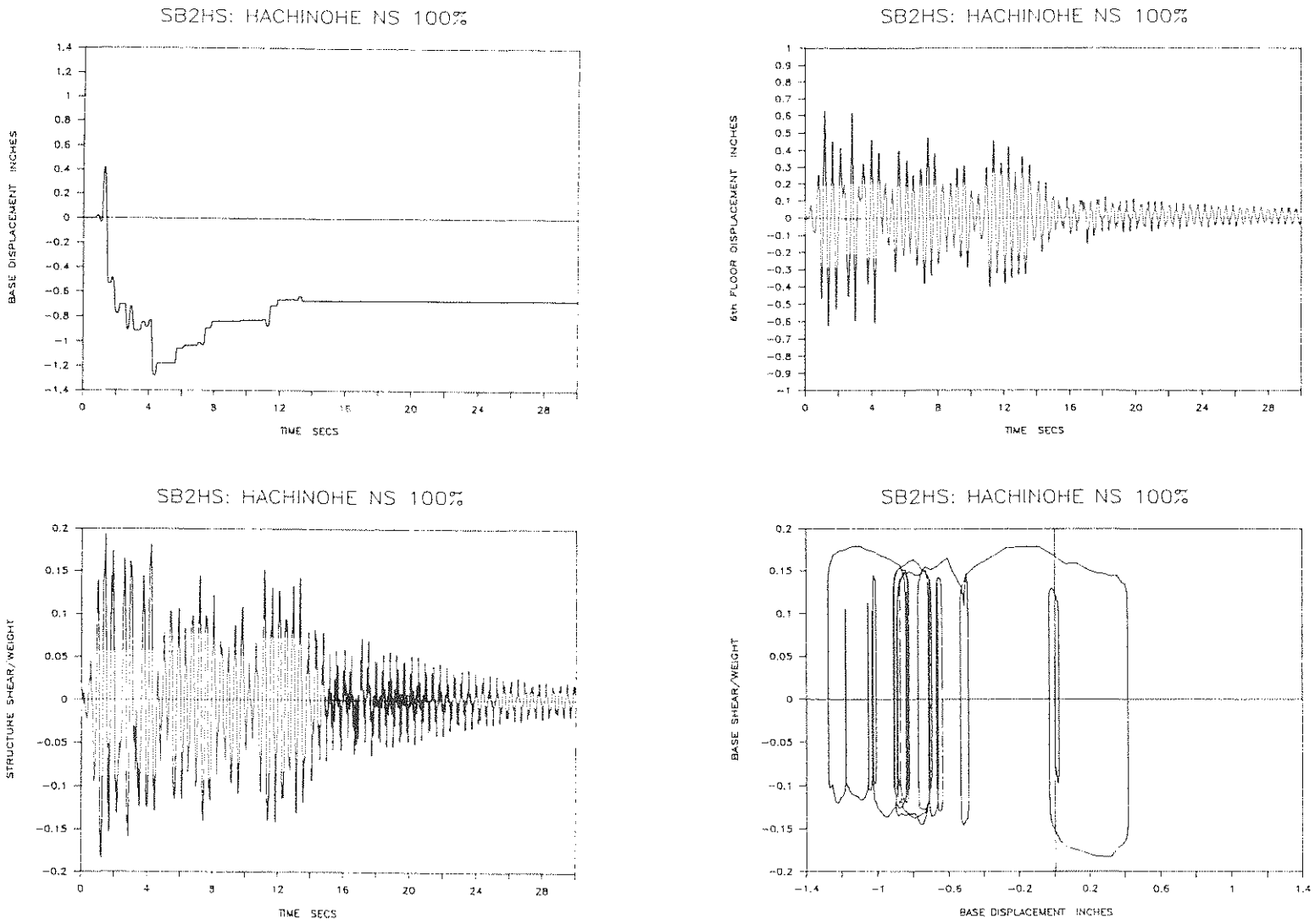

Fig. 5-35 - Experimental Time Histories of Base (Bearing) Displacement, Structure Shear and Sixth-Floor Displacement with Respect to Base and Base Shear-Bearing Displacement Loop in Case of Isolation System with Two Spring Units and for Hachinohe NS Input (0.22g peak table acceleration).

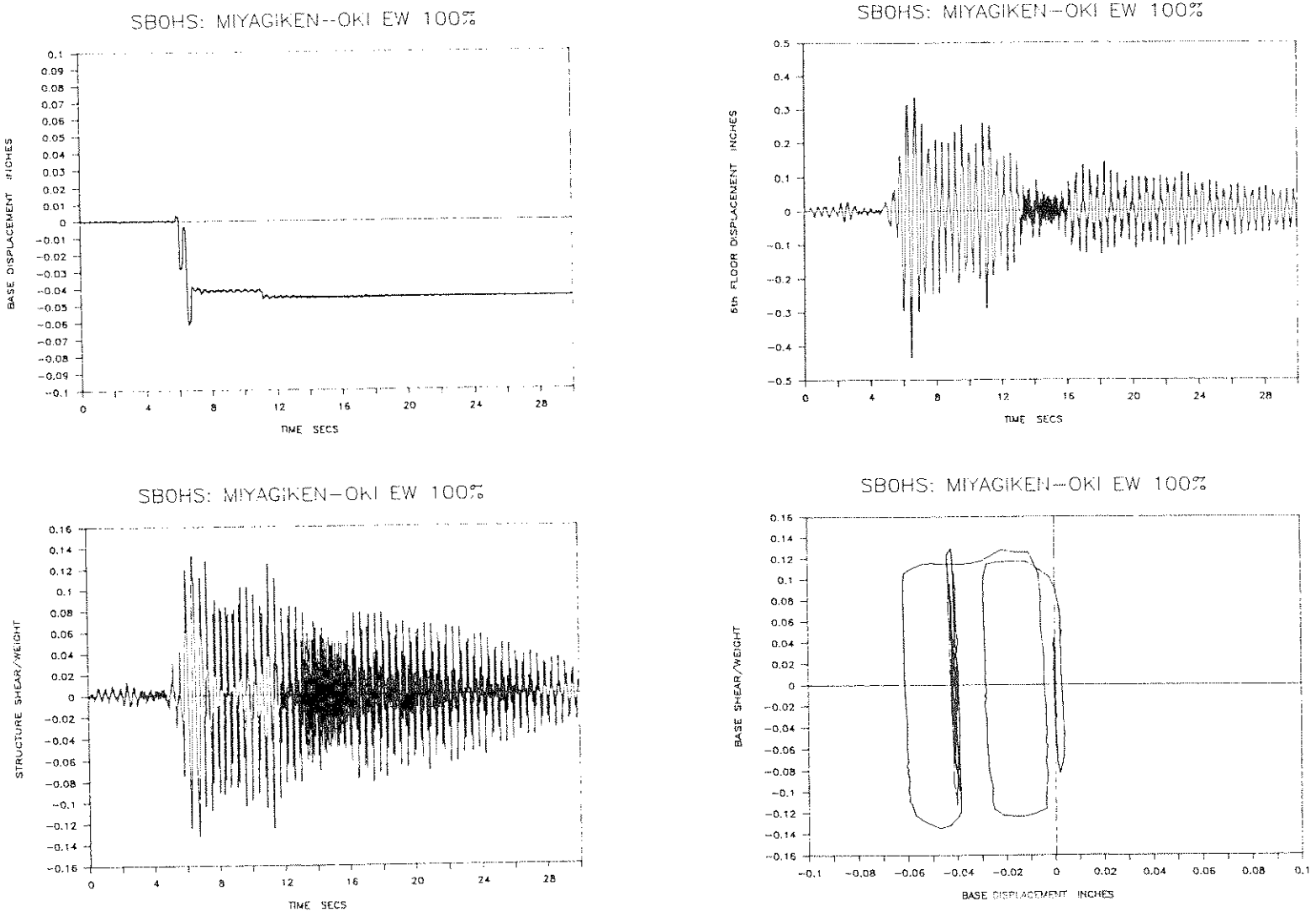

Fig. 5-36 - Experimental Time Histories of Base (Bearing) Displacement, Structure Shear and Sixth-Floor Displacement with Respect to Base and Base Shear-Bearing Displacement Loop in Case of Isolation System Without Spring Units and for Miyagiken-Oki EW Input (0.14g peak table acceleration).

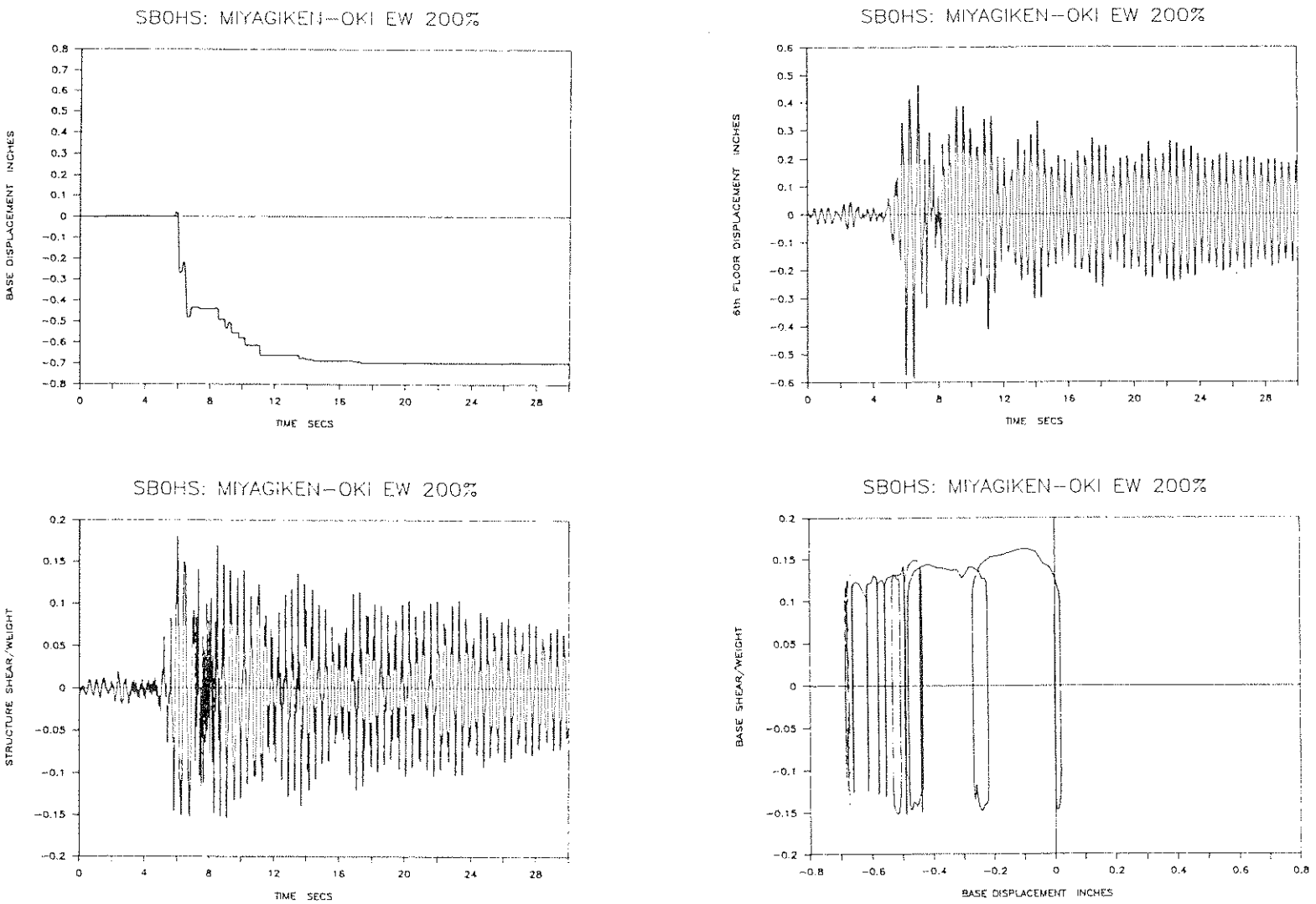

Fig. 5-37 - Experimental Time Histories of Base (Bearing) Displacement, Structure Shear and Sixth-Floor Displacement with Respect to Base and Base Shear-Bearing Displacement Loop in Case of Isolation System Without Spring Units and for Miyagiken-Oki EW Input (0.28g peak table acceleration).

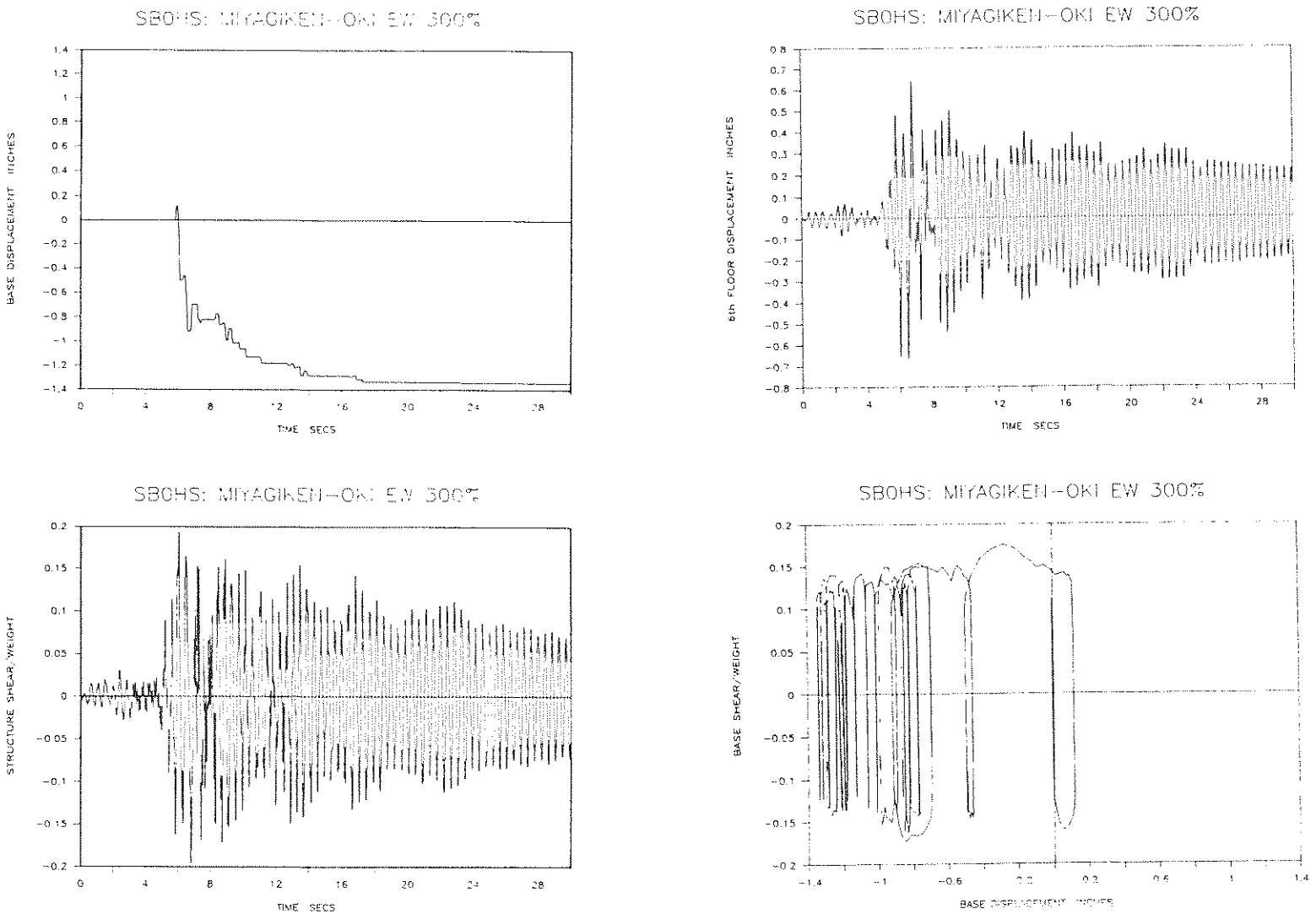

Fig. 5-38 - Experimental Time Histories of Base (Bearing) Displacement, Structure Shear and Sixth-Floor Displacement with Respect to Base and Base Shear-Bearing Displacement Loop in Case of Isolation System Without Spring Units and for Miyagiken-Oki EW Input (0.43g peak table acceleration).

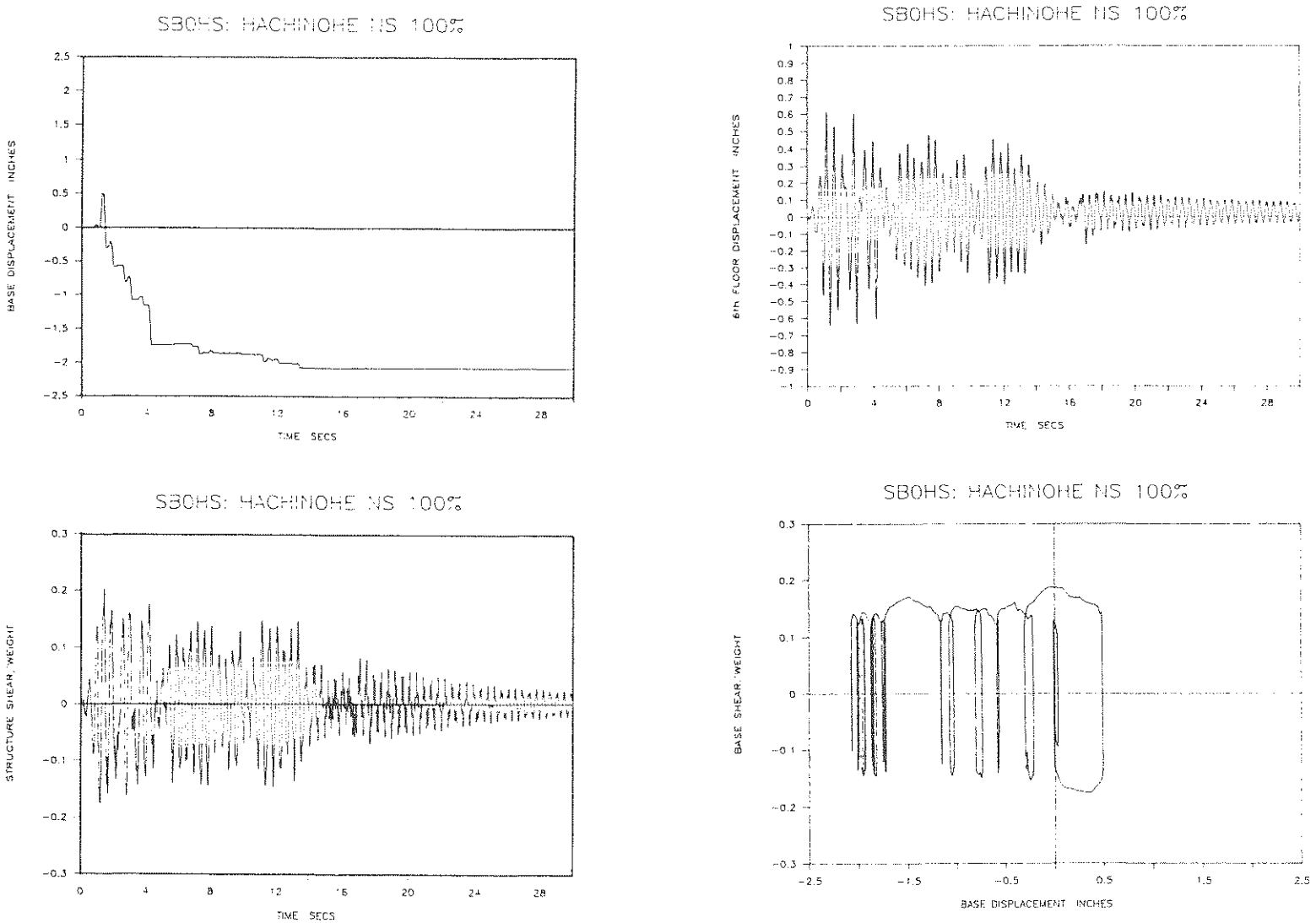

Fig. 5-39 - Experimental Time Histories of Base (Bearing) Displacement, Structure Shear and Sixth-Floor Displacement with Respect to Base and Base Shear-Bearing Displacement Loop in Case of Isolation System Without Spring Units and for Hachinohe NS Input (0.21g peak table acceleration).

SECTION 6
ANALYTICAL PREDICTION OF RESPONSE

The "Tentative General Requirements for the Design and Construction of Seismic-Isolated Structures" document which was prepared by the Structural Engineers Association of California (SEAOC, 1990) specifies analysis procedures for base-isolated structures. The document requires the use of dynamic time history analysis for specific cases, one of which is when the structure is located on a soil profile with site factor S_4. Of course, this requires the availability of analytical techniques for the reliable prediction of response.

A lumped mass model with degrees of freedom being the floor and base displacements was used for the analytical prediction of the response of the tested system. The equations of motion are:

$$[M]\{\ddot{U}\}+[C]\{\dot{U}\}+[K]\{U\}=-[M]\{1\}(\ddot{U}_b+\ddot{U}_g) \tag{6.1}$$

$$\sum_{i=1}^{6} m_i(\ddot{U}_i+\ddot{U}_b+\ddot{U}_g)+m_b(\ddot{U}_b+\ddot{U}_g)+F_f+F_r=0 \tag{6.2}$$

Equation (6.1) is the equation of motion of the six story superstructure with [M], [C] and [K] being the mass, damping and stiffness matrices, respectively. Equation (6.2) is that of dynamic equilibrium of the entire structure in the horizontal direction. {U} is the vector of floor displacements with respect to the base, U_b is the base displacement with respect to the table and U_g is the table displacement. A dot denotes differentiation with respect to time. m_i and m_b (i = 1 to 6) are the floor and base masses.

Matrices [K] and [C] were constructed analytically using the analytical modal shapes and frequencies of Table 2-I (see Mokha et al, 1990a for details). The modal damping factors used in the construction of matrix [C] were those determined experimentally (see Table 2-I).

F_f and F_r are the frictional and restoring forces, respectively, at the isolation interface. The frictional force is given by:

$$F_f = [\mu(\dot{U}_b)\cos\delta - sgn(\dot{U}_b)\sin\delta]WZ \qquad (6.3)$$

where sgn stands for the signum function and $\mu(\dot{U}_b)$ is the coefficient of sliding friction of the Teflon bearing which depends on the velocity of sliding in accordance to Eq. (3.2). δ is the accidental average inclination of the sliding interface which was determined to be 0.4 degrees. Effectively, the mobilized frictional force is lower when sliding occurs in the downhill direction and larger when sliding occurs in the uphill direction. The difference from the average value is $\sin\delta$ W, where W is the weight of the model. This small difference amounts to only 0.36 Kips (1.6 kN). This difference is visible in the frictional force-displacement loops of Figures 3-4a. These loops were adjusted for symmetry so that reliable measurements of the coefficient of frictional could be made. In the loop of Figure 3-4a at frequency of 0.016 Hz, the starting point of the loop is shown with a dot which starts at a force of about -0.3 Kips.

Variable Z in Eq. (6.3) is used to account for the conditions of separation and reattachment (Constantinou et al, 1990) and is governed by the following differential equation:

$$Y\dot{Z} + \gamma|\dot{U}_b|Z|Z|^{+} + \beta\dot{U}_b Z^2 - \dot{U}_b = 0 \qquad (6.4)$$

in which Y = 0.005 in (0.127 mm) and $\beta + \gamma = 1$.

The restoring force is given by:

$$F_r = \begin{cases} K_1 U_b & , |U_b| \le D_1 \\ (K_1 - K_2) D_1 sgn(U_b) + K_2 U_b & , |U_b| > D_1 \end{cases} \qquad (6.5)$$

in which K_1 is the initial low value of the spring stiffness, valid for displacements less than the limit D_1 and K_2 is the stiffness beyond the limit D_1. Equation (6.5) describes the force in an elastic bilinear spring. For the system with four spring units, K_1 = 1.54 Kip/in (0.27 kN/mm), K_2 = 2.68 Kip/in (0.47 kN/mm) and D_1 = 0.5 in (12.7 mm).

As noted earlier, the coefficient of friction was not constant, but rather increased with repeated testing. In general, the coefficient of sliding friction followed the law of Eq. (3.2) with parameter a equal to approximately 0.55 sec/in (21.6 sec/m) but with parameters D_f and f_{max} increasing with repeated testing. At the initial tests, f_{max} was 0.12 and D_f was 0.088. The value of f_{max} could be obtained from recorded base shear-bearing displacement loops during the sequence of earthquake loading tests. It was found to increase from 0.12 to almost 0.19, where it became stable. It was not possible to accurately determine the value of D_f in each

test. It was approximately determined from recorded loops of base shear-displacement to be in the range of 0.06 to 0.13. For example, in the test on the system with four spring units and Pacoima S16E 85% (peak table acceleration of 0.84g) input, these parameters had values of f_{max} = 0.17 and D_f = 0.10. In the test on the system without spring units and Hachinohe 100% (0.21g) input, these parameters changed to f_{max} = 0.185 and D_f = 0.13. This was the last test in the testing sequence.

Analyses have been performed in selected cases and the results are presented in Figures 6-1 through 6-9. The results are presented in the same terms as the experimental results of Figures 5-13 through 5-39, to which they should be compared. For the numerical solution of Eqs. (6.1) through (6.5) a technique appropriate for stiff differential equations has been used as described by Mokha et al, 1990a.

The analytical results on the bearing displacement history and base shear-displacement loop compare favorably to the experimental results. It is particularly important to note the ability of the analytical model to predict permanent bearing displacements in the systems with two or no spring units. However, the accuracy of the analytical prediction is not as good as in earlier studies of the authors with other sliding isolation systems (Mokha et al, 1990a). Major reason for this difference is the lack of precise knowledge of the coefficient of friction.

The analytical results on the structural shear and sixth floor displacement histories compare well to the experimental results only in the initial portion of each record and show marked differences in the tail of each record. As discussed earlier, this difference in the tail is caused by the rocking motion of the table which was not accounted for in the analysis.

In an attempt to provide analytical interpretation of this phenomenon we selected the case of the system with four spring units and Pacoima S16E (0.84g) input (Figures 5-24 and 6-2). This is a case with marked difference between the tails of analytical and experimental responses. We determined the rocking motion of the table from the vertical acceleration records from accelerometers which were placed above each sliding bearing (see Figure 2-2 for instrumentation diagram). This was not the exact rocking motion of the table as some filtering occurred in the Adiprene discs of the sliding bearings. The equations of motion were modified to account for rocking input and the results of this analysis are shown in Figure 6-10. A comparison of this figure to Figure 5-24 (experimental response) shows a good agreement between the analytical and experimental results. Indeed the rocking table input is responsible for the peculiar tail of the observed response.

The importance of the accidental average bearing inclination is demonstrated in Figure 6-11, which compares analytical bearing displacement histories to the experimental one for the system without spring units and Hachinohe 100% (0.21g) input. When the measured value of $\delta = 0.4$ degrees was used, the analysis gave results in very

good accord with the experiment. However, when a value of $\delta = 0$ (perfectly leveled bearings) was used, the bearing followed a different path with much lower permanent displacement.

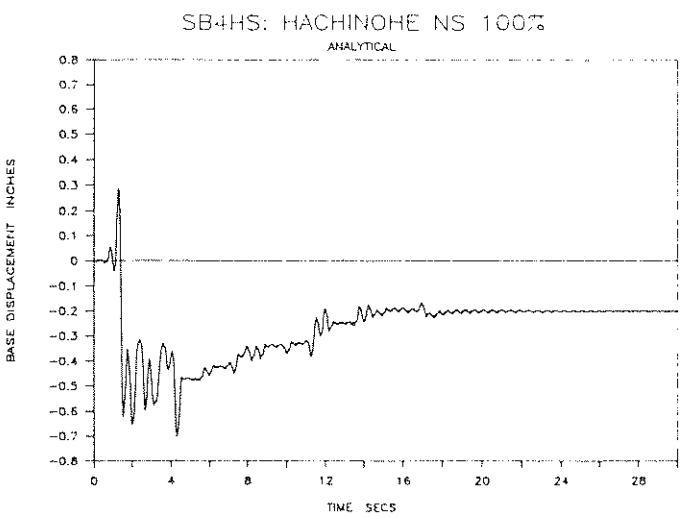

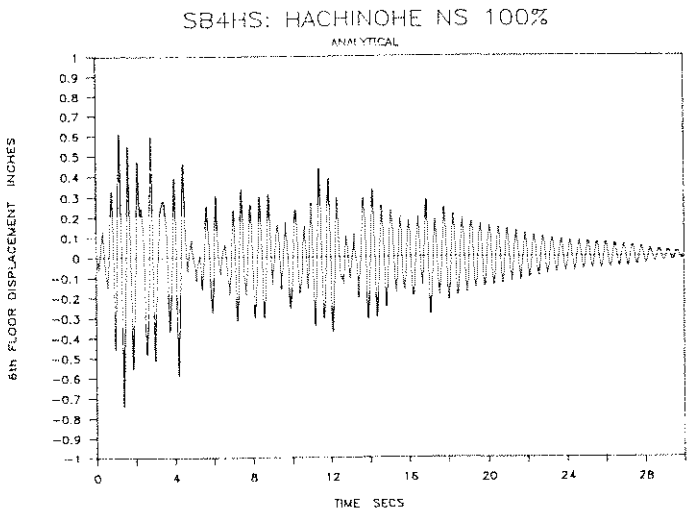

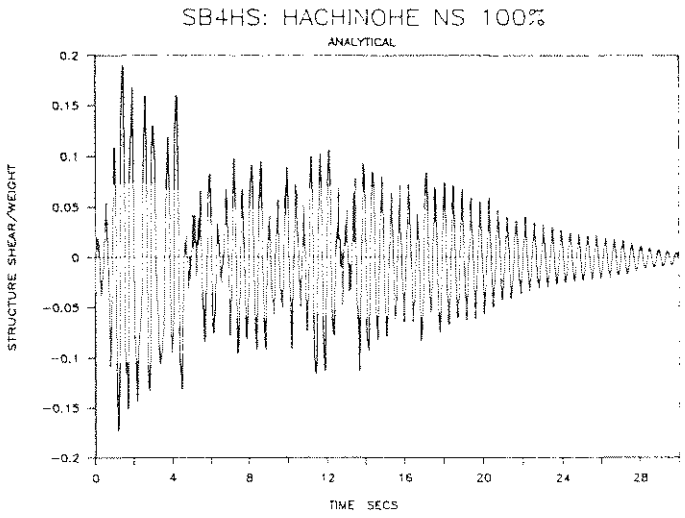

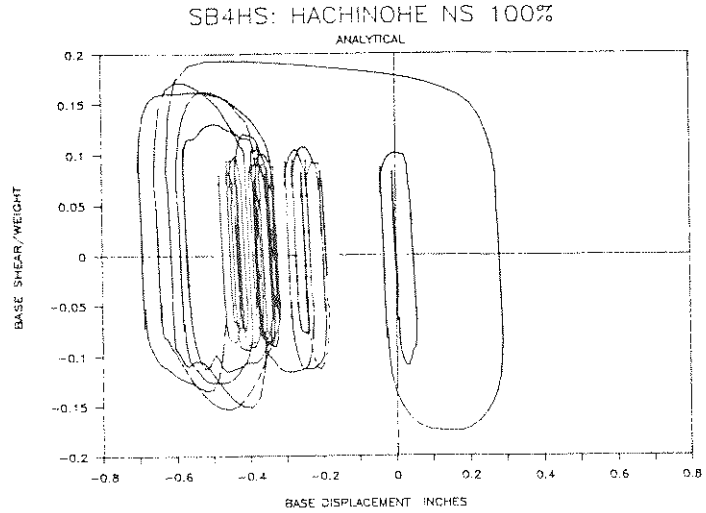

Fig. 6-1 - Analytical Time Histories of Base (Bearing) Displacement, Structure Shear and Sixth-Floor Displacement with Respect to Base and Base Shear-Bearing Displacement Loop in Case of Isolation System with Four Spring Units and for Hachinohe NS Input (0.22g peak table acceleration). Compare with Figure 5-14.

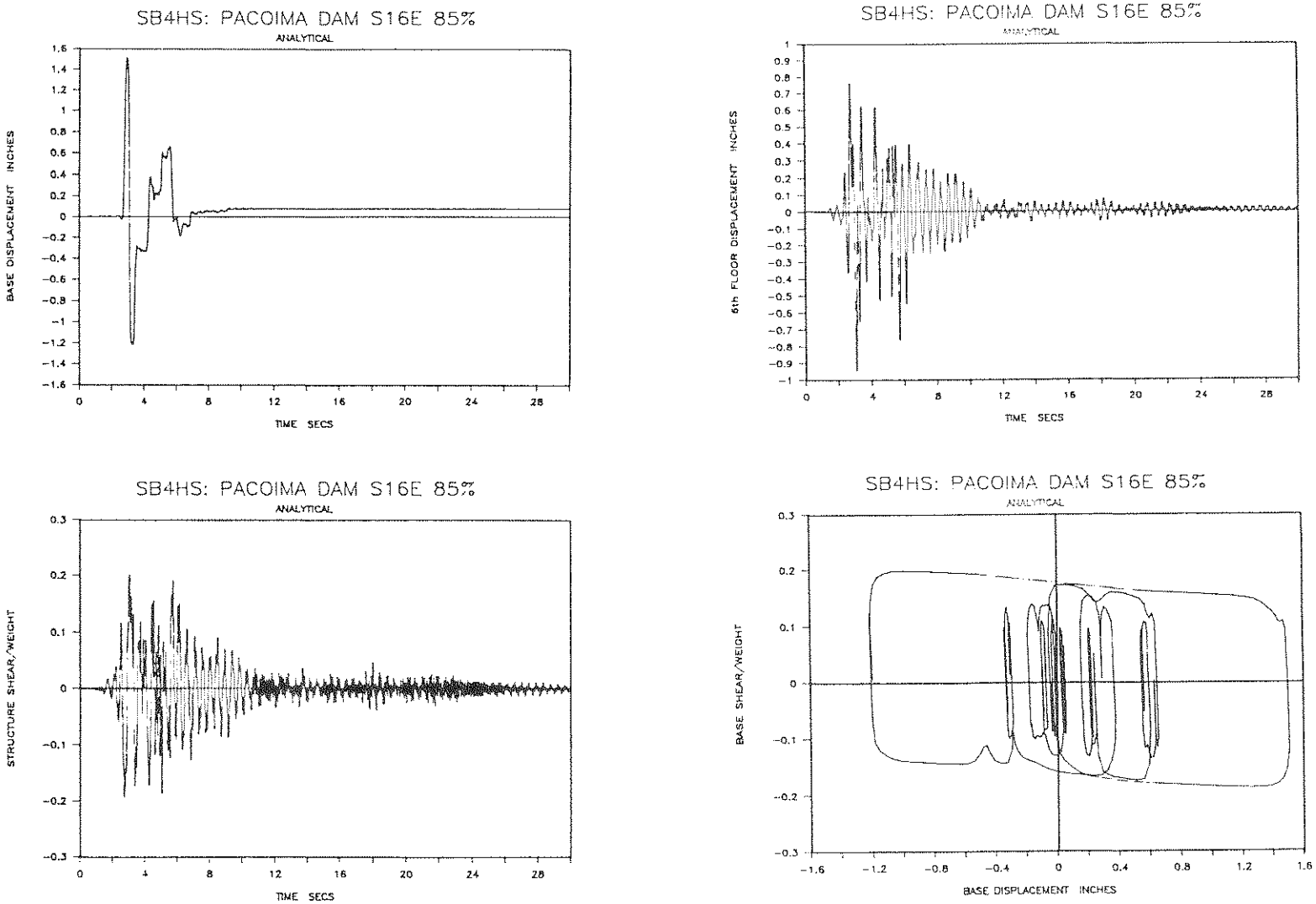

Fig. 6-2 - Analytical Time Histories of Base (Bearing) Displacement, Structure Shear and Sixth-Floor Displacement with Respect to Base and Base Shear-Bearing Displacement Loop in Case of Isolation System with Four Spring Units and for Pacoima S16E Input (0.84g peak table acceleration). Compare with Figure 5-24.

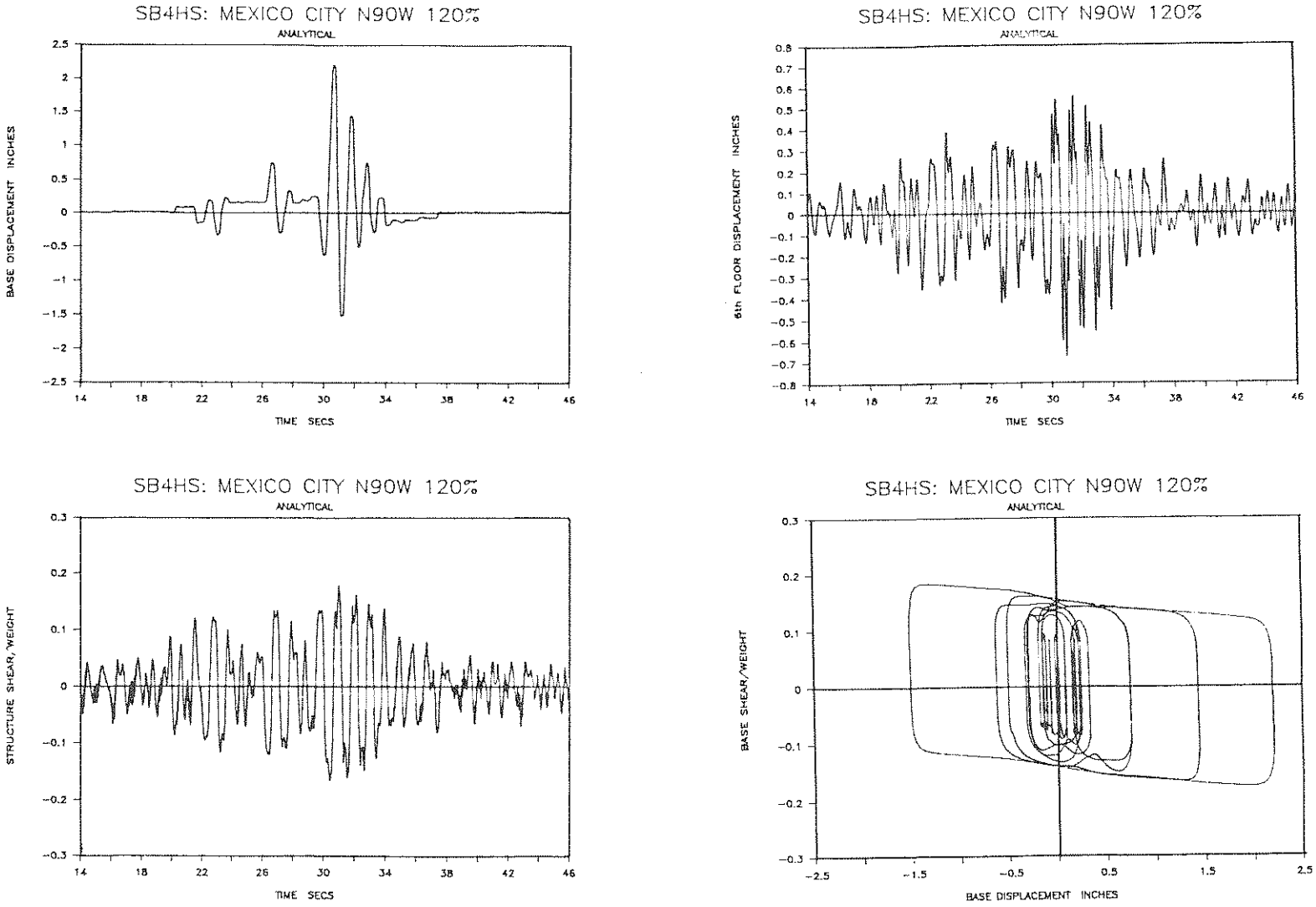

Fig. 6-3 - Analytical Time Histories of Base (Bearing) Displacement, Structure Shear and Sixth-Floor Displacement with Respect to Base and Base Shear-Bearing Displacement Loop in Case of Isolation System with Four Spring Units and for Mexico City N90W Input (0.21g peak table acceleration). Compare with Figure 5-28.

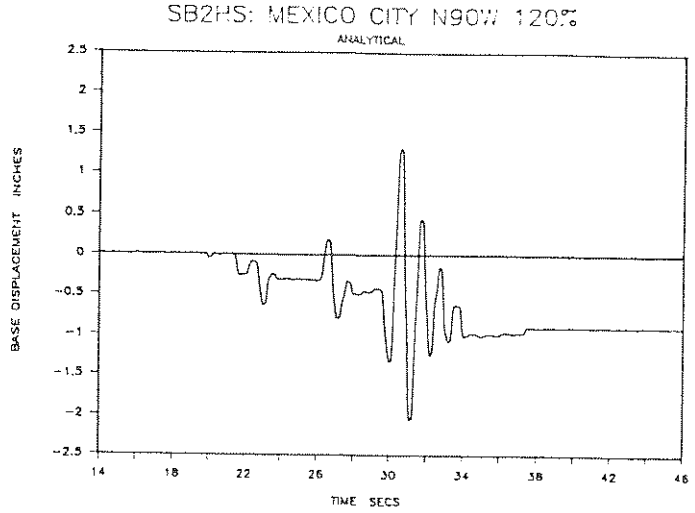

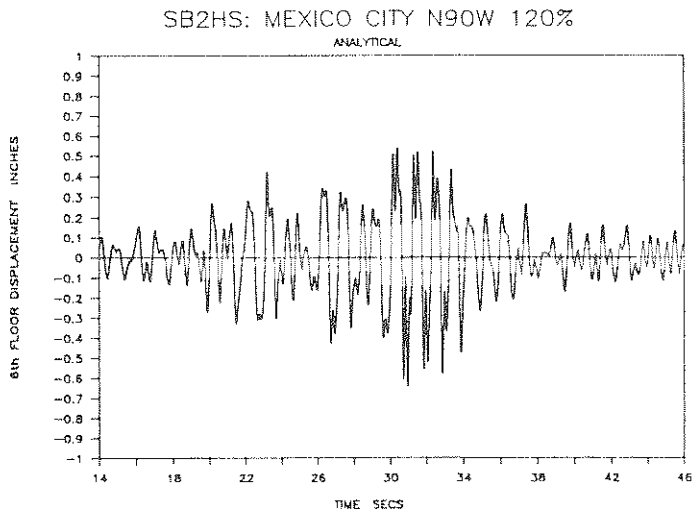

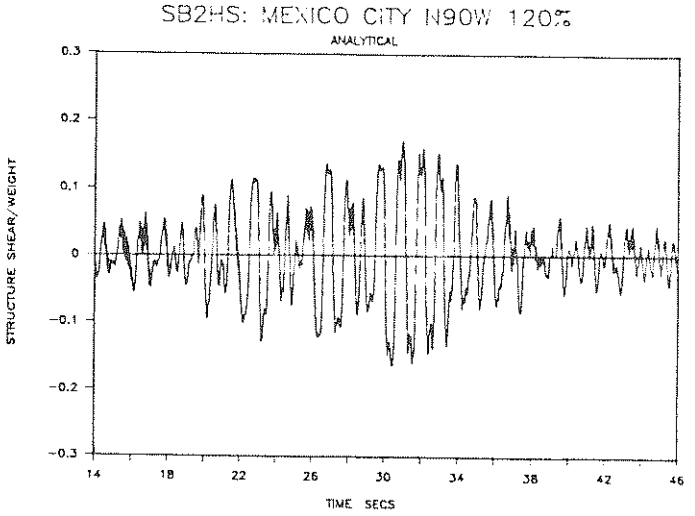

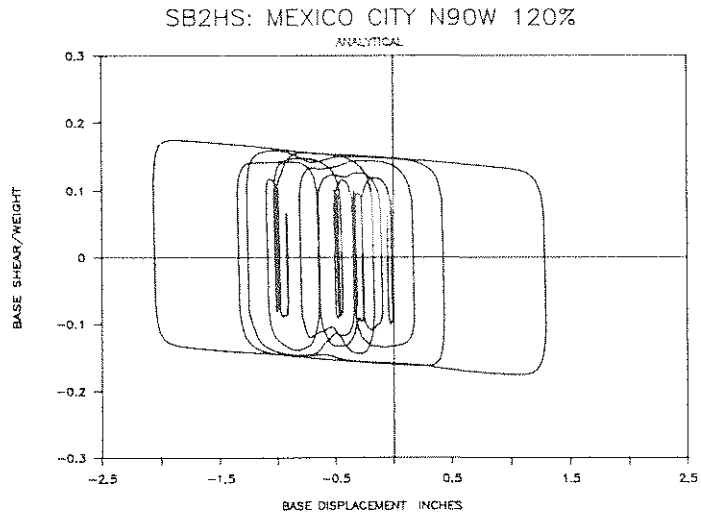

Fig. 6-4 - Analytical Time Histories of Base (Bearing) Displacement, Structure Shear and Sixth-Floor Displacement with Respect to Base and Base Shear-Bearing Displacement Loop in Case of Isolation System with Two Spring Units and for Mexico City N90W Input (0.21g peak table acceleration). Compare with Figure 5-29.

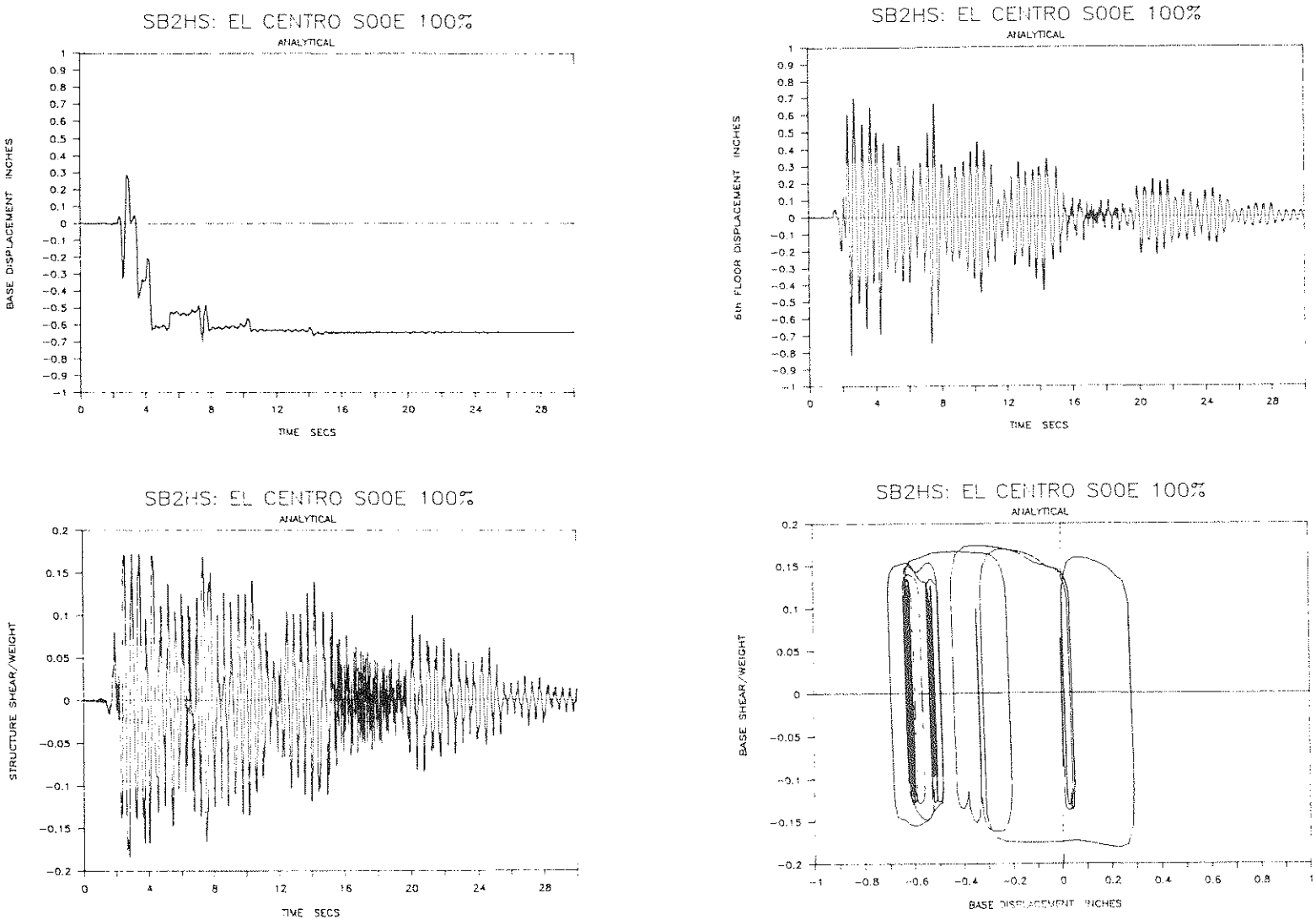

Fig. 6-5 - Analytical Time Histories of Base (Bearing) Displacement, Structure Shear and Sixth-Floor Displacement with Respect to Base and Base Shear-Bearing Displacement Loop in Case of Isolation System with Two Spring Units and for El Centro S00E Input (0.28g peak table acceleration). Compare with Figure 5-30.

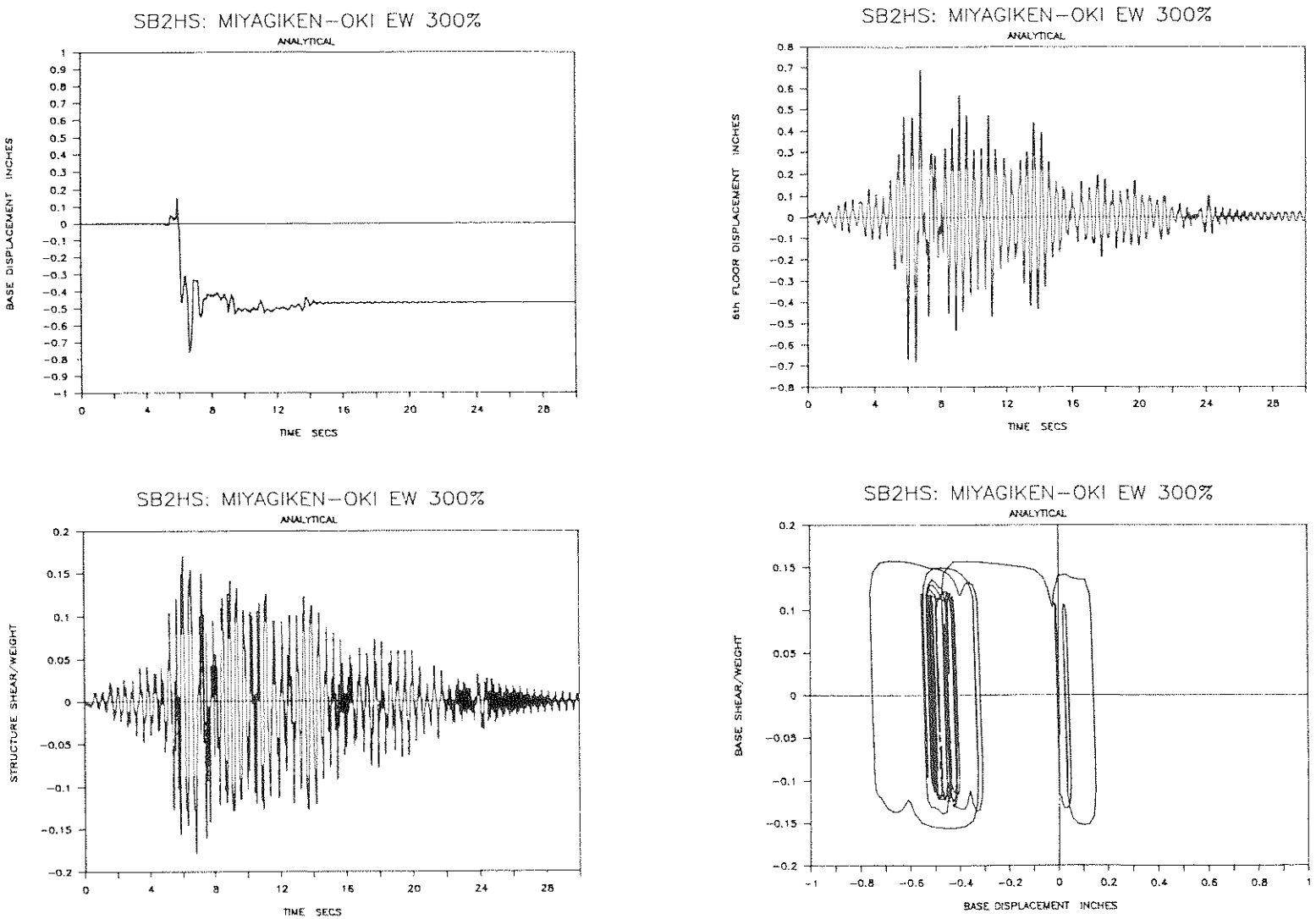

Fig. 6-6 - Analytical Time Histories of Base (Bearing) Displacement, Structure Shear and Sixth-Floor Displacement with Respect to Base and Base Shear-Bearing Displacement Loop in Case of Isolation System with Two Spring Units and for Miyagiken-Oki Input (0.42g peak table acceleration). Compare with Figure 5-32.

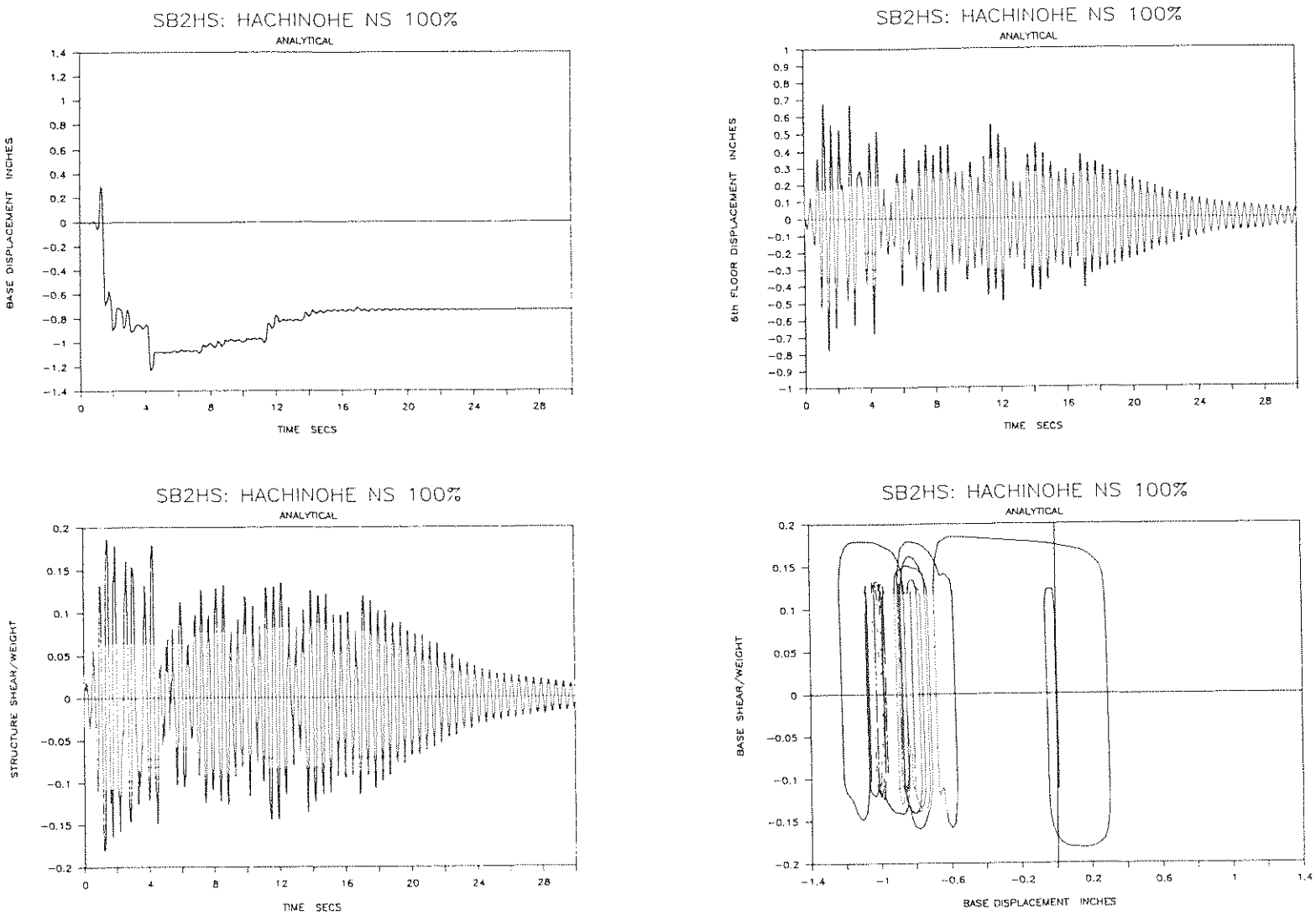

Fig. 6-7 - Analytical Time Histories of Base (Bearing) Displacement, Structure Shear and Sixth-Floor Displacement with Respect to Base and Base Shear-Bearing Displacement Loop in Case of Isolation System with Two Spring Units and for Hachinohe NS Input (0.22g peak table acceleration). Compare with Figure 5-35.

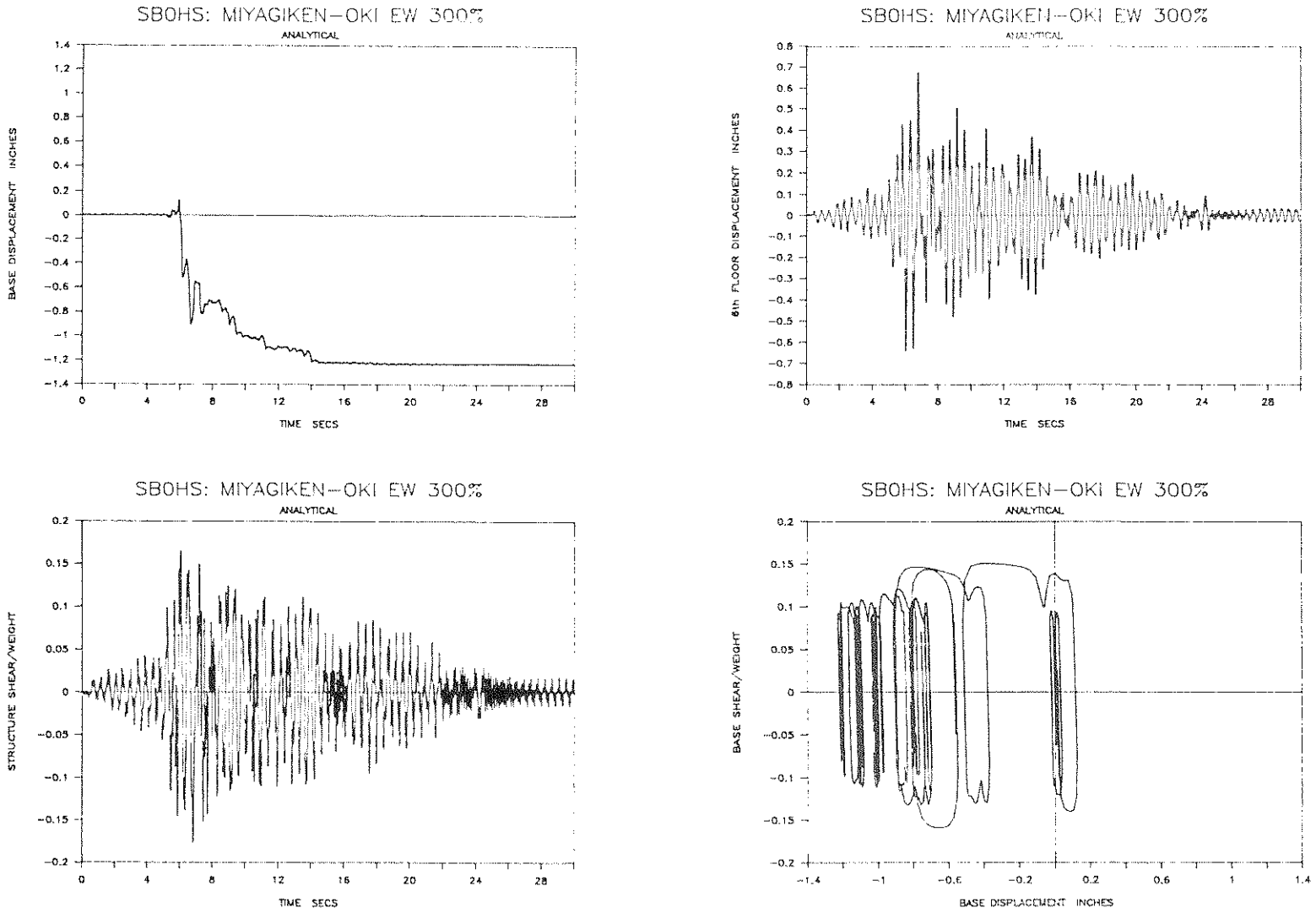

Fig. 6-8 - Analytical Time Histories of Base (Bearing) Displacement, Structure Shear and Sixth-Floor Displacement with Respect to Base and Base Shear-Bearing Displacement Loop in Case of Isolation System Without Spring Units and for Miyagiken-Oki EW Input (0.43g peak table acceleration). Compare with Figure 5-38.

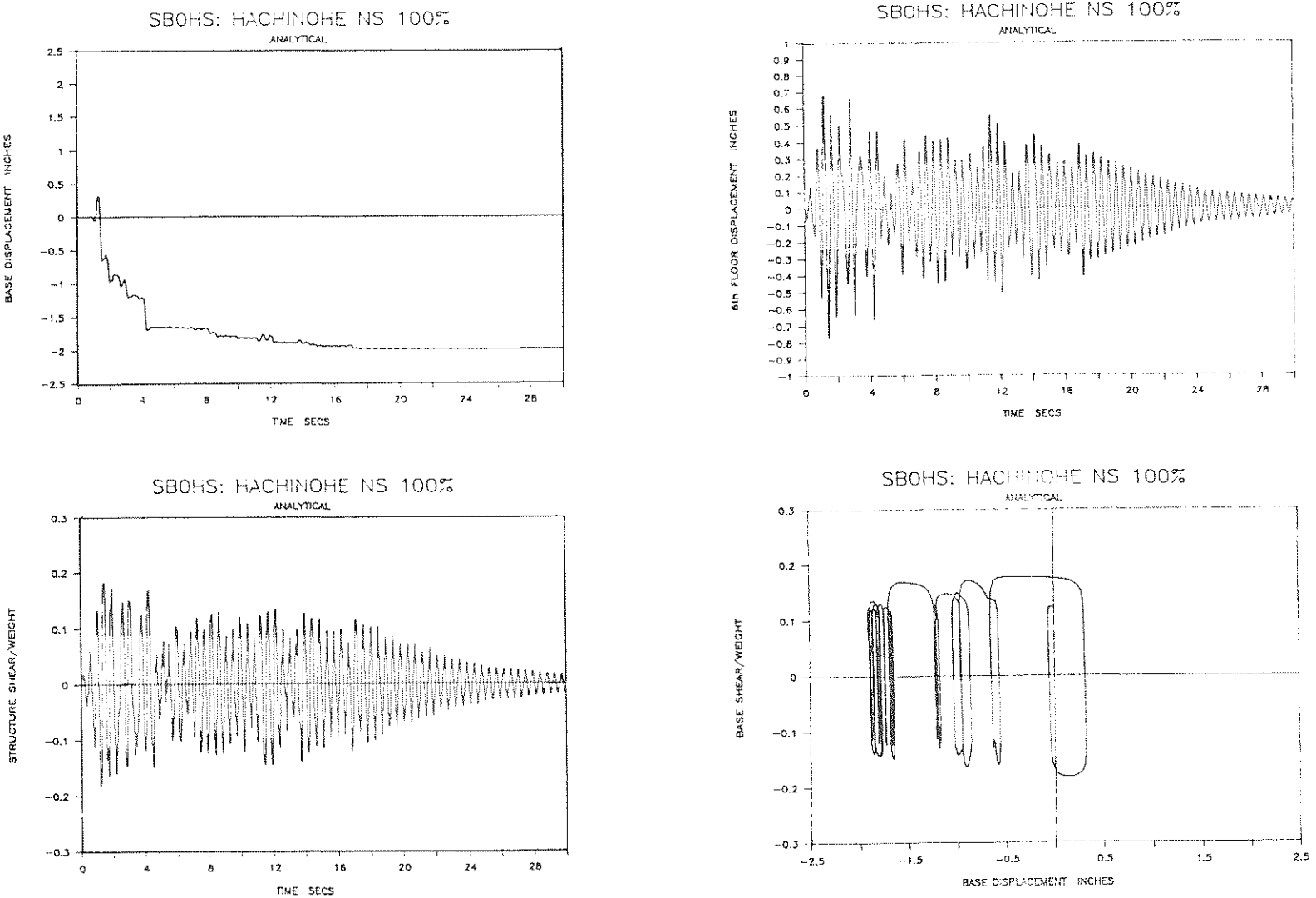

Fig. 6-9 - Analytical Time Histories of Base (Bearing) Displacement, Structure Shear and Sixth-Floor Displacement with Respect to Base and Base Shear-Bearing Displacement Loop in Case of Isolation System Without Spring Units and for Hachinohe NS Input (0.21g peak table acceleration). Compare with Figure 5-39.

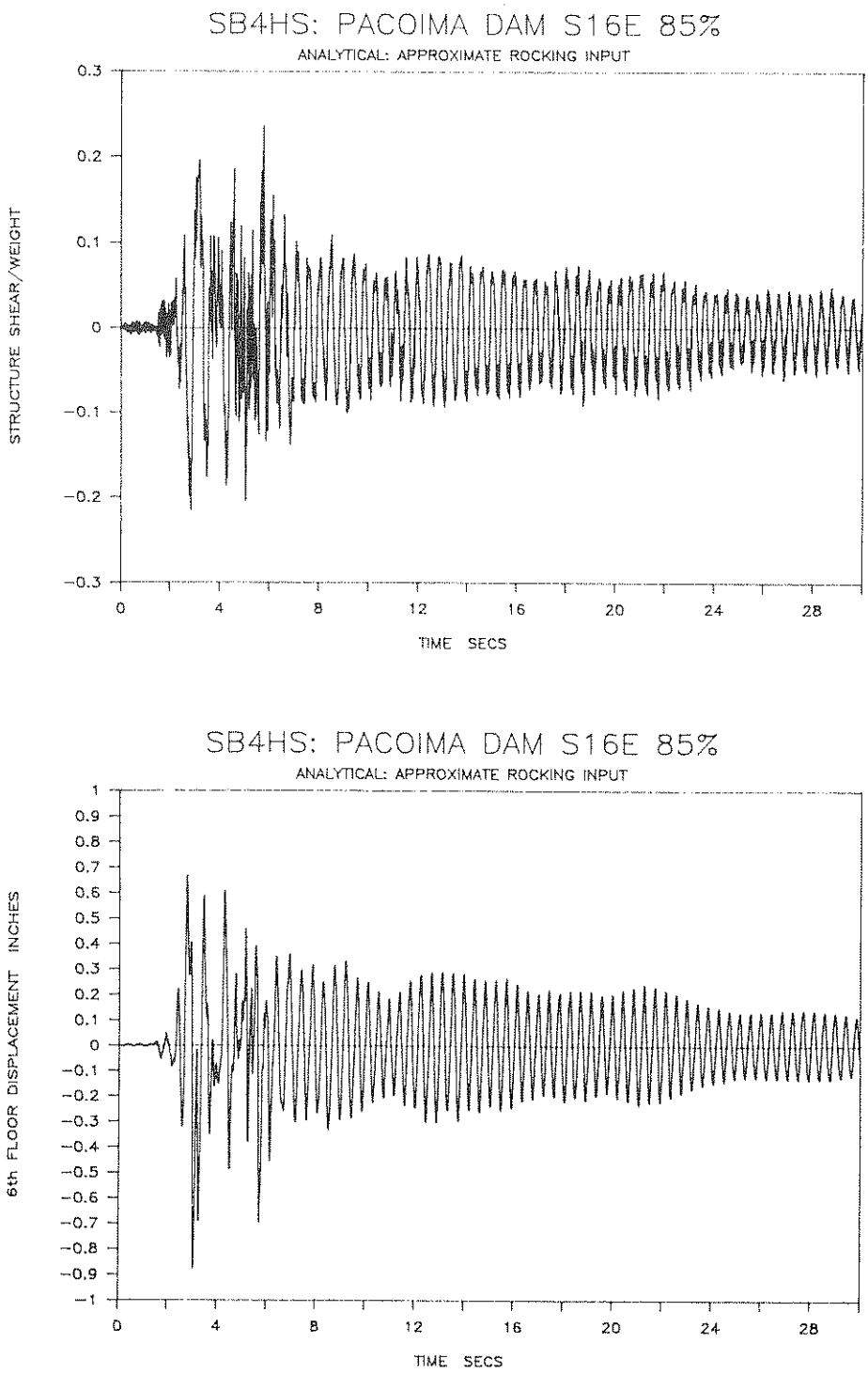

Fig. 6-10 - Analytical Time Histories of Structure Shear and Sixth-Floor Displacement in Case of Isolation System with Four Spring Units and Pacoima S16E Input (0.84g peak table acceleration). The Rocking Motion of Table Has Been Accounted for. Compare with Figure 5-24.

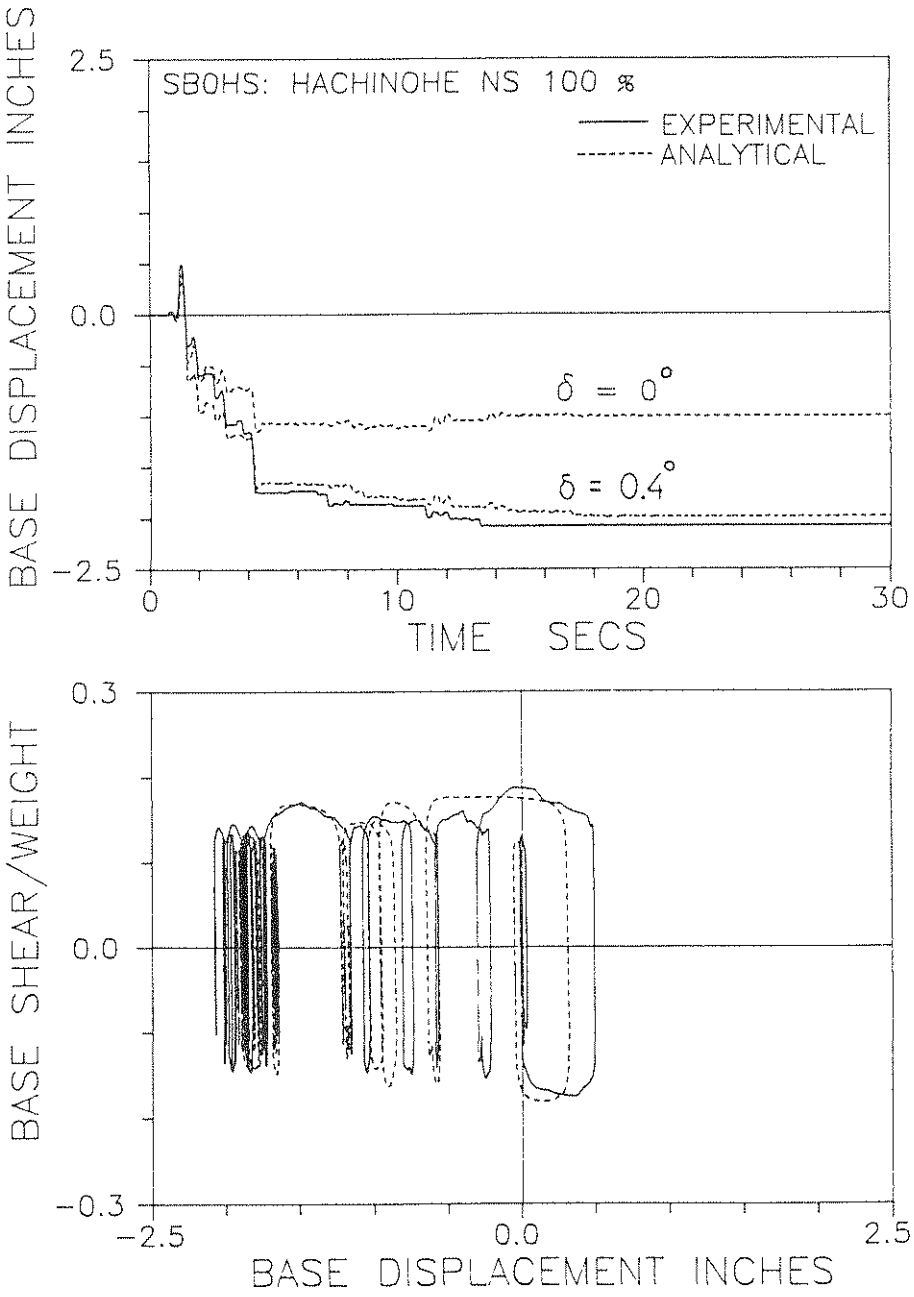

Fig. 6-11 - Comparison of Analytical and Experimental Base (Bearing) Displacement Histories in Case of System Without Spring Units and Hachinohe NS Input (0.21g peak table acceleration). Observe Difference in Bearing Permanent Displacement When Accidental Bearing Inclination is not Accounted.

SECTION 7
CONCLUSIONS

A sliding isolation system consisting of Teflon disc bearings and helical steel springs has been tested with a quarter scale, six-story large aspect ratio model. The helical steel springs provided weak peak restoring force which was always less, by at least a factor of two, than the mobilized peak frictional force. The results show:

1. The system has low sensitivity to the frequency content of input motion. The system performed well for motions of significantly different frequency content, ranging from high frequency like the 1940 El Centro and the 1978 Japanese Miyagiken-Oki to low frequency like the 1985 Mexico City earthquake.
2. The restoring force devices were only effective in reducing bearing displacements and, in particular, in reducing permanent bearing displacements. In the configuration with four spring units, these permanent displacements were less than six percent of the bearing design displacement.
3. Isolation was provided by limiting the force at the isolation interface and not by shifting the fundamental frequency of the system to low values. Actually, the spring units did not at all change the frequency characteristics of the structure.
4. An important consideration in the design of sliding isolation systems is the possible accidental average inclination of the sliding interfaces. As a result of this inclination, friction

is asymmetric. The stiffness of the restoring force devices should be large enough to counteract the effects of this asymmetry.

5. The response of the structure is out of phase with large floor accelerations. However, owing to the out of phase response the accelerations point to opposing directions and lead to reduced story shear, overturning moment and drift.
6. In tests with the El Centro motion the isolated structure could sustain, while elastic, a table acceleration at least three times more than it could sustain under fixed-base conditions.
7. The response of the system could be reliably predicted by analytical techniques.

SECTION 8

REFERENCES

Buckle, I. (1986). "Development and Application of Base Isolation and Passive Energy Dissipation: A World Overview." Proceeding of ATC-17 Seminar on Base Isolation and Passive Energy Dissipation, Applied Technology Council, Palo Alto, Calif., 153-174.

Chalhoub, M.S. and Kelly, J.M. (1989). "Earthquake Simulator Evaluation of a Combined Sliding Bearing and Tension Controlled Rubber Bearing Isolation System." Proceeding, 1989 ASME Pressure Vessels and Piping Conference, American Society of Mechanical Engineers, Hawaii, Vol. 181, 59-64.

Constantinou, M.C., Mokha, A. and Reinhorn, A.M. (1990). "Teflon Bearings in Base Isolation II: Modeling," J. Structural Engng, ASCE, 116(2), 455-474.

Griffith, M.C., Aiken, I.D. and Kelly, J.M. (1988). "Experimental Evaluation of Seismic Isolation of a 9-story Braced Steel Frame Subject to Uplift," Report No. UCB/EERC-88/05, Earthquake Engineering Research Center, University of California, Berkeley, Calif., May.

Kawamura, S. Kitazawa, K., Hisano, M. and Nagashima, I. (1988). "Study of a Sliding-Type Base Isolation System. System Composition and Element Properties." Proceedings of 9th World Conference on Earthquake Engineering, Tokyo-Kyoto, Japan, Vol. V, 735-740.

Kelly, J.M. (1988). "Base Isolation in Japan, 1988". Report No. UCB/EERC-88/20, Earthquake Engineering Research Center, University of California, Berkeley, Calif., December.

Mokha, A. Constantinou, M.C. and Reinhorn, A.M. (1988). "Teflon Bearings in Aseismic Base Isolation. Experimental Studies and Mathematical Modeling." Report No. NCEER-88-0038, National Center for Earthquake Engineering Research, State University of New York, Buffalo, N.Y.

Mokha, A, Constantinou, M.C. and Reinhorn, A.M. (1990a). "Experimental Study and Analytical Prediction of Earthquake Response of The Friction Pendulum Isolation System (FPS)." Report of the National Center for Earthquake Engineering Research, State University of New York, Buffalo, NY, to appear.

Mokha, A., Constantinou and Reinhorn, A.M. (1990b). "Teflon Bearings in Base Isolation I: Testing." J. Structural Engng., ASCE, 116(2), 438-454.

Mokha, A., Constantinou, M.C. and Reinhorn, A.M. (1990c). "Further Results on the Frictional Properties of Teflon Bearings." J. Structural Engineering, ASCE, to appear.

Mostaghel, N. and Khodaverdian, M. (1987). "Dynamics of Resilient Friction Base Isolator (R-FBI)." Earthquake Engineering and Structural Dynamics, 15(3), 379-390.

Structural Engineers Association of California (1990). "Tentative General Requirements for the Design and Construction of Seismic-Isolated Structures." Appendix IL of Recommended Lateral Force Requirements and Commentary (Blue Book).

Zayas, V., Low, S.S. and Mahin, S.A. (1987). "The FPS Earthquake Resisting System, Experimental Report." Report No. UCB/EERC- 87/01, Earthquake Engineering Research Center, University of California, Berkeley, Calif., June.

NATIONAL CENTER FOR EARTHQUAKE ENGINEERING RESEARCH
LIST OF TECHNICAL REPORTS

The National Center for Earthquake Engineering Research (NCEER) publishes technical reports on a variety of subjects related to earthquake engineering written by authors funded through NCEER. These reports are available from both NCEER's Publications Department and the National Technical Information Service (NTIS). Requests for reports should be directed to the Publications Department, National Center for Earthquake Engineering Research, State University of New York at Buffalo, Red Jacket Quadrangle, Buffalo, New York 14261. Reports can also be requested through NTIS, 5285 Port Royal Road, Springfield, Virginia 22161. NTIS accession numbers are shown in parenthesis, if available.

NCEER-87-0001 "First-Year Program in Research, Education and Technology Transfer," 3/5/87, (PB88-134275/AS).

NCEER-87-0002 "Experimental Evaluation of Instantaneous Optimal Algorithms for Structural Control," by R.C. Lin, T.T. Soong and A.M. Reinhorn, 4/20/87, (PB88-134341/AS).

NCEER-87-0003 "Experimentation Using the Earthquake Simulation Facilities at University at Buffalo," by A.M. Reinhorn and R.L. Ketter, to be published.

NCEER-87-0004 "The System Characteristics and Performance of a Shaking Table," by J.S. Hwang, K.C. Chang and G.C. Lee, 6/1/87, (PB88-134259/AS). This report is available only through NTIS (see address given above).

NCEER-87-0005 "A Finite Element Formulation for Nonlinear Viscoplastic Material Using a Q Model," by O. Gyebi and G. Dasgupta, 11/2/87, (PB88-213764/AS).

NCEER-87-0006 "Symbolic Manipulation Program (SMP) - Algebraic Codes for Two and Three Dimensional Finite Element Formulations," by X. Lee and G. Dasgupta, 11/9/87, (PB88-219522/AS).

NCEER-87-0007 "Instantaneous Optimal Control Laws for Tall Buildings Under Seismic Excitations," by J.N. Yang, A. Akbarpour and P. Ghaemmaghami, 6/10/87, (PB88-134333/AS).

NCEER-87-0008 "IDARC: Inelastic Damage Analysis of Reinforced Concrete Frame - Shear-Wall Structures," by Y.J. Park, A.M. Reinhorn and S.K. Kunnath, 7/20/87, (PB88-134325/AS).

NCEER-87-0009 "Liquefaction Potential for New York State: A Preliminary Report on Sites in Manhattan and Buffalo," by M. Budhu, V. Vijayakumar, R.F. Giese and L. Baumgras, 8/31/87, (PB88-163704/AS). This report is available only through NTIS (see address given above).

NCEER-87-0010 "Vertical and Torsional Vibration of Foundations in Inhomogeneous Media," by A.S. Veletsos and K.W. Dotson, 6/1/87, (PB88-134291/AS).

NCEER-87-0011 "Seismic Probabilistic Risk Assessment and Seismic Margins Studies for Nuclear Power Plants," by Howard H.M. Hwang, 6/15/87, (PB88-134267/AS).

NCEER-87-0012 "Parametric Studies of Frequency Response of Secondary Systems Under Ground-Acceleration Excitations," by Y. Yong and Y.K. Lin, 6/10/87, (PB88-134309/AS).

NCEER-87-0013 "Frequency Response of Secondary Systems Under Seismic Excitation," by J.A. HoLung, J. Cai and Y.K. Lin, 7/31/87, (PB88-134317/AS).

NCEER-87-0014 "Modelling Earthquake Ground Motions in Seismically Active Regions Using Parametric Time Series Methods," by G.W. Ellis and A.S. Cakmak, 8/25/87, (PB88-134283/AS).

NCEER-87-0015 "Detection and Assessment of Seismic Structural Damage," by E. DiPasquale and A.S. Cakmak, 8/25/87, (PB88-163712/AS).

NCEER-87-0016 "Pipeline Experiment at Parkfield, California," by J. Isenberg and E. Richardson, 9/15/87, (PB88-163720/AS). This report is available only through NTIS (see address given above).

NCEER-87-0017 "Digital Simulation of Seismic Ground Motion," by M. Shinozuka, G. Deodatis and T. Harada, 8/31/87, (PB88-155197/AS). This report is available only through NTIS (see address given above).

NCEER-87-0018 "Practical Considerations for Structural Control: System Uncertainty, System Time Delay and Truncation of Small Control Forces," J.N. Yang and A. Akbarpour, 8/10/87, (PB88-163738/AS).

NCEER-87-0019 "Modal Analysis of Nonclassically Damped Structural Systems Using Canonical Transformation," by J.N. Yang, S. Sarkani and F.X. Long, 9/27/87, (PB88-187851/AS).

NCEER-87-0020 "A Nonstationary Solution in Random Vibration Theory," by J.R. Red-Horse and P.D. Spanos, 11/3/87, (PB88-163746/AS).

NCEER-87-0021 "Horizontal Impedances for Radially Inhomogeneous Viscoelastic Soil Layers," by A.S. Veletsos and K.W. Dotson, 10/15/87, (PB88-150859/AS).

NCEER-87-0022 "Seismic Damage Assessment of Reinforced Concrete Members," by Y.S. Chung, C. Meyer and M. Shinozuka, 10/9/87, (PB88-150867/AS). This report is available only through NTIS (see address given above).

NCEER-87-0023 "Active Structural Control in Civil Engineering," by T.T. Soong, 11/11/87, (PB88-187778/AS).

NCEER-87-0024 Vertical and Torsional Impedances for Radially Inhomogeneous Viscoelastic Soil Layers," by K.W. Dotson and A.S. Veletsos, 12/87, (PB88-187786/AS).

NCEER-87-0025 "Proceedings from the Symposium on Seismic Hazards, Ground Motions, Soil-Liquefaction and Engineering Practice in Eastern North America," October 20-22, 1987, edited by K.H. Jacob, 12/87, (PB88-188115/AS).

NCEER-87-0026 "Report on the Whittier-Narrows, California, Earthquake of October 1, 1987," by J. Pantelic and A. Reinhorn, 11/87, (PB88-187752/AS). This report is available only through NTIS (see address given above).

NCEER-87-0027 "Design of a Modular Program for Transient Nonlinear Analysis of Large 3-D Building Structures," by S. Srivastav and J.F. Abel, 12/30/87, (PB88-187950/AS).

NCEER-87-0028 "Second-Year Program in Research, Education and Technology Transfer," 3/8/88, (PB88-219480/AS).

NCEER-88-0001 "Workshop on Seismic Computer Analysis and Design of Buildings With Interactive Graphics," by W. McGuire, J.F. Abel and C.H. Conley, 1/18/88, (PB88-187760/AS).

NCEER-88-0002 "Optimal Control of Nonlinear Flexible Structures," by J.N. Yang, F.X. Long and D. Wong, 1/22/88, (PB88-213772/AS).

NCEER-88-0003 "Substructuring Techniques in the Time Domain for Primary-Secondary Structural Systems," by G.D. Manolis and G. Juhn, 2/10/88, (PB88-213780/AS).

NCEER-88-0004 "Iterative Seismic Analysis of Primary-Secondary Systems," by A. Singhal, L.D. Lutes and P.D. Spanos, 2/23/88, (PB88-213798/AS).

NCEER-88-0005 "Stochastic Finite Element Expansion for Random Media," by P.D. Spanos and R. Ghanem, 3/14/88, (PB88-213806/AS).

NCEER-88-0006 "Combining Structural Optimization and Structural Control," by F.Y. Cheng and C.P. Pantelides, 1/10/88, (PB88-213814/AS).

NCEER-88-0007 "Seismic Performance Assessment of Code-Designed Structures," by H.H-M. Hwang, J-W. Jaw and H-J. Shau, 3/20/88, (PB88-219423/AS).

NCEER-88-0008 "Reliability Analysis of Code-Designed Structures Under Natural Hazards," by H.H-M. Hwang, H. Ushiba and M. Shinozuka, 2/29/88, (PB88-229471/AS).

NCEER-88-0009 "Seismic Fragility Analysis of Shear Wall Structures," by J-W Jaw and H.H-M. Hwang, 4/30/88, (PB89-102867/AS).

NCEER-88-0010 "Base Isolation of a Multi-Story Building Under a Harmonic Ground Motion - A Comparison of Performances of Various Systems," by F-G Fan, G. Ahmadi and I.G. Tadjbakhsh, 5/18/88, (PB89-122238/AS).

NCEER-88-0011 "Seismic Floor Response Spectra for a Combined System by Green's Functions," by F.M. Lavelle, L.A. Bergman and P.D. Spanos, 5/1/88, (PB89-102875/AS).

NCEER-88-0012 "A New Solution Technique for Randomly Excited Hysteretic Structures," by G.Q. Cai and Y.K. Lin, 5/16/88, (PB89-102883/AS).

NCEER-88-0013 "A Study of Radiation Damping and Soil-Structure Interaction Effects in the Centrifuge," by K. Weissman, supervised by J.H. Prevost, 5/24/88, (PB89-144703/AS).

NCEER-88-0014 "Parameter Identification and Implementation of a Kinematic Plasticity Model for Frictional Soils," by J.H. Prevost and D.V. Griffiths, to be published.

NCEER-88-0015 "Two- and Three- Dimensional Dynamic Finite Element Analyses of the Long Valley Dam," by D.V. Griffiths and J.H. Prevost, 6/17/88, (PB89-144711/AS).

NCEER-88-0016 "Damage Assessment of Reinforced Concrete Structures in Eastern United States," by A.M. Reinhorn, M.J. Seidel, S.K. Kunnath and Y.J. Park, 6/15/88, (PB89-122220/AS).

NCEER-88-0017 "Dynamic Compliance of Vertically Loaded Strip Foundations in Multilayered Viscoelastic Soils," by S. Ahmad and A.S.M. Israil, 6/17/88, (PB89-102891/AS).

NCEER-88-0018 "An Experimental Study of Seismic Structural Response With Added Viscoelastic Dampers," by R.C. Lin, Z. Liang, T.T. Soong and R.H. Zhang, 6/30/88, (PB89-122212/AS).

NCEER-88-0019 "Experimental Investigation of Primary - Secondary System Interaction," by G.D. Manolis, G. Juhn and A.M. Reinhorn, 5/27/88, (PB89-122204/AS).

NCEER-88-0020 "A Response Spectrum Approach For Analysis of Nonclassically Damped Structures," by J.N. Yang, S. Sarkani and F.X. Long, 4/22/88, (PB89-102909/AS).

NCEER-88-0021 "Seismic Interaction of Structures and Soils: Stochastic Approach," by A.S. Veletsos and A.M. Prasad, 7/21/88, (PB89-122196/AS).

NCEER-88-0022 "Identification of the Serviceability Limit State and Detection of Seismic Structural Damage," by E. DiPasquale and A.S. Cakmak, 6/15/88, (PB89-122188/AS).

NCEER-88-0023 "Multi-Hazard Risk Analysis: Case of a Simple Offshore Structure," by B.K. Bhartia and E.H. Vanmarcke, 7/21/88, (PB89-145213/AS).

NCEER-88-0024 "Automated Seismic Design of Reinforced Concrete Buildings," by Y.S. Chung, C. Meyer and M. Shinozuka, 7/5/88, (PB89-122170/AS).

NCEER-88-0025 "Experimental Study of Active Control of MDOF Structures Under Seismic Excitations," by L.L. Chung, R.C. Lin, T.T. Soong and A.M. Reinhorn, 7/10/88, (PB89-122600/AS).

NCEER-88-0026 "Earthquake Simulation Tests of a Low-Rise Metal Structure," by J.S. Hwang, K.C. Chang, G.C. Lee and R.L. Ketter, 8/1/88, (PB89-102917/AS).

NCEER-88-0027 "Systems Study of Urban Response and Reconstruction Due to Catastrophic Earthquakes," by F. Kozin and H.K. Zhou, 9/22/88, (PB90-162348/AS).

NCEER-88-0028 "Seismic Fragility Analysis of Plane Frame Structures," by H.H-M. Hwang and Y.K. Low, 7/31/88, (PB89-131445/AS).

NCEER-88-0029 "Response Analysis of Stochastic Structures," by A. Kardara, C. Bucher and M. Shinozuka, 9/22/88, (PB89-174429/AS).

NCEER-88-0030 "Nonnormal Accelerations Due to Yielding in a Primary Structure," by D.C.K. Chen and L.D. Lutes, 9/19/88, (PB89-131437/AS).

NCEER-88-0031 "Design Approaches for Soil-Structure Interaction," by A.S. Veletsos, A.M. Prasad and Y. Tang, 12/30/88, (PB89-174437/AS).

NCEER-88-0032 "A Re-evaluation of Design Spectra for Seismic Damage Control," by C.J. Turkstra and A.G. Tallin, 11/7/88, (PB89-145221/AS).

NCEER-88-0033 "The Behavior and Design of Noncontact Lap Splices Subjected to Repeated Inelastic Tensile Loading," by V.E. Sagan, P. Gergely and R.N. White, 12/8/88, (PB89-163737/AS).

NCEER-88-0034 "Seismic Response of Pile Foundations," by S.M. Mamoon, P.K. Banerjee and S. Ahmad, 11/1/88, (PB89-145239/AS).

NCEER-88-0035 "Modeling of R/C Building Structures With Flexible Floor Diaphragms (IDARC2)," by A.M. Reinhorn, S.K. Kunnath and N. Panahshahi, 9/7/88, (PB89-207153/AS).

NCEER-88-0036 "Solution of the Dam-Reservoir Interaction Problem Using a Combination of FEM, BEM with Particular Integrals, Modal Analysis, and Substructuring," by C-S. Tsai, G.C. Lee and R.L. Ketter, 12/31/88, (PB89-207146/AS).

NCEER-88-0037 "Optimal Placement of Actuators for Structural Control," by F.Y. Cheng and C.P. Pantelides, 8/15/88, (PB89-162846/AS).

NCEER-88-0038 "Teflon Bearings in Aseismic Base Isolation: Experimental Studies and Mathematical Modeling," by A. Mokha, M.C. Constantinou and A.M. Reinhorn, 12/5/88, (PB89-218457/AS).

NCEER-88-0039 "Seismic Behavior of Flat Slab High-Rise Buildings in the New York City Area," by P. Weidlinger and M. Ettouney, 10/15/88, (PB90-145681/AS).

NCEER-88-0040 "Evaluation of the Earthquake Resistance of Existing Buildings in New York City," by P. Weidlinger and M. Ettouney, 10/15/88, to be published.

NCEER-88-0041 "Small-Scale Modeling Techniques for Reinforced Concrete Structures Subjected to Seismic Loads," by W. Kim, A. El-Attar and R.N. White, 11/22/88, (PB89-189625/AS).

NCEER-88-0042 "Modeling Strong Ground Motion from Multiple Event Earthquakes," by G.W. Ellis and A.S. Cakmak, 10/15/88, (PB89-174445/AS).

NCEER-88-0043 "Nonstationary Models of Seismic Ground Acceleration," by M. Grigoriu, S.E. Ruiz and E. Rosenblueth, 7/15/88, (PB89-189617/AS).

NCEER-88-0044 "SARCF User's Guide: Seismic Analysis of Reinforced Concrete Frames," by Y.S. Chung, C. Meyer and M. Shinozuka, 11/9/88, (PB89-174452/AS).

NCEER-88-0045 "First Expert Panel Meeting on Disaster Research and Planning," edited by J. Pantelic and J. Stoyle, 9/15/88, (PB89-174460/AS).

NCEER-88-0046 "Preliminary Studies of the Effect of Degrading Infill Walls on the Nonlinear Seismic Response of Steel Frames," by C.Z. Chrysostomou, P. Gergely and J.F. Abel, 12/19/88, (PB89-208383/AS).

NCEER-88-0047 "Reinforced Concrete Frame Component Testing Facility - Design, Construction, Instrumentation and Operation," by S.P. Pessiki, C. Conley, T. Bond, P. Gergely and R.N. White, 12/16/88, (PB89-174478/AS).

NCEER-89-0001 "Effects of Protective Cushion and Soil Compliancy on the Response of Equipment Within a Seismically Excited Building," by J.A. HoLung, 2/16/89, (PB89-207179/AS).

NCEER-89-0002 "Statistical Evaluation of Response Modification Factors for Reinforced Concrete Structures," by H.H-M. Hwang and J-W. Jaw, 2/17/89, (PB89-207187/AS).

NCEER-89-0003 "Hysteretic Columns Under Random Excitation," by G-Q. Cai and Y.K. Lin, 1/9/89, (PB89-196513/AS).

NCEER-89-0004 "Experimental Study of 'Elephant Foot Bulge' Instability of Thin-Walled Metal Tanks," by Z-H. Jia and R.L. Ketter, 2/22/89, (PB89-207195/AS).

NCEER-89-0005 "Experiment on Performance of Buried Pipelines Across San Andreas Fault," by J. Isenberg, E. Richardson and T.D. O'Rourke, 3/10/89, (PB89-218440/AS).

NCEER-89-0006 "A Knowledge-Based Approach to Structural Design of Earthquake-Resistant Buildings," by M. Subramani, P. Gergely, C.H. Conley, J.F. Abel and A.H. Zaghw, 1/15/89, (PB89-218465/AS).

NCEER-89-0007 "Liquefaction Hazards and Their Effects on Buried Pipelines," by T.D. O'Rourke and P.A. Lane, 2/1/89, (PB89-218481).

NCEER-89-0008 "Fundamentals of System Identification in Structural Dynamics," by H. Imai, C-B. Yun, O. Maruyama and M. Shinozuka, 1/26/89, (PB89-207211/AS).

NCEER-89-0009 "Effects of the 1985 Michoacan Earthquake on Water Systems and Other Buried Lifelines in Mexico," by A.G. Ayala and M.J. O'Rourke, 3/8/89, (PB89-207229/AS).

NCEER-89-R010 "NCEER Bibliography of Earthquake Education Materials," by K.E.K. Ross, Second Revision, 9/1/89, (PB90-125352/AS).

NCEER-89-0011 "Inelastic Three-Dimensional Response Analysis of Reinforced Concrete Building Structures (IDARC-3D), Part I - Modeling," by S.K. Kunnath and A.M. Reinhorn, 4/17/89, (PB90-114612/AS).

NCEER-89-0012 "Recommended Modifications to ATC-14," by C.D. Poland and J.O. Malley, 4/12/89, (PB90-108648/AS).

NCEER-89-0013 "Repair and Strengthening of Beam-to-Column Connections Subjected to Earthquake Loading," by M. Corazao and A.J. Durrani, 2/28/89, (PB90-109885/AS).

NCEER-89-0014 "Program EXKAL2 for Identification of Structural Dynamic Systems," by O. Maruyama, C-B. Yun, M. Hoshiya and M. Shinozuka, 5/19/89, (PB90-109877/AS).

NCEER-89-0015 "Response of Frames With Bolted Semi-Rigid Connections, Part I - Experimental Study and Analytical Predictions," by P.J. DiCorso, A.M. Reinhorn, J.R. Dickerson, J.B. Radziminski and W.L. Harper, 6/1/89, to be published.

NCEER-89-0016 "ARMA Monte Carlo Simulation in Probabilistic Structural Analysis," by P.D. Spanos and M.P. Mignolet, 7/10/89, (PB90-109893/AS).

NCEER-89-P017 "Preliminary Proceedings from the Conference on Disaster Preparedness - The Place of Earthquake Education in Our Schools," Edited by K.E.K. Ross, 6/23/89.

NCEER-89-0017 "Proceedings from the Conference on Disaster Preparedness - The Place of Earthquake Education in Our Schools," Edited by K.E.K. Ross, 12/31/89, (PB90-207895).

NCEER-89-0018 "Multidimensional Models of Hysteretic Material Behavior for Vibration Analysis of Shape Memory Energy Absorbing Devices, by E.J. Graesser and F.A. Cozzarelli, 6/7/89, (PB90-164146/AS).

NCEER-89-0019 "Nonlinear Dynamic Analysis of Three-Dimensional Base Isolated Structures (3D-BASIS)," by S. Nagarajaiah, A.M. Reinhorn and M.C. Constantinou, 8/3/89, (PB90-161936/AS).

NCEER-89-0020 "Structural Control Considering Time-Rate of Control Forces and Control Rate Constraints," by F.Y. Cheng and C.P. Pantelides, 8/3/89, (PB90-120445/AS).

NCEER-89-0021 "Subsurface Conditions of Memphis and Shelby County," by K.W. Ng, T-S. Chang and H-H.M. Hwang, 7/26/89, (PB90-120437/AS).

NCEER-89-0022 "Seismic Wave Propagation Effects on Straight Jointed Buried Pipelines," by K. Elhmadi and M.J. O'Rourke, 8/24/89, (PB90-162322/AS).

NCEER-89-0023 "Workshop on Serviceability Analysis of Water Delivery Systems," edited by M. Grigoriu, 3/6/89, (PB90-127424/AS).

NCEER-89-0024 "Shaking Table Study of a 1/5 Scale Steel Frame Composed of Tapered Members," by K.C. Chang, J.S. Hwang and G.C. Lee, 9/18/89, (PB90-160169/AS).

NCEER-89-0025 "DYNA1D: A Computer Program for Nonlinear Seismic Site Response Analysis - Technical Documentation," by Jean H. Prevost, 9/14/89, (PB90-161944/AS).

NCEER-89-0026 "1:4 Scale Model Studies of Active Tendon Systems and Active Mass Dampers for Aseismic Protection," by A.M. Reinhorn, T.T. Soong, R.C. Lin, Y.P. Yang, Y. Fukao, H. Abe and M. Nakai, 9/15/89, (PB90-173246/AS).

NCEER-89-0027 "Scattering of Waves by Inclusions in a Nonhomogeneous Elastic Half Space Solved by Boundary Element Methods," by P.K. Hadley, A. Askar and A.S. Cakmak, 6/15/89, (PB90-145699/AS).

NCEER-89-0028 "Statistical Evaluation of Deflection Amplification Factors for Reinforced Concrete Structures," by H.H.M. Hwang, J-W. Jaw and A.L. Ch'ng, 8/31/89, (PB90-164633/AS).

NCEER-89-0029 "Bedrock Accelerations in Memphis Area Due to Large New Madrid Earthquakes," by H.H.M. Hwang, C.H.S. Chen and G. Yu, 11/7/89, (PB90-162330/AS).

NCEER-89-0030 "Seismic Behavior and Response Sensitivity of Secondary Structural Systems," by Y.Q. Chen and T.T. Soong, 10/23/89, (PB90-164658/AS).

NCEER-89-0031 "Random Vibration and Reliability Analysis of Primary-Secondary Structural Systems," by Y. Ibrahim, M. Grigoriu and T.T. Soong, 11/10/89, (PB90-161951/AS).

NCEER-89-0032 "Proceedings from the Second U.S. - Japan Workshop on Liquefaction, Large Ground Deformation and Their Effects on Lifelines, September 26-29, 1989," Edited by T.D. O'Rourke and M. Hamada, 12/1/89, (PB90-209388/AS).

NCEER-89-0033 "Deterministic Model for Seismic Damage Evaluation of Reinforced Concrete Structures," by J.M. Bracci, A.M. Reinhorn, J.B. Mander and S.K. Kunnath, 9/27/89.

NCEER-89-0034 "On the Relation Between Local and Global Damage Indices," by E. DiPasquale and A.S. Cakmak, 8/15/89, (PB90-173865).

NCEER-89-0035 "Cyclic Undrained Behavior of Nonplastic and Low Plasticity Silts," by A.J. Walker and H.E. Stewart, 7/26/89, (PB90-183518/AS).

NCEER-89-0036 "Liquefaction Potential of Surficial Deposits in the City of Buffalo, New York," by M. Budhu, R. Giese and L. Baumgrass, 1/17/89, (PB90-208455/AS).

NCEER-89-0037 "A Determinstic Assessment of Effects of Ground Motion Incoherence," by A.S. Veletsos and Y. Tang, 7/15/89, (PB90-164294/AS).

NCEER-89-0038 "Workshop on Ground Motion Parameters for Seismic Hazard Mapping," July 17-18, 1989, edited by R.V. Whitman, 12/1/89, (PB90-173923/AS).

NCEER-89-0039 "Seismic Effects on Elevated Transit Lines of the New York City Transit Authority," by C.J. Costantino, C.A. Miller and E. Heymsfield, 12/26/89, (PB90-207887/AS).

NCEER-89-0040 "Centrifugal Modeling of Dynamic Soil-Structure Interaction," by K. Weissman, Supervised by J.H. Prevost, 5/10/89, (PB90-207879/AS).

NCEER-89-0041 "Linearized Identification of Buildings With Cores for Seismic Vulnerability Assessment," by I-K. Ho and A.E. Aktan, 11/1/89.

NCEER-90-0001 "Geotechnical and Lifeline Aspects of the October 17, 1989 Loma Prieta Earthquake in San Francisco," by T.D. O'Rourke, H.E. Stewart, F.T. Blackburn and T.S. Dickerman, 1/90, (PB90-208596/AS).

NCEER-90-0002 "Nonnormal Secondary Response Due to Yielding in a Primary Structure," by D.C.K. Chen and L.D. Lutes, 2/28/90.

NCEER-90-0003 "Earthquake Education Materials for Grades K-12," by K.E.K. Ross, 4/16/90.

NCEER-90-0004 "Catalog of Strong Motion Stations in Eastern North America," by R.W. Busby, 4/3/90.

NCEER-90-0005 "NCEER Strong-Motion Data Base: A User Manuel for the GeoBase Release (Version 1.0 for the Sun3)," by P. Friberg and K. Jacob, 3/31/90.

NCEER-90-0006 "Seismic Hazard Along a Crude Oil Pipeline in the Event of an 1811-1812 Type New Madrid Earthquake," by H.H.M. Hwang and C-H.S. Chen, 4/16/90.

NCEER-90-0007 "Site-Specific Response Spectra for Memphis Sheahan Pumping Station," by H.H.M. Hwang and C.S. Lee, 5/15/90.

NCEER-90-0008 "Pilot Study on Seismic Vulnerability of Crude Oil Transmission Systems," by T. Ariman, R. Dobry, M. Grigoriu, F. Kozin, M. O'Rourke, T. O'Rourke and M. Shinozuka, 5/25/90.

NCEER-90-0009 "A Program to Generate Site Dependent Time Histories: EQGEN," by G.W. Ellis, M. Srinivasan and A.S. Cakmak, 1/30/90.

NCEER-90-0010 "Active Isolation for Seismic Protection of Operating Rooms," by M.E. Talbott, Supervised by M. Shinozuka, 6/8/9.

NCEER-90-0011 "Program LINEARID for Identification of Linear Structural Dynamic Systems," by C-B. Yun and M. Shinozuka, 6/25/90.

NCEER-90-0012 "Two-Dimensional Two-Phase Elasto-Plastic Seismic Response of Earth Dams," by A.N. Yiagos, Supervised by J.H. Prevost, 6/20/90.

NCEER-90-0013 "Secondary Systems in Base-Isolated Structures: Experimental Investigation, Stochastic Response and Stochastic Sensitivity," by G.D. Manolis, G. Juhn, M.C. Constantinou and A.M. Reinhorn, 7/1/90.

NCEER-90-0014 "Seismic Behavior of Lightly-Reinforced Concrete Column and Beam-Column Joint Details," by S.P. Pessiki, C.H. Conley, P. Gergely and R.N. White, 8/22/90.

NCEER-90-0015 "Two Hybrid Control Systems for Building Structures Under Strong Earthquakes," by J.N. Yang and A. Danielians, 6/29/90.

NCEER-90-0016 "Instantaneous Optimal Control with Acceleration and Velocity Feedback," by J.N. Yang and Z. Li, 6/29/90.

NCEER-90-0017 "Reconnaissance Report on the Northern Iran Earthquake of June 21, 1990," by M. Mehrain, 10/4/90.

NCEER-90-0018 "Evaluation of Liquefaction Potential in Memphis and Shelby County," by T.S. Chang, P.S. Tang, C.S. Lee and H. Hwang, 8/10/90.

NCEER-90-0019 "Experimental and Analytical Study of a Combined Sliding Disc Bearing and Helical Steel Spring Isolation System," by M.C. Constantinou, A.S. Mokha and A.M. Reinhorn, 10/4/90.